

RETHINKING GNNs AND MISSING FEATURES: CHALLENGES, EVALUATION AND A ROBUST SOLUTION

005 **Anonymous authors**

006 Paper under double-blind review

ABSTRACT

012 Handling missing node features is a key challenge for deploying Graph Neural
 013 Networks (GNNs) in real-world domains such as healthcare and sensor networks.
 014 Existing studies mostly address relatively benign scenarios, namely benchmark
 015 datasets with (a) high-dimensional but sparse node features and (b) incomplete
 016 data generated under *Missing Completely At Random (MCAR)* mechanisms. For
 017 (a), we theoretically prove that high sparsity substantially limits the information
 018 loss caused by missingness, making all models appear robust and preventing a
 019 meaningful comparison of their performance. To overcome this limitation, we
 020 introduce one synthetic and three real-world datasets with dense, semantically
 021 meaningful features. For (b), we move beyond MCAR and design evaluation
 022 protocols with more realistic missingness mechanisms. Moreover, we provide a
 023 theoretical background to state explicit assumptions on the missingness process
 024 and analyze their implications for different methods. Building on this analysis,
 025 we propose GNNmim, a simple yet effective [baseline](#) for node classification with
 026 incomplete feature data. Experiments show that GNNmim [is competitive with respect to](#)
 027 specialized architectures across diverse datasets and missingness regimes.

1 INTRODUCTION

031 Learning with missing features is a pervasive and often unavoidable challenge in many real-world
 032 machine learning applications, such as healthcare (Braem et al., 2024; Mirkes et al., 2016), IoT
 033 sensor networks (Faizin et al., 2019; Okafor & Delaney, 2021; Agbo et al., 2022), and recommender
 034 systems (Marlin & Zemel, 2009; He et al., 2017; Marlin et al., 2011). This issue naturally extends to
 035 Graph Neural Networks (GNNs), which are increasingly applied in domains where missing features
 036 are common. In this work, we focus specifically on the problem of *missing node feature data*, a
 037 setting that has received growing attention in the GNN literature (Um et al., 2023; Yun et al., 2024;
 038 Rossi et al., 2022; Guo et al., 2023; Taguchi et al., 2021; Errica & Niepert, 2024; Um et al., 2025)

039 A wide range of methods have been proposed, from simple mean imputation (You et al., 2020) to
 040 architectures that jointly impute and predict during training (Guo et al., 2023). These approaches are
 041 typically evaluated by synthetically removing features from widely used node classification bench-
 042 marks such as CORA, CITESEER, and PUBMED (Yang et al., 2016). However, despite the growing
 043 number of models, little attention has been paid to the validity of these evaluation protocols. We
 044 argue that two critical issues remained largely unaddressed: (i) the datasets used for evaluation, and
 045 (ii) the missingness mechanisms applied to generate incomplete features.

046 Regarding (i), existing evaluations rely on datasets with *extremely sparse* node features, typically
 047 bag-of-words representations where the vast majority of entries are zero. This raises a crucial ques-
 048 tion: *can robustness to missing features be meaningfully assessed when most features are already*
 049 *absent?* Our theoretical analysis shows that in highly sparse settings, the mutual information be-
 050 between features and labels is barely affected by additional missingness, except at extremely high
 051 missing rates. Empirically, we find that all the existing GNN-based methods maintain high per-
 052 formance across a wide range of missingness levels on these benchmarks, with performance degrading
 053 only when more than 90% of entries are removed. These results cast serious doubt on the ability of
 current benchmarks to meaningfully assess the robustness of the models.

To move beyond this limitation, we identify a set of datasets, one synthetic and three real-world, with dense, raw features that are naturally low-dimensional and semantically meaningful (e.g., physical measurements). These datasets offer a more realistic setting for studying GNNs under feature missingness. This focus on dataset quality aligns with recent calls for more careful benchmark design in graph machine learning (Bechler-Speicher et al., 2025; Coupette et al., 2025).

Regarding (ii), the design of the missingness mechanisms used during evaluation is overly simplistic. Most prior works consider only *Missing Completely At Random (MCAR)* mechanisms (Rubin, 1976; Little & Rubin, 2019), where feature deletion is independent of the data. In practice, however, missingness is often related to the feature values or prediction target (Carreras et al., 2021; Hazewinkel et al., 2022; Kopra et al., 2015). For example, a patient might be less likely to report their weight if it is above a certain threshold. This corresponds to a Missing Not At Random (MNAR) mechanism (Rubin, 1976), in which the probability of missingness depends on the unobserved feature value itself. A further limitation of existing evaluation protocols is the implicit assumption that the missingness mechanism remains identical across training and test data. In practice, however, this is often not the case: for example, training data may be historical and collected with obsolete sensors prone to failures, while test data come from newer sensors with little or no missingness. To overcome this limitation of the current evaluation procedure, we design more realistic evaluation protocols. These include new, more representative instances of MCAR and MNAR mechanisms, as well as train–test distribution shifts. Such conditions more accurately capture real-world deployment challenges, where both the causes and the distributions of missing data may vary across stages.

Finally, we introduce a simple yet effective GNN model, **GNNmim**, based on the Missing Indicator Method (MIM) (Van Ness et al., 2023). GNNmim augments the node feature matrix with a binary mask indicating which features are missing. The resulting representation is processed by a standard GNN without requiring any learned imputation. **GNNmim** does not rely on any assumption on the distribution of the missingness and, despite its simplicity, it is competitive with respect to several state-of-the-art methods showing robustness under a variety of missingness settings.

Contributions. To summarize, our main contributions are:

1. We provide a theoretical analysis showing that the impact of missing features depends strongly on feature sparsity, and derive an information-theoretic bound on the resulting loss.
2. We introduce one synthetic and three real-world datasets with dense, informative features, and show experimentally that models appearing robust on sparse benchmarks fail on these datasets.
3. We propose realistic evaluation protocols, including new, more representative instances of MCAR and MNAR mechanisms and train–test distribution shifts, and demonstrate that existing methods are not robust to all the possible settings.
4. We introduce **GNNmim**, a simple yet effective method, and show that it is competitive with respect to existing approaches across datasets, missingness types, and distribution shifts.

The core aim of this paper is to redefine how research on GNNs with missing features should move forward. We show that apparent progress in this area has been largely constrained by the evaluation itself: existing benchmarks rely on sparse, weakly informative features and overly benign missingness mechanisms, making current results difficult to interpret and obscuring the true robustness of existing methods. By introducing dense, semantically meaningful datasets, realistic missingness protocols, and a clear theoretical framing, we establish a foundation that enables more meaningful and reliable research directions. Within this improved evaluation setup, **GNNmim** is intentionally simple: once evaluation artifacts are removed, a lightweight, assumption-free model can outperform more complex approaches. Thus, **GNNmim** serves as an effective baseline that naturally arises from the identification and analysis of the limitations of the current evaluation setup. The broader contribution of this work lies in establishing a principled and realistic evaluation framework, with **GNNmim** serving as a clear baseline within it.

2 LEARNING FROM INCOMPLETE GRAPH DATA

We consider an attributed graph $G = (V, E, \mathbf{X}, \mathbf{Y})$, where $V = \{1, \dots, n\}$ is the set of nodes, $E \subseteq V \times V$ is the set of edges represented by the adjacency matrix $\mathbf{A} \in \{0, 1\}^{n \times n}$, $\mathbf{X} \in \mathbb{R}^{n \times d}$ is

108 the node feature matrix with entry X_{ij} denoting feature j of node i , and $\mathbf{Y} \in \mathcal{Y}^n$ is the vector of
109 node labels.

110 When data is incomplete, some entries of \mathbf{X} are unobserved. Let $\mathbf{M} \in \{0, 1\}^{n \times d}$ be the missingness
111 indicator matrix that has $M_{ij} = 1$ if x_{ij} is missing and 0 otherwise. In our setting, the missingness
112 indicator matrix \mathbf{M} is directly and deterministically constructed from the observed dataset. Missing
113 values are explicitly marked in the raw data, so the mask \mathbf{M} is uniquely defined and contains no
114 uncertainty. Let \mathbf{X}^{obs} be the elements of \mathbf{X} for which $M_{ij} = 0$, and \mathbf{X}^{miss} the elements for which
115 $M_{ij} = 1$. The observed data from which we learn then can be written as $\mathbf{X}^{obs}, \mathbf{Y}, \mathbf{M}$. We note
116 that we here make the assumption that \mathbf{Y} is fully observed in the (training) data, and that there is no
117 uncertainty about the graph structure E . The distribution of the data then can be parameterized as
118

$$P_{\theta, \gamma, \lambda}(\mathbf{X}^{obs}, \mathbf{Y}, \mathbf{M}) = \int_{\mathbf{X}^{miss}} P_{\theta}(\mathbf{X}) P_{\gamma}(\mathbf{Y}|\mathbf{X}) P_{\lambda}(\mathbf{M}|\mathbf{X}, \mathbf{Y}), \quad (1)$$

121 where $\mathbf{X} = \mathbf{X}^{obs} \cup \mathbf{X}^{miss}$, P_{θ} is the node feature distribution, P_{γ} is the conditional label distribution,
122 and P_{λ} represents the *missingness mechanism*. Though not explicitly reflected in the notation, all
123 these distributions will usually depend on the underlying graph structure, which will typically induce
124 dependencies among the rows of \mathbf{X} , and among the elements of \mathbf{Y} .

125 A GNN for node classification with complete feature data is a model $P_{\gamma}(\mathbf{Y}|\mathbf{X})$ with γ the weights
126 of the GNN. For classification with incomplete data we need to learn the conditional model
127

$$P_{\theta, \gamma, \lambda}(\mathbf{Y}|\mathbf{X}^{obs}, \mathbf{M}) = \int_{\mathbf{X}^{miss}} P_{\theta, \gamma, \lambda}(\mathbf{Y}|\mathbf{X}, \mathbf{M}) P_{\theta, \gamma, \lambda}(\mathbf{X}^{miss}|\mathbf{X}^{obs}, \mathbf{M}). \quad (2)$$

130 The classical *missing (completely) at random (M(C)AR)* assumptions (Rubin, 1976) simplify this
131 problem. The original M(C)AR assumptions have been formulated in the context of estimating the
132 parameter of a generative distribution. It has been observed that more specialized variations of the
133 original definitions can be more pertinent in the context of classification (Ding & Simonoff, 2010;
134 Ghorbani & Zou, 2018). In the following we give formulations of M(C)AR for classification that
135 provide the foundations for our theoretical analysis.

136 **Definition 1.** The joint distribution $P_{\theta, \gamma, \lambda}$ is *feature-MAR*, if

$$P_{\gamma, \lambda}(\mathbf{M}|\mathbf{X}^{miss}, \mathbf{X}^{obs}) = P_{\theta, \gamma, \lambda}(\mathbf{M}|\mathbf{X}^{obs}). \quad (3)$$

137 It is *label-MAR* if

$$P_{\lambda}(\mathbf{M}|\mathbf{X}, \mathbf{Y}) = P_{\gamma, \lambda}(\mathbf{M}|\mathbf{X}). \quad (4)$$

138 The distribution is *MCAR*, if

$$P_{\lambda}(\mathbf{M}|\mathbf{X}, \mathbf{Y}) = P_{\theta, \gamma, \lambda}(\mathbf{M}). \quad (5)$$

139 In (3)-(5) all probability functions are indexed with the parameters they actually depend on. Note,
140 for example, that the conditional of \mathbf{M} given \mathbf{X} requires marginalization over \mathbf{Y} , and thereby also
141 depends on the parameter γ . MCAR implies both feature- and label-MAR.

142 The simplest realization of an MCAR mechanism is *uniform missingness (U-MCAR)* in which
143 entries of \mathbf{X} are independently missing with a fixed missingness probability μ . This can be generalized
144 by defining a missingness probability matrix $\mu \in [0, 1]^{n \times d}$ specifying potentially different missing-
145 ness probabilities for different entries of \mathbf{X} .

146 MAR assumptions allow us to eliminate the missingness model P_{λ} from (2). The following proposition
147 states this classical *ignorability* result in a version most suitable in our context.

148 **Theorem 1.** If $P_{\theta, \gamma, \lambda}$ is feature-MAR and label-MAR, then (2) simplifies to

$$\int_{\mathbf{X}^{miss}} P_{\gamma}(\mathbf{Y}|\mathbf{X}) P_{\theta}(\mathbf{X}^{miss}|\mathbf{X}^{obs}). \quad (6)$$

149 **Intuition.** Under feature-MAR and label-MAR, the missingness pattern carries no predictive in-
150 formation. The learning problem reduces to the usual classification task with imputed features,
151 meaning that methods explicitly modeling the missingness mask do not gain theoretical advantage
152 in this regime.

The proof is straightforward by rewriting the two factors on the right of (2) using Bayes’s rule, and plugging in (3) and (4). Formulation (6) still poses two major challenges: it requires a feature distribution model P_θ when in reality we only are interested in the conditional model P_γ , and the integration over \mathbf{X}^{miss} is usually intractable (Ipsen et al., 2022). The simplest approach to address these problems is to approximate the integral (6) by evaluating $P_\gamma(\mathbf{Y}|\mathbf{X})$ at a single imputed value $\mathbf{X} = \text{impute}(\mathbf{X}^{miss})$ (Rubin, 1988). This does not require an explicit model for P_θ , but relies on the implicit assumption that the imputed value $\text{impute}(\mathbf{X}^{miss})$ has high probability under P_θ . A simple example is *mean-imputation*, in which missing values of a given feature are filled with the mean of that feature; we will refer to this approach combined with a standard GNN as GNN_{mi} (You et al., 2020). In addition, we also consider *zero-imputation*, where missing entries are replaced with zeros (GNN_{zero}), and *median-imputation*, where they are filled with the feature median (GNN_{median}). Similarly, PCFI (Um et al., 2023) does not require an explicit model for P_θ ; it introduces a confidence-guided imputation scheme where pseudo-confidence is derived from the shortest-path distance to observed features, and combines channel-wise diffusion with inter-channel propagation to recover a single estimate of \mathbf{X} . GOODIE (Yun et al., 2024) approximates the integral in (6) using a combination of label propagation and FP (Rossi et al., 2022), which propagates features by minimizing a Dirichlet energy function, whereas FairAC (Guo et al., 2023) does so by aggregating, via an attention mechanism, the representations from neighbors of nodes with missing features.

Other methods explicitly model P_θ . The GCNmf approach of Taguchi et al. (2021) introduces a model of P_θ in the form of a mixture of Gaussians, and approximates (6) by $P_\gamma(\mathbf{Y}, |, \mathbb{E}_\theta[\mathbf{L}_1 | \mathbf{X}^{obs}])$, where $\mathbb{E}_\theta[\mathbf{L}_1 | \mathbf{X}^{obs}]$ is the expected activation at the first layer of the GNN defining P_γ . Finally, GSPN (Errica & Niepert, 2024) explicitly models P_θ with graph-induced sum–product networks, so missing features are handled by exact marginalization.

An alternative to all these approaches that work entirely with models P_θ, P_γ for the (complete) data distribution is to include the missingness mechanism explicitly in a model $P_{\gamma^+}(\mathbf{Y} | \mathbf{X}^{obs}, \mathbf{M})$, that directly captures the left side of (2). We here write γ^+ for the parameters of the model to emphasize that it can be structurally similar to a model $P_\gamma(\mathbf{Y} | \mathbf{X})$, but different in that it has the missingness matrix \mathbf{M} as an explicit extra input.

This modeling strategy, often referred to as the Missing Indicator Method (MIM), has been studied in the context of supervised learning with missing features (Van Ness et al., 2023), but, to the best of our knowledge, it has not been explored in the context of graph machine learning. In this work, we propose a GNN-based instantiation of the MIM framework, which we call GNN_{mim}. In GNN_{mim}, we implement P_{γ^+} as a GNN, we construct the matrix *zero-pad*(\mathbf{X}^{obs}) in which missing values are filled in by zeros, and use the concatenation *zero-pad*(\mathbf{X}^{obs})[$i, :||\mathbf{M}[i, :]$ as the feature vector for node i in an otherwise standard GNN architecture¹. GNN_{mim} does not rely on any MAR assumptions, and thereby can be expected to perform more robustly than other approaches under different missingness mechanisms. As our experiments in Section 5 show, this simple yet principled strategy yields robust performance across a wide variety of missingness scenarios. In Appendix I, we provide additional analyses where the missing-feature mask is applied not only to zero imputation but also to the existing models presented in this section.

3 ARE WE EVALUATING GNNS FOR MISSING FEATURES ON THE RIGHT DATA?

A rigorous evaluation of GNNs under feature missingness requires not only well-designed models, but also datasets that are suitable for the problem at hand. Recent work in the graph learning community has emphasized the importance of dataset suitability in benchmarking (Bechler-Speicher et al., 2025; Coupette et al., 2025). In the context of learning with missing node features, dataset suitability is even more critical. Models designed to handle missingness should be tested on datasets where the

¹We deliberately here say “zero-padding” rather than “zero-imputation”. The latter would imply that we view the zeros as somehow reasonable stand-ins for the true unobserved values. We view the zeros as arbitrary placeholders. Ideally, the trained model will learn to ignore these values when the corresponding missingness indicator is 1.

presence of missing features meaningfully affects model performance and where reasoning under missingness is necessary and non-trivial.

The current standard practice in the literature is to evaluate state-of-the-art methods on a set of widely-used benchmarks for node-level tasks, namely, CORA, CITESEER, PUBMED, AMAZON-COMPUTERS, and AMAZONPHOTO. In these datasets, node features are constructed as follows: CORA, CITESEER and PUBMED use binary bag-of-words features, while AMAZONCOMPUTERS and AMAZONPHOTO use TF-IDF vectors (Aizawa, 2003). These feature matrices are typically very sparse, which we quantify using the notion of *feature sparsity*, formally defined as below:

Definition 2 (Feature Sparsity). Given a node feature matrix $\mathbf{X} \in \mathbb{R}^{n \times d}$, the *feature sparsity* is defined as the proportion of zero entries: $s(\mathbf{X}) = \frac{1}{nd} \sum_{i=1}^n \sum_{j=1}^d \mathbf{1}[X_{ij} = 0]$, where $\mathbf{1}[\cdot]$ denotes the indicator function.

The sparsity values of the benchmark datasets are reported in Table 1 (first three rows). All datasets exhibit substantial sparsity, with more than 50% of features being zero across all the datasets, with Citeseer reaching an extreme sparsity level of approximately 99%. This raises a crucial question: does it make sense to evaluate models designed to handle missing features on datasets where the feature representations are already extremely sparse? In such sparse settings, a high probability of missingness is needed to induce a meaningful information loss. Otherwise, the observed model performance under missingness may reflect artifacts of the dataset rather than the robustness of the method. We formalize this observation in the following theorem.

Theorem 2. Let $\mathbf{X} \in \mathbb{R}^{n \times d}$ and $\mathbf{Y} \in \mathcal{Y}^n$ be random variables, $\mathbf{M} \in \{0, 1\}^{n \times d}$ be a missingness mask and \mathbf{X}^{obs} denotes the observed (incomplete) data. We encode the pair $(\mathbf{X}^{obs}, \mathbf{M})$ with the random variable $\tilde{\mathbf{X}}$ with

$$\tilde{X}_{ij} = \begin{cases} X_{ij}, & M_{ij} = 0, \\ ?, & M_{ij} = 1. \end{cases}$$

Let the change in the information be defined as $\Delta := I(\mathbf{Y}; \tilde{\mathbf{X}}) - I(\mathbf{Y}; \mathbf{X})$, where $I(\cdot; \cdot)$ denotes the mutual information. Then,

1. If the missingness is label-MAR, then $\Delta \leq 0$.
2. If $\mathbf{X} \in \{0, 1\}^{n \times d}$ and the missingness is U-MCAR with missingness probability μ , and $s(\mathbf{X})$ is the sample sparsity as in Definition 2, then

$$-nd\mu h_2(\mathbb{E}[s(\mathbf{X})]) \leq \Delta \leq 0,$$

where $h_2(u) = -u \log u - (1-u) \log(1-u)$.

Intuition. When node features are extremely sparse (e.g., BoW/TF-IDF), the information loss induced by missingness is provably negligible unless missingness is extremely high. As a result, existing sparse benchmarks inherently make all methods appear robust, preventing meaningful comparison.

The proof can be found in Appendix A. Theorem 2 demonstrates that when feature sparsity is high, a very large amount of missingness is required to produce a meaningful loss of information. This confirms that such benchmarks do not meaningfully differentiate between approaches, casting doubt on their suitability for evaluating GNNs under feature missingness. As a consequence, we argue for the use of datasets where missingness poses a real challenge. In particular, we introduce a set of four alternative datasets, one new synthetic and three real-world. More details about the datasets are reported in Appendix C.

Table 1: Feature sparsity across benchmarks and custom datasets.

Dataset	#Features	Sparsity ↓	Type of features
CORA	1433	0.9873	BoW (binary)
CITESEER	3703	0.9915	BoW (binary)
PUBMED	500	0.8998	BoW (binary)
SYNTHETIC	5	0.0000	Gaussian
AIR	7	0.1615	Raw
ELECTRIC	5	0.2000	Raw
TADPOLE	15	0.0000	Raw

(1) **A synthetic dataset tailored to controlled missingness.** We construct a dataset based on a Barabási–Albert graph topology, where node features are sampled from a Gaussian distribution. Node labels are assigned using a fixed two-layer GCN applied to the full, complete features, ensuring that a GNN model has the capacity to achieve high classification accuracy in the absence of missingness. This controlled setting provides a testbed for isolating the effects of missingness under varying sparsity, while maintaining a well-defined ground truth.

(2) **Real-world datasets with semantically meaningful features.** We also advocate for the use of real datasets in which node features correspond to raw, observable properties: 1) **AIR** (Zheng et al., 2015), a sensor network dataset from IoT applications, where node features correspond to environmental measurements and node labels indicate sensor status categories; 2) **ELECTRIC** (Birchfield et al., 2016; Baek & Birchfield, 2023), a dataset of interconnected electrical sensors, with real-valued measurements as features and operational condition classification as the target task; 3) **TADPOLE** (Zhu et al., 2019), a medical graph dataset derived from the TADPOLE challenge, where each node represents a patient, node features include clinical and imaging biomarkers, and the goal is to predict diagnostic labels.

Table 2: Evaluation of P1 (feature-structure separability) and P2 (feature-structure complementarity) on our custom datasets. Each cell reports the KS statistic and associated p -value for separability under six perturbation settings. $\gamma_{1,1}$ indicates the feature-structure complementarity. Datasets satisfying each property (as per Couppete et al. (2025)) are marked with \checkmark .

Dataset	Empty Feat.	Random Feat.	Complete Feat.	Empty Graph	Random Graph	Complete Graph	$\gamma_{1,1}$	P1	P2
SYNTHETIC	1.00 (8.80e-62)	1.00 (8.80e-62)	1.00 (1.93e-14)	1.00 (1.03e-17)	1.00 (8.80e-62)	1.00 (8.80e-62)	0.62	\checkmark	\checkmark
AIR	1.00 (8.80e-62)	1.00 (8.80e-62)	1.00 (8.80e-62)	0.67 (1.53e-30)	1.00 (8.80e-62)	1.00 (8.80e-62)	0.68	\checkmark	\checkmark
ELECTRIC	1.00 (8.80e-62)	1.00 (8.80e-62)	1.00 (8.80e-62)	0.98 (1.90e-57)	1.00 (8.80e-62)	1.00 (8.80e-62)	0.69	\checkmark	\checkmark
TADPOLE	1.00 (8.80e-62)	0.90 (5.31e-44)	0.61 (4.22e-18)	0.77 (1.53e-30)	1.00 (8.80e-62)	1.00 (8.80e-62)	0.64	\checkmark	\checkmark

Both the synthetic and real-world datasets exhibit low feature sparsity (Table 1), a necessary condition for studying missingness. However, sparsity alone is not sufficient: suitable datasets must also ensure that both features and structure are task-informative and interact non-trivially. We assess this using the RINGS framework (Couppete et al., 2025), which measures performance separability via KS statistics under perturbations (e.g., removing all edges or replacing features with noise), and features-topology complementarity via the normalized Gromov–Wasserstein distance $\gamma_{1,1}$ between the structural and feature-induced metric spaces (values above 0.5 are considered satisfactory). As shown in Table 2, all proposed datasets satisfy both mode complementarity and performance separability. Combined with their low feature sparsity, these properties make the datasets more suitable than traditional benchmarks for evaluating robustness to incomplete node attributes.

While the real-world datasets we introduce have moderate numbers of nodes and features (Table 3), they satisfy the three key requirements for evaluating robustness to missing node attributes: (i) dense, semantically meaningful, low-dimensional features; (ii) non-trivial predictive signal under complete information; and (iii) complementary and separable contributions of features and structure. To the best of our knowledge, no existing large-scale graph datasets simultaneously meet all these criteria. This limitation is structural to current benchmarks and has been noted in recent work (Bechler-Speicher et al., 2025). Importantly, the effect of missingness on model performance does not depend on graph size: in Appendix E we replicate our experiments on a larger variant of the **SYNTHETIC** dataset (both in number of nodes and features) and observe trends fully consistent with those reported in the main analysis.

4 BEYOND UNIFORM MISSINGNESS

Dataset suitability is only one dimension of the evaluation problem. A second, equally important factor is the choice of the missingness mechanism under which models are tested. In the literature, nearly all prior works adopt a masking scheme based on *U-MCAR* mechanism. In other works (Taguchi et al., 2021; Um et al., 2023), a different variant is used where entire feature vectors of randomly selected nodes are masked. We denote this as **Structural MCAR (S-MCAR)**. These two settings have become the default evaluation standards in the context of graph learning. We argue that more challenging and realistic missing data patterns need to be considered for a more infor-

324 mative evaluation of different methods’ capabilities. We first introduce a more challenging MCAR
 325 mechanism:

327 **Label-Dependent MCAR (LD-MCAR).** Missingness here is applied at the feature (column) level,
 328 assigning higher missingness probability to features X_j that are more informative for the label, as
 329 measured by the mutual information $I(X_j; Y)$. Then, each entry X_{ij} is masked independently with
 330 probability $P(M_{ij} = 1) = \rho \cdot I(X_j; Y)$, where $\rho \in [0, 1]$ is a scaling factor selected to achieve
 331 the overall desired expected missingness rate across the dataset. Importantly, this mechanism is still
 332 MCAR: the probability that a specific entry is missing does not depend on the actual value of the
 333 feature or the label, but only on the mutual information of the feature column and the label.

334 Outside of graph learning, authors have also emphasized the importance of MAR and MNAR mech-
 335 anisms that reflect more realistically the kinds of missingness encountered in real-world applica-
 336 tions(Ghorbani & Zou, 2018; Mohan & Pearl, 2021; Jaeger, 2022; Van Ness et al., 2023). In many
 337 practical scenarios, missing features are indeed related to their values or to the prediction target. For
 338 instance, a patient might be less likely to report their weight if it is above a certain threshold. This
 339 corresponds to a Missing Not At Random (MNAR) mechanism (Rubin, 1976). Testing GNN mod-
 340 els exclusively under MCAR conditions thus fails to capture the challenge of more realistic settings.
 341 We therefore propose two different MNAR scenarios:

342 **Feature-Dependant MNAR (FD-MNAR).** In this mechanism the probability of missingness de-
 343 pends on the value of the feature itself. In particular, we assume that extreme feature values, e.g.,
 344 high quantiles, are more likely to be missing, as often observed in real-world settings such as health-
 345 care, where abnormal values may be withheld. Formally, for each feature column j , let $q_j^{(\tau)}$ denote
 346 the τ -quantile of the observed values. We define the missingness probability for entry X_{ij} as:

$$P(M_{ij} = 1) = \begin{cases} \mu^{\text{hi}} & \text{if } X_{ij} \geq q_j^{(\tau)}, \\ \mu^{\text{lo}} & \text{otherwise,} \end{cases}$$

351 with $\mu^{\text{hi}} > \mu^{\text{lo}}$ and both chosen selected to match a desired overall missingness rate.

352 **Class-Dependent MNAR (CD-MNAR).** In this mechanism, features whose values are informative
 353 for the label, are more likely to be omitted. For example, in medical datasets, patients may be less
 354 likely to disclose whether they smoke, a feature strongly associated with the label indicating a history
 355 of heart attack. To identify such dependencies, we train a decision tree classifier in a one-vs-rest
 356 setting, using the observed features to predict class membership. For each class $c \in \{1, \dots, C\}$, we
 357 extract decision paths that lead to leaf nodes predicting c . These paths define a set of feature-value
 358 conditions that contribute to the prediction of class c , which we denote as \mathcal{R}_c . Let $\text{Cond}_c(j, X_{ij})$
 359 be a predicate that evaluates to true if the value of feature j for node i satisfies at least one condition
 360 in \mathcal{R}_c . Then, the missingness probability is defined as:

$$P(M_{ij} = 1 \mid Y_i = c) = \begin{cases} \mu^{\text{hi}} & \text{if } \text{Cond}_c(j, X_{ij}) = \text{true,} \\ \mu^{\text{lo}} & \text{otherwise,} \end{cases}$$

364 where $\mu^{\text{hi}} > \mu^{\text{lo}}$, and both are selected to meet a target overall missingness rate.

366 In almost all existing experimental studies the missingness mechanism is the same in training and
 367 test data. An exception is (Ding & Simonoff, 2010), where two types of test data are considered:
 368 data that underlies the same missingness as the training data, and complete data. We consider a
 369 possible distribution shift in $P_{\lambda}(\mathbf{M}|\mathbf{X}, \mathbf{Y})$ to be an important concern for two reasons: first, it
 370 represents a realistic scenario in practical applications. For instance, training data may consist of
 371 historical records collected over time, which may contain missing features due to manual entry or
 372 outdated systems. In contrast, test data are collected in real time with modern infrastructure, and
 373 all feature values are available. This results in a shift from incomplete to complete data between
 374 training and testing. The second reason for considering distribution shifts in P_{λ} is to assess a pos-
 375 sible weakness of GNNmim: as a model of the form $P_{\gamma^+}(\mathbf{Y}|\mathbf{X}^{\text{obs}}, \mathbf{M})$ it explicitly incorporates a
 376 model of the missingness mechanism, and thereby could be expected to be less robust under miss-
 377 ingness distribution shifts than models that are based on MAR assumptions and (6) (which would
 378 be expected to be robust as long as the mechanism is feature and label MAR in both training and
 379 test data). We therefore define two evaluation regimes (R1 and R2) with and without a shift in the

378 missingness process. Let $\mu_{\text{tr}}(\mathbf{M} \mid \mathbf{X}, \mathbf{Y})$ and $\mu_{\text{te}}(\mathbf{M} \mid \mathbf{X}, \mathbf{Y})$ denote the missingness distributions
 379 in training and testing, respectively.
 380

381 **R1: i.i.d. missingness (no shift).** The same missingness mechanism (*U-MCAR*, *S-MCAR*, *LD-MCAR*, *FD-MNAR*, *CD-MNAR*) and rate are applied to training and test data, i.e., $\mu_{\text{tr}} = \mu_{\text{te}}$.
 382

383 **R2: missingness distribution shift (train \neq test).** In this setting, we evaluate combinations of
 384 a training missingness mechanism $M_{\text{tr}} \in \{\text{FD-MNAR}, \text{CD-MNAR}\}$ with missingness probability
 385 $\mu_{\text{tr}} = 50\%$, and a test missingness mechanism $M_{\text{te}} = \text{U-MCAR}$ with missingness probability $\mu_{\text{te}} \in$
 386 $\{0\%, 25\%, 50\%\}$.
 387

389 5 EXPERIMENTAL RESULTS

390 We conduct experiments on node classification task using the datasets introduced in Section 3 and
 391 the more realistic missingness protocols described in Section 4. We compare a range of GNN-based
 392 models specifically designed to handle missing features described in Section 2, namely `GNNzero`,
 393 `GNNmedian`, `GNNmi`, `GCNmf`, `GOODIE`, `GSPN`, `PCFI`, `FP`, and `FairAC` as well as our proposed
 394 method, `GNNmim`. [Following the evaluation protocol adopted by these competitors, we perform all
 395 main experiments in a transductive setting. However, we note that `GNNmim` can also be applied in
 396 an inductive scenario; for completeness, in Appendix H we report additional experiments conducted
 397 under an inductive setting.](#) For all the experiments, we decide to treat the specific GNN layer type in
 398 `GNNmim` as a hyperparameter. Full implementation details and hyperparameter settings are provided
 399 in Appendix D. The code is provided in the supplementary material. The experiments are designed
 400 to answer the following research questions:
 401

- 402 • **Q1:** Do the datasets of Section 3 provide new and complementary insights regarding the robust-
 403 ness of GNNs under varying rates of missing features?
- 404 • **Q2:** How robust are different models for handling incomplete features to different types of
 405 missingness?
- 406 • **Q3:** Do different models maintain their performance under distribution shifts in missingness
 407 between training and test sets?

408 **Q1:** To assess the impact of the dataset on evaluating robustness under different missingness rates,
 409 we compute the F1 score for each model as a function of the missingness rate μ . Figure 1 re-
 410 ports these curves under *Structural MCAR* (*S-MCAR*) under R1 regimes (see Section 4) for both the
 411 standard benchmarks (`CORA`, `CITESEER`, `PUBMED`) and the datasets we propose (`ELECTRIC`, `AIR`,
 412 `TADPOLE`, and `SYNTHETIC`). Results for other missingness mechanisms lead to equal conclusions
 413 and are included in Appendix B.
 414

415 On `CORA`, `CITESEER`, `PUBMED`, all models appear robust, as their F1 score remains high across
 416 a wide range of μ , and only drops at very high missingness rates (85-90%). In contrast, on our
 417 proposed datasets, performance drops much earlier, often already at low missingness rates. On
 418 `TADPOLE`, the degradation is less pronounced at low μ overall; however, two models, `GOODIE` and
 419 `GSPN`, notably diverge from the rest, showing much weaker performance even with limited miss-
 420 ingness.
 421

422 These results show that evaluating robustness solely on traditional benchmarks may lead to overly
 423 optimistic conclusions on the robustness of the methods. To properly assess the behavior of GNNs
 424 under different missing rates, it is essential to use more challenging datasets.
 425

426 **Q2:** To assess robustness across mechanisms, we compute the area under the F1-missingness curve
 427 (AUC) for each dataset, model, and missingness mechanism under R1 regimes (complete F1 results
 428 by model, dataset, missingness rate, and mechanism are reported in Appendix F).
 429

430 Figure 2 reports the AUC scores as heatmaps, where lighter colors indicate better model performance
 431 for each mechanism within each dataset. We observe that many existing methods exhibit strong
 432 sensitivity to the missingness type. For example, `FairAC` performs well under *S-MCAR* settings on
 433 `ELECTRIC` (0.870 AUC, ranking first among all the models), but its performance degrades signif-
 434 icantly under *FD-MNAR* on `SYNTHETIC` (0.641, ranking second-last). Similarly, `GOODIE` ranks
 435 highest on `SYNTHETIC` with uniform missingness (0.771), yet drops to 0.587 under *CD-MNAR*.
 436

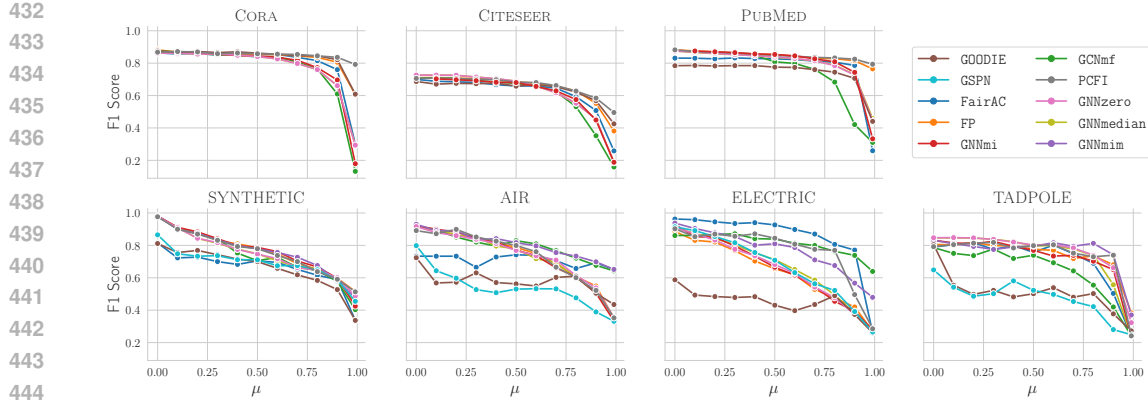


Figure 1: Mean F1-score across 5 runs as a function of the missingness probability μ on the proposed datasets and established benchmarks. Each panel reports the performance of all models on a specific dataset under the **S-MCAR** setting. The complete tables for all missingness mechanisms are provided in Appendix B.

These results confirm that performance under **U-MCAR** is not predictive of robustness under more realistic **FD-MNAR** scenarios. This calls into question the validity of evaluations based only on uniform or structure-based missingness. Our proposed method, **GNNmim**, exhibits consistently high AUC across all missingness types and datasets. These results suggest that broad robustness to diverse and realistic missingness mechanisms is achievable, even with lightweight models that do not rely on any MAR assumptions.

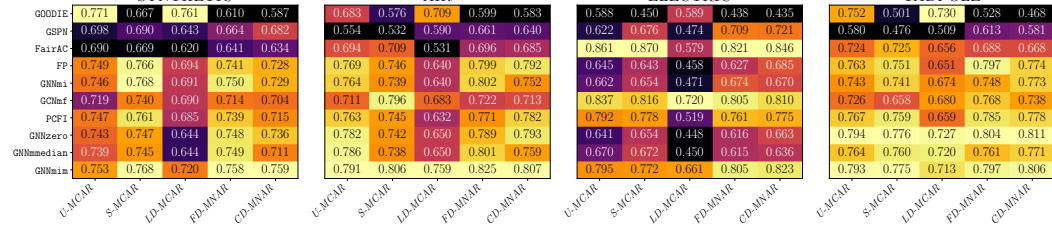


Figure 2: Column-normalized heatmaps showing the AUC (area under the F1 vs. missingness rate μ curve) for each model, dataset, and missingness mechanism. Higher values (lighter colors) indicate better overall robustness across increasing levels of missingness.

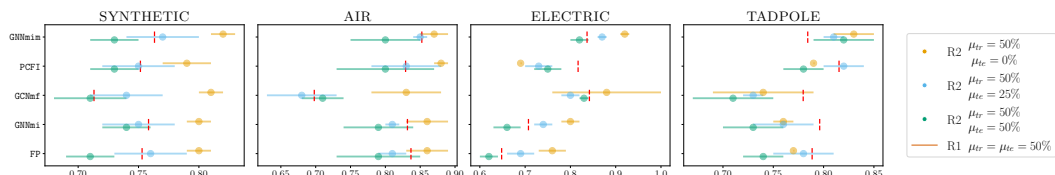
Q3: To evaluate model robustness under distribution shifts in missingness, we compute the F1 score (mean \pm standard deviation over 5 runs) for each dataset, model, and shift configuration of the R2 regime (Section 4). Full results are in Appendix G; Figure 3 shows a representative subset of the best-performing models from Q2 (GNNmim, GNNmi, GCNmf, FP, PCFI), trained on **FD-MNAR** with $\mu_{tr} = 50\%$ and tested on **U-MCAR** with $\mu_{te} \in \{0\%, 25\%, 50\%\}$. Similar results hold for other models and for the case where the training missing mechanisms is **CD-MNAR** (Appendix G).

Each panel shows one dataset, with F1 on the x-axis, models on the y-axis, and color indicating μ_{te} (yellow 0%, blue 25%, green 50%). Dots show mean F1, horizontal lines the standard deviation, and the red vertical bar marks the results obtained in the regime R1 with **FD-MNAR** mechanism on both training and test and $\mu_{tr} = \mu_{te} = 50\%$. We observe two findings.

1. Distribution shift generalization is challenging: in almost all cases, performance under R2 test conditions **U-MCAR** 25% is lower than in the i.i.d. R1 setting, despite the test missingness being less severe. This is visible when the blue dot ($\mu_{te} = 25\%$) lies to the left of the red vertical bar ($\mu_{tr} = \mu_{te} = 50\%$). This shows that distribution shifts in missingness create a harder generalization challenge that is not explained solely by missingness severity. The effect

486 is also dataset-dependent, further reinforcing the need to evaluate robustness under these shifts
 487 and under different datasets.

488 2. GNNmim **is competitive with respect to** other models even under R2 conditions. Across datasets
 489 and levels of test missingness, GNNmim tends to achieve the highest F1 scores (i.e., yellow,
 490 blue, and green dots are consistently farther to the right). In spite of its potential vulnerability
 491 in the R2 setting, GNNmim is seen to maintain its advantage over the alternative approaches.



500 Figure 3: F1 scores (mean \pm std over 5 runs) under distribution shifts in missingness between training
 501 and test data. All models are trained with *FD-MNAR* missingness at 50%. Each panel corresponds
 502 to a dataset; each row to a model. Colored dots represent test-time F1 under *U-MCAR* with varying
 503 missingness rates: yellow = 0%, blue = 25%, green = 50%. Vertical red lines indicate the F1
 504 achieved in the i.i.d. setting (*FD-MNAR* 50% at both train and test).

506 6 CONCLUSION AND FUTURE WORK

507 We revisited the problem of learning GNNs under missing node features, highlighting fundamental
 508 limitations of current evaluation protocols, namely the reliance on benchmarks with sparse features
 509 and oversimplified missingness mechanisms. To address these issues, we introduced new datasets
 510 with dense, informative features and more realistic missingness patterns that go beyond MCAR,
 511 and proposed GNNmim, a simple yet effective method that explicitly models missingness through
 512 the missing-indicator approach. Our experiments show that GNNmim **is competitive with respect to**
 513 more complex architectures across diverse datasets, missingness types, and train–test shifts. This
 514 work calls for a shift towards more realistic evaluation settings and demonstrates that lightweight
 515 yet principled strategies can achieve strong robustness in challenging missing-feature scenarios.

516 As a direction for future work, our study underscores the need for larger and more diverse benchmarks
 517 specifically designed for missing features, aligning with recent calls for better datasets in
 518 graph learning (Bechler-Speicher et al., 2025), and reveals that there remains substantial room for
 519 developing models that are robust to diverse rates and types of missingness. **Another promising**
 520 **direction concerns the development of more realistic MNAR mechanisms, potentially incorporating**
 521 **graph-specific dependencies where missingness is influenced by structural properties of the graph**
 522 **itself. Designing richer, structurally grounded MNAR processes would allow for more faithful stress-**
 523 **testing of models in settings that better reflect more complex patterns.**

525
 526
 527
 528
 529
 530
 531
 532
 533
 534
 535
 536
 537
 538
 539

540 USE OF LARGE LANGUAGE MODELS (LLMs)
541542 We used LLMs to improve the readability of the manuscript, rephrase selected passages, and assist
543 in code debugging. All content was initially written by the authors, with LLMs employed solely to
544 enhance clarity and presentation.
545546 ETHICS STATEMENT
547548 Our study does not involve human subjects or personally identifiable data. The datasets used are
549 publicly available benchmarks or synthetically generated. We follow the ICLR Code of Ethics and
550 note that our work raises no foreseeable ethical concerns beyond those inherent to the general study
551 of machine learning with missing data.
552553 REPRODUCIBILITY STATEMENT
554555 We have made every effort to ensure reproducibility. Details of the experimental setup are pro-
556 vided in Section 5, with dataset descriptions in Appendix 3 and complete training configurations
557 in Appendix D. All proofs are included in Appendix A. Anonymous source code to reproduce our
558 experiments is provided in the supplementary material.
559560 REFERENCES
561562 Benjamin Agbo, Hussain Al-Aqrabi, Richard Hill, and Tariq Alsouqi. Missing data imputation in
563 the internet of things sensor networks. *Future Internet*, 14(5):143, 2022.564 Akiko Aizawa. An information-theoretic perspective of tf–idf measures. *Information Processing &*
565 *Management*, 39(1):45–65, 2003.566 Jongoh Baek and Adam B Birchfield. A tuning method for exciters and governors in realistic syn-
567 thetic grids with dynamics. In *2023 North American Power Symposium (NAPS)*, pp. 1–6. IEEE,
568 2023.569 Maya Bechler-Speicher, Ben Finkelshtein, Fabrizio Frasca, Luis Müller, Jan Tönshoff, Antoine Sir-
570 audin, Viktor Zaverkin, Michael M Bronstein, Mathias Niepert, Bryan Perozzi, et al. Position:
571 Graph learning will lose relevance due to poor benchmarks. *arXiv preprint arXiv:2502.14546*,
572 2025.573 Adam B Birchfield, Ti Xu, Kathleen M Gegner, Komal S Shetye, and Thomas J Overbye. Grid struc-
574 tural characteristics as validation criteria for synthetic networks. *IEEE Transactions on power*
575 *systems*, 32(4):3258–3265, 2016.576 Carlijn IR Braem, Utku S Yavuz, Hermie J Hermens, and Peter H Veltink. Missing data statistics
577 provide causal insights into data loss in diabetes health monitoring by wearable sensors. *Sensors*,
578 24(5):1526, 2024.579 Giulia Carreras, Guido Miccinesi, Andrew Wilcock, Nancy Preston, Daan Nieboer, Luc Deliens,
580 Mogensm Groenvold, Urska Lunder, Agnes van der Heide, Michela Baccini, et al. Missing not at
581 random in end of life care studies: multiple imputation and sensitivity analysis on data from the
582 action study. *BMC medical research methodology*, 21(1):13, 2021.583 Corinna Coupette, Jeremy Wayland, Emily Simons, and Bastian Rieck. No metric to rule them
584 all: Toward principled evaluations of graph-learning datasets. *arXiv preprint arXiv:2502.02379*,
585 2025.586 Yufeng Ding and Jeffrey S Simonoff. An investigation of missing data methods for classification
587 trees applied to binary response data. *Journal of Machine Learning Research*, 11(1), 2010.588 Federico Errica and Mathias Niepert. Tractable probabilistic graph representation learning with
589 graph-induced sum-product networks. In *The Twelfth International Conference on Learning Rep-
590 resentations*, 2024. URL <https://openreview.net/forum?id=h7nOCxFsPg>.

594 Rahmat Nur Faizin, Mardhani Riasetiawan, and Ahmad Ashari. A review of missing sensor data
 595 imputation methods. In *2019 5th International Conference on Science and Technology (ICST)*,
 596 volume 1, pp. 1–6. IEEE, 2019.

597

598 Amirata Ghorbani and James Y Zou. Embedding for informative missingness: Deep learning with
 599 incomplete data. In *2018 56th Annual Allerton Conference on Communication, Control, and
 600 Computing (Allerton)*, pp. 437–445. IEEE, 2018.

601 Dongliang Guo, Zhixuan Chu, and Sheng Li. Fair attribute completion on graph with missing
 602 attributes. *arXiv preprint arXiv:2302.12977*, 2023.

603

604 Audinga-Dea Hazewinkel, Jack Bowden, Kaitlin H Wade, Tom Palmer, Nicola J Wiles, and Kate
 605 Tilling. Sensitivity to missing not at random dropout in clinical trials: Use and interpretation of
 606 the trimmed means estimator. *Statistics in Medicine*, 41(8):1462–1481, 2022.

607

608 Xiangnan He, Lizi Liao, Hanwang Zhang, Liqiang Nie, Xia Hu, and Tat-Seng Chua. Neural col-
 609 laborative filtering. In *Proceedings of the 26th international conference on world wide web*, pp.
 173–182, 2017.

610

611 Niels Bruun Ipsen, Pierre-Alexandre Mattei, and Jes Frellsen. How to deal with missing data in
 612 supervised deep learning? In *10th International Conference on Learning Representations*, 2022.

613

614 Manfred Jaeger. The aim and em algorithms for learning from coarse data. *Journal of Machine
 Learning Research*, 23(62):1–55, 2022.

615

616 Juho Kopra, Tommi Härkänen, Hanna Tolonen, and Juha Karvanen. Correcting for non-ignorable
 617 missingness in smoking trends. *Stat*, 4(1):1–14, 2015.

618

619 Roderick JA Little and Donald B Rubin. *Statistical analysis with missing data*. John Wiley & Sons,
 2019.

620

621 Benjamin M Marlin and Richard S Zemel. Collaborative filtering and the missing at random as-
 622 sumption. In *Proceedings of the 23rd Conference on Uncertainty in Artificial Intelligence (UAI)*,
 623 pp. 267–275, 2009.

624

625 Benjamin M Marlin, Richard S Zemel, Sam T Roweis, and Malcolm Slaney. Recommender systems,
 626 missing data and statistical model estimation. In *IJCAI proceedings-international joint conference
 on artificial intelligence*, volume 22, pp. 2686, 2011.

627

628 Eugenij Moiseevich Mirkes, Timothy J Coats, Jeremy Levesley, and Alexander N Gorban. Handling
 629 missing data in large healthcare dataset: A case study of unknown trauma outcomes. *Computers
 in biology and medicine*, 75:203–216, 2016.

630

631 Karthika Mohan and Judea Pearl. Graphical models for processing missing data. *Journal of the
 632 American Statistical Association*, 116(534):1023–1037, 2021.

633

634 Nwamaka U Okafor and Declan T Delaney. Missing data imputation on iot sensor networks: Impli-
 635 cations for on-site sensor calibration. *IEEE Sensors journal*, 21(20):22833–22845, 2021.

636

637 Emanuele Rossi, Henry Kenlay, Maria I Gorinova, Benjamin Paul Chamberlain, Xiaowen Dong,
 638 and Michael M Bronstein. On the unreasonable effectiveness of feature propagation in learning
 on graphs with missing node features. In *Learning on graphs conference*, pp. 11–1. PMLR, 2022.

639

640 Donald B Rubin. Inference and missing data. *Biometrika*, 63(3):581–592, 1976.

641

642 Donald B Rubin. An overview of multiple imputation. In *Proceedings of the survey research
 methods section of the American statistical association*, volume 79, pp. 84, 1988.

643

644 Hibiki Taguchi, Xin Liu, and Tsuyoshi Murata. Graph convolutional networks for graphs containing
 645 missing features. *Future Generation Computer Systems*, 117:155–168, 2021.

646

647 Daeho Um, Jiwoong Park, Seulki Park, and Jin young Choi. Confidence-based feature imputation
 for graphs with partially known features. In *The Eleventh International Conference on Learning
 Representations*, 2023. URL <https://openreview.net/forum?id=YPKBIILy-Kt>.

648 Daeho Um, Sunoh Kim, Jiwoong Park, Jongin Lim, Seong Jin Ahn, and Seulki Park. Propagate
649 and inject: Revisiting propagation-based feature imputation for graphs with partially observed
650 features. In *Forty-second International Conference on Machine Learning*, 2025. URL <https://openreview.net/forum?id=QfKrcgyase>.

651

652 Mike Van Ness, Tomas M Bosschier, Roberto Halpin-Gregorio, and Madeleine Udell. The missing
653 indicator method: From low to high dimensions. In *Proceedings of the 29th ACM SIGKDD*
654 *Conference on Knowledge Discovery and Data Mining*, pp. 5004–5015, 2023.

655

656 Zhilin Yang, William W. Cohen, and Ruslan Salakhutdinov. Revisiting semi-supervised learning
657 with graph embeddings. *CoRR*, abs/1603.08861, 2016. URL <http://arxiv.org/abs/1603.08861>.

658

659 Jiaxuan You, Xiaobai Ma, Yi Ding, Mykel J Kochenderfer, and Jure Leskovec. Handling missing
660 data with graph representation learning. *Advances in Neural Information Processing Systems*, 33:
661 19075–19087, 2020.

662

663 Sukwon Yun, Xin Liu, Yunhak Oh, Junseok Lee, Tianlong Chen, Tsuyoshi Murata, and Chanyoung
664 Park. Oldie but goodie: Re-illuminating label propagation on graphs with partially observed
665 features, 2024. URL <https://openreview.net/forum?id=T1FDFKyEIQ>.

666

667 Yu Zheng, Xiuwen Yi, Ming Li, Ruiyuan Li, Zhangqing Shan, Eric Chang, and Tianrui Li. Fore-
668 casting fine-grained air quality based on big data. In *Proceedings of the 21th ACM SIGKDD*
669 *international conference on knowledge discovery and data mining*, pp. 2267–2276, 2015.

670

671 Qikui Zhu, Bo Du, and Pingkun Yan. Multi-hop convolutions on weighted graphs. *arXiv preprint*
arXiv:1911.04978, 2019.

672

673

674

675

676

677

678

679

680

681

682

683

684

685

686

687

688

689

690

691

692

693

694

695

696

697

698

699

700

701

A PROOFS

Theorem 1. If $P_{\theta, \gamma, \lambda}$ is feature-MAR and label-MAR, then (2) simplifies to

$$\int_{\mathbf{X}^{\text{miss}}} P_{\gamma}(\mathbf{Y}|\mathbf{X}) P_{\theta}(\mathbf{X}^{\text{miss}}|\mathbf{X}^{\text{obs}}). \quad (6)$$

Proof.

$$\begin{aligned} P_{\theta, \gamma, \lambda}(\mathbf{Y}|\mathbf{X}, \mathbf{M}) &= P_{\lambda}(\mathbf{M}|\mathbf{X}, \mathbf{Y}) \frac{P_{\gamma}(\mathbf{Y}|\mathbf{X})}{P_{\gamma, \lambda}(\mathbf{M}|\mathbf{X})} \stackrel{(4)}{=} P_{\gamma}(\mathbf{Y}|\mathbf{X}) \\ P_{\theta, \gamma, \lambda}(\mathbf{X}^{\text{miss}}|\mathbf{X}^{\text{obs}}, \mathbf{M}) &= P_{\gamma, \lambda}(\mathbf{M}|\mathbf{X}^{\text{obs}}, \mathbf{X}^{\text{miss}}) \frac{P_{\theta}(\mathbf{X}^{\text{miss}}|\mathbf{X}^{\text{obs}})}{P_{\theta, \gamma, \lambda}(\mathbf{M}|\mathbf{X}^{\text{obs}})} \stackrel{(3)}{=} P_{\theta}(\mathbf{X}^{\text{miss}}|\mathbf{X}^{\text{obs}}) \end{aligned}$$

□

Theorem 2. Let $\mathbf{X} \in \mathbb{R}^{n \times d}$ and $\mathbf{Y} \in \mathcal{Y}^n$ be random variables, $\mathbf{M} \in \{0, 1\}^{n \times d}$ be a missingness mask and \mathbf{X}^{obs} denotes the observed (incomplete) data. We encode the pair $(\mathbf{X}^{\text{obs}}, \mathbf{M})$ with the random variable $\tilde{\mathbf{X}}$ with

$$\tilde{X}_{ij} = \begin{cases} X_{ij}, & M_{ij} = 0, \\ ?, & M_{ij} = 1. \end{cases}$$

Let the change in the information be defined as $\Delta := I(\mathbf{Y}; \tilde{\mathbf{X}}) - I(\mathbf{Y}; \mathbf{X})$, where $I(\cdot; \cdot)$ denotes the mutual information. Then,

1. If the missingness is label-MAR, then $\Delta \leq 0$.
2. If $\mathbf{X} \in \{0, 1\}^{n \times d}$ and the missingness is U-MCAR with missingness probability μ , and $s(\mathbf{X})$ is the sample sparsity as in Definition 2, then

$$-nd\mu h_2(\mathbb{E}[s(\mathbf{X})]) \leq \Delta \leq 0,$$

where $h_2(u) = -u \log u - (1-u) \log(1-u)$.

Proof. By construction $\tilde{\mathbf{X}} = g(\mathbf{X}, \mathbf{M})$ for some measurable g . Thus $(\mathbf{Y}) \rightarrow (\mathbf{X}, \mathbf{M}) \rightarrow \tilde{\mathbf{X}}$ is a Markov chain, and the data-processing inequality implies

$$I(\mathbf{Y}; \tilde{\mathbf{X}}) \leq I(\mathbf{Y}; \mathbf{X}, \mathbf{M}). \quad (7)$$

Moreover, for any three random elements (A, B, C) we have the chain-rule identities

$$I(A; B, C) = I(A; C) + I(A; B | C). \quad (8)$$

(1) Label-MAR $\Delta \leq 0$. Assume label-MAR: $\mathbb{P}(\mathbf{M} | \mathbf{X}, \mathbf{Y}) = \mathbb{P}(\mathbf{M} | \mathbf{X})$, which is equivalent to $\mathbf{Y} \perp \mathbf{M} | \mathbf{X}$. Applying equation 8 with $(A, B, C) = (\mathbf{Y}, \mathbf{X}, \mathbf{M})$,

$$I(\mathbf{Y}; \mathbf{X}, \mathbf{M}) = I(\mathbf{Y}; \mathbf{X}) + I(\mathbf{Y}; \mathbf{M} | \mathbf{X}).$$

Under label-MAR, $I(\mathbf{Y}; \mathbf{M} | \mathbf{X}) = 0$, hence

$$I(\mathbf{Y}; \mathbf{X}, \mathbf{M}) = I(\mathbf{Y}; \mathbf{X}). \quad (9)$$

Combining equation 7 and equation 9 yields

$$I(\mathbf{Y}; \tilde{\mathbf{X}}) \leq I(\mathbf{Y}; \mathbf{X}) \iff \Delta = I(\mathbf{Y}; \tilde{\mathbf{X}}) - I(\mathbf{Y}; \mathbf{X}) \leq 0.$$

(2) Two-sided bound under uniform MCAR and α - β sparsity. Assume uniform MCAR: $M_{ij} \sim \text{Bernoulli}(1 - \mu)$ independently of (\mathbf{X}, \mathbf{Y}) and i.i.d. across (i, j) , and that $\mathbb{P}(s(\mathbf{X}) \geq \alpha) \geq \beta$, where $s(\mathbf{X}) = \frac{1}{nd} \sum_{i,j} \mathbb{I}\{X_{ij} = 0\}$.

Upper side. MCAR implies label-MAR, so by part (1): $\Delta \leq 0$.

756 *Lower side.* We start from the chain-rule identity applied to $(A, B, C) = (\mathbf{Y}, \mathbf{X}, \tilde{\mathbf{X}})$:

$$757 \quad I(\mathbf{Y}; \mathbf{X}, \tilde{\mathbf{X}}) = I(\mathbf{Y}; \tilde{\mathbf{X}}) + I(\mathbf{Y}; \mathbf{X} \mid \tilde{\mathbf{X}}) = I(\mathbf{Y}; \mathbf{X}) + I(\mathbf{Y}; \tilde{\mathbf{X}} \mid \mathbf{X}).$$

759 Rearranging gives

$$760 \quad -\Delta = I(\mathbf{Y}; \mathbf{X}) - I(\mathbf{Y}; \tilde{\mathbf{X}}) = I(\mathbf{Y}; \mathbf{X} \mid \tilde{\mathbf{X}}) - I(\mathbf{Y}; \tilde{\mathbf{X}} \mid \mathbf{X}). \quad (10)$$

762 The second term on the right is nonnegative, hence

$$763 \quad -\Delta \leq I(\mathbf{Y}; \mathbf{X} \mid \tilde{\mathbf{X}}). \quad (11)$$

764 Using the bound $I(U; V \mid W) \leq H(V \mid W)$, we get

$$765 \quad -\Delta \leq H(\mathbf{X} \mid \tilde{\mathbf{X}}). \quad (12)$$

767 Index the matrix entries by a total order \prec on pairs (i, j) and apply the chain rule:

$$769 \quad H(\mathbf{X} \mid \tilde{\mathbf{X}}) = \sum_{(i,j)} H(X_{ij} \mid \tilde{\mathbf{X}}, \{X_{kl} : (k, l) \prec (i, j)\}).$$

771 Since conditioning reduces entropy,

$$772 \quad H(\mathbf{X} \mid \tilde{\mathbf{X}}) \leq \sum_{i,j} H(X_{ij} \mid \tilde{X}_{ij}). \quad (13)$$

775 Fix (i, j) and denote $\pi_{ij} = \Pr[X_{ij} = 1]$. Under uniform MCAR,

$$777 \quad \Pr[\tilde{X}_{ij} = ?] = \mu, \quad \Pr[\tilde{X}_{ij} = x] = (1 - \mu) \Pr[X_{ij} = x], \quad x \in \{0, 1\}.$$

778 Hence: (i) if $\tilde{X}_{ij} \in \{0, 1\}$ then X_{ij} is revealed, so $H(X_{ij} \mid \tilde{X}_{ij} \in \{0, 1\}) = 0$; (ii) if $\tilde{X}_{ij} = ?$, then
779 $\Pr[X_{ij} = 1 \mid \tilde{X}_{ij} = ?] = \pi_{ij}$ and $H(X_{ij} \mid \tilde{X}_{ij} = ?) = h_2(\pi_{ij})$. Averaging over \tilde{X}_{ij} gives

$$781 \quad H(X_{ij} \mid \tilde{X}_{ij}) = \mu h_2(\pi_{ij}). \quad (14)$$

782 Combining equation 13 and equation 14:

$$784 \quad H(\mathbf{X} \mid \tilde{\mathbf{X}}) \leq \sum_{i,j} \mu h_2(\pi_{ij}) = nd \mu \cdot \frac{1}{nd} \sum_{i,j} h_2(\pi_{ij}) \leq nd \mu \cdot h_2\left(\frac{1}{nd} \sum_{i,j} \pi_{ij}\right),$$

787 since h_2 is concave. Note that

$$789 \quad \frac{1}{nd} \sum_{i,j} \pi_{ij} = \frac{1}{nd} \sum_{i,j} \Pr[X_{ij} = 1] = \mathbb{E}\left[\frac{1}{nd} \sum_{i,j} \mathbb{I}\{X_{ij} = 1\}\right] = 1 - \mathbb{E}[s(\mathbf{X})].$$

792 Using the symmetry $h_2(u) = h_2(1 - u)$, we conclude

$$793 \quad H(\mathbf{X} \mid \tilde{\mathbf{X}}) \leq nd \mu \cdot h_2(\mathbb{E}[s(\mathbf{X})]).$$

794 Combining with $-\Delta \leq H(\mathbf{X} \mid \tilde{\mathbf{X}})$ gives

$$796 \quad -nd \mu h_2(\mathbb{E}[s(\mathbf{X})]) \leq \Delta \leq 0.$$

797 This concludes the proof. \square

799 B ADDITIONAL RESULTS ON BENCHMARKS AND PROPOSED DATASETS

801 This section presents the full plots of the results under the R1 regime introduced in Section 4.

803 Figure 4 shows the complete set of results across all datasets, whose statistics are summarized in
804 Table 3. The top three rows correspond to the classic benchmarks (CORA, CITESEER, PUBMED).
805 Consistently with Proposition 2, models maintain nearly constant F1 scores up to extremely high
806 missingness levels ($\sim 90\%$), confirming that these benchmarks are of limited value for evaluating
807 robustness to missing features.

808 The bottom four rows correspond to our proposed datasets (SYNTHETIC, AIR, ELECTRIC, TAD-
809 POLE). In these cases, performance degrades much earlier and more severely, highlighting the higher
realism and difficulty of our benchmarks.

810
 811 Table 3: Dataset statistics and feature sparsity. Classic benchmarks (CORA, CITESEER, PUBMED)
 812 exhibit extremely sparse bag-of-words features, while our proposed datasets (SYNTHETIC, AIR,
 813 ELECTRIC, TADPOLE) provide less sparse representations.

814 Dataset	815 #Nodes	816 #Features	817 Sparsity ↓	818 Type of features
CORA	2708	1433	0.9873	BoW (binary)
CITESEER	3327	3703	0.9915	BoW (binary)
PUBMED	19717	500	0.8998	BoW (binary)
SYNTHETIC	1000	5	0.0000	Gaussian
AIR	430	7	0.1615	Raw
ELECTRIC	2000	5	0.2000	Raw
TADPOLE	555	15	0.0000	Raw

823 C MORE CHALLENGING DATASETS

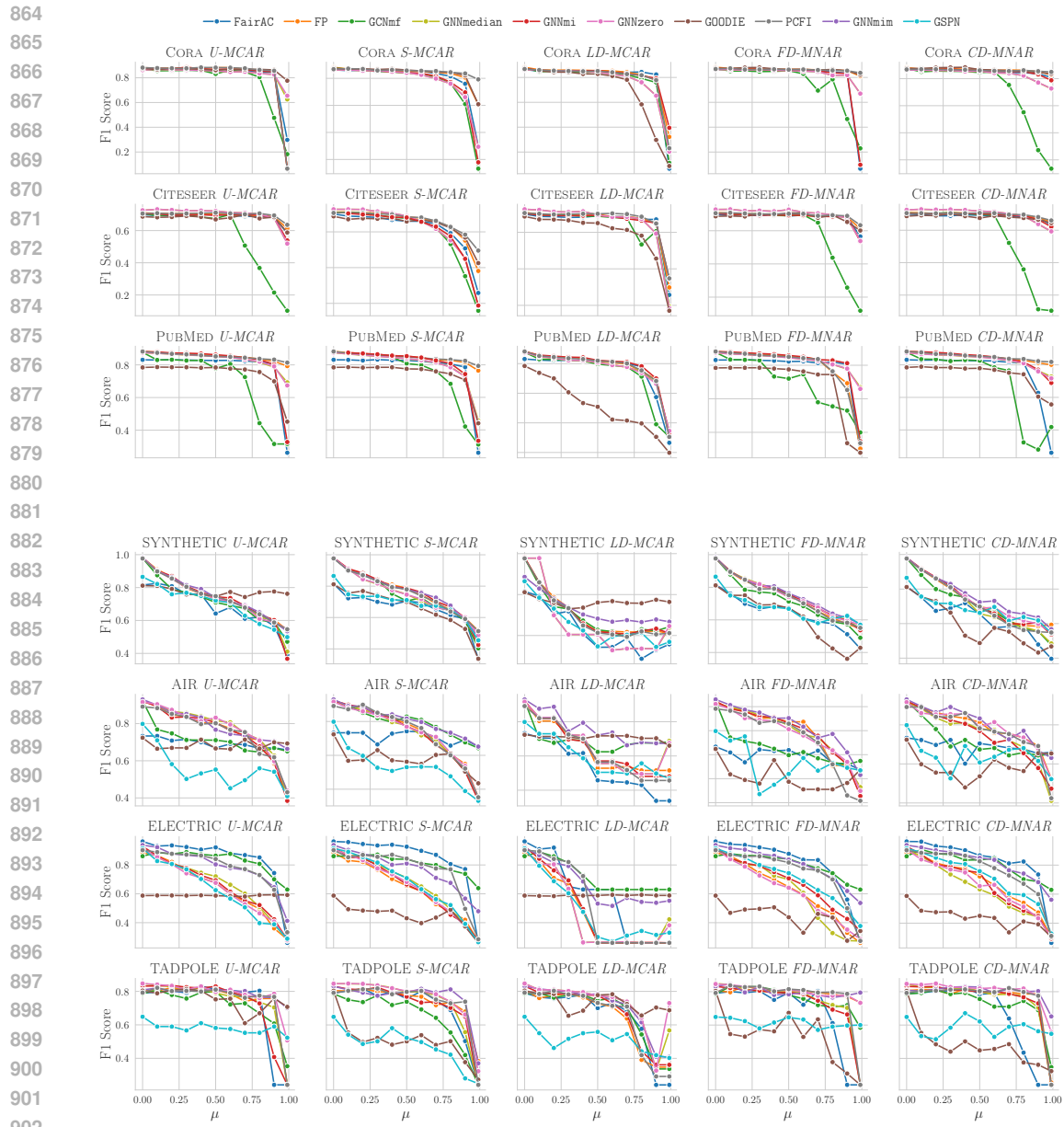
825 In Section 3, we introduced the synthetic and real-world datasets employed in our experiments. We
 826 now provide additional details on their construction and characteristics.

828 **SYNTHETIC** Synthetic dataset based on a Barabási–Albert graph topology. Each node is associated
 829 with five real-valued features sampled from a Gaussian distribution. Node labels are generated
 830 deterministically by applying a fixed two-layer GCN with hard-coded weights to the complete feature
 831 matrix. This construction ensures that the ground-truth labeling function is fully expressible
 832 by a GNN, allowing models to achieve near-perfect accuracy in the absence of missingness. The
 833 resulting task is a binary node classification problem, with classes separated according to structured
 834 feature combinations defined by the fixed GCN. This controlled setup provides a principled
 835 testbed to isolate and analyze the effects of different missingness mechanisms, while preserving a
 836 well-defined ground truth.

837 **AIR** Dataset (Zheng et al., 2015) built from a network of air quality monitoring stations de-
 838 ployed in an urban area. Each node corresponds to a station and is associated with a set of en-
 839 vironmental measurements. The node features include both air pollutant concentrations (CO, NO₂,
 840 PM₁₀, O₃, SO₂) and meteorological variables (temperature, humidity, wind speed, wind
 841 direction). Edges are constructed based on the geographical distance between stations, with
 842 two nodes connected if their distance is below a given threshold. The target variable is derived from
 843 the PM_{2.5} concentration, which is discretized into three balanced categories (low, medium, high)
 844 according to the distribution of observed values. This formulation allows us to frame the problem as
 845 a semi-supervised node classification task with three classes.

846 **ELECTRIC** Dataset (Birchfield et al., 2016; Baek & Birchfield, 2023) derived from a large-scale
 847 model of the Texas power grid. Nodes correspond to buses in the electrical network, each enriched
 848 with both structural and operational attributes. The node features include identifiers (area, zone),
 849 electrical measurements (voltage magnitude, voltage angle), and a topological prop-
 850 erty (betweenness centrality). Edges are constructed directly from the transmission lines
 851 specified in the raw grid data, connecting pairs of buses. The classification target is the nominal
 852 voltage level of each bus (base kV), which we discretize into three categories: low voltage (<100
 853 kV), medium voltage (100–200 kV), and high voltage (>200 kV). This setup results in a three-class
 854 node classification problem reflecting operational conditions across the grid.

856 **TADPOLE** The TADPOLE dataset (Zhu et al., 2019) originates from the TADPOLE challenge,
 857 which provides longitudinal clinical and imaging data for patients at risk of developing Alzheimer’s
 858 disease. In our graph formulation, each node corresponds to a patient and is associated with a set
 859 of features encompassing clinical scores, cerebrospinal fluid (CSF) biomarkers, and neuroimaging
 860 measures such as MRI- and PET-derived variables. Since the original dataset does not provide graph
 861 connectivity, we construct edges using a k -nearest neighbors approach over the most informative
 862 biomarkers, so that patients with similar profiles are connected. The target variable is the diagnostic
 863 label, categorized into three classes (cognitively normal, mild cognitive impairment, Alzheimer’s
 864 disease). This results in a semi-supervised node classification problem where the goal is to pre-



903 Figure 4: F1 score as a function of feature missingness (μ) for both classic benchmarks (top three
904 rows) and our proposed datasets (bottom four rows), under the mechanisms described in Section 4.
905 Classic benchmarks show almost no degradation until extremely high μ , while the proposed datasets
906 reveal model weaknesses at more realistic missingness levels. Tables for numeric results are in App.
907 F

908
909
910
911 dict the diagnostic status of patients based on multimodal biomedical features and patient similarity
912 structure.

913 Table 3 reports, for each dataset, the number of nodes, number of features, feature sparsity, and the
914 type of features. While the number of nodes and features may seem small compared to standard
915 benchmark graph datasets, we emphasize that using real features (as in AIR, ELECTRIC, and TAD-
916 POLE) is more realistic in the context of feature missingness. In fact, it is not meaningful to study
917 missingness on pre-computed embeddings, since embeddings are typically high-dimensional repre-
918 sentations mapped to wide feature spaces and are not expected to exhibit missingness in practice.

918 **D EXPERIMENTAL DETAILS**
919

920 All baseline and competitor methods are implemented using the official code released in their re-
921 spective repositories, following the recommended training protocols and hyperparameter settings.
922 For GNNmi and GNNmim, we adopt a standard GNN architecture where the convolutional layer type
923 (Table 4), the number of layers (1-3), the learning rate (10^{-4} - 10^{-2}), and the weight decay (10^{-5} -
924 10^{-3}) are tuned via grid search on the validation set. All models are trained on the same data splits
925 with early stopping to ensure a fair comparison.

926 Table 4: Best GNN encoder selected within GNNmim for each dataset and missingness mechanism.
927

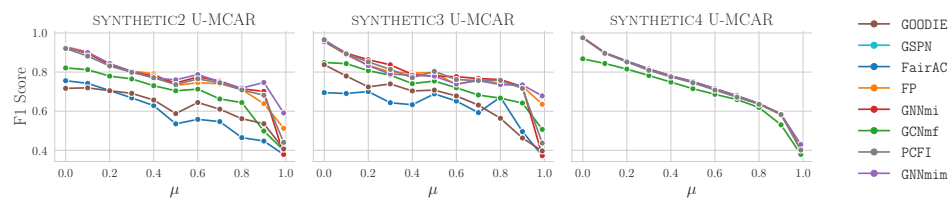
929 Dataset	<i>U-MCAR</i>	<i>S-MCAR</i>	<i>LD-MCAR</i>	<i>FD-MNAR</i>	<i>CD-MNAR</i>
930 SYNTHETIC	GCN	GCN	GraphSAGE	GCN	GCN
931 AIR	GraphSAGE	GraphSAGE	GraphSAGE	GraphSAGE	GraphSAGE
932 ELECTRIC	GIN	GIN	GraphSAGE	GIN	GIN
933 TADPOLE	GCN	GraphSAGE	GraphSAGE	GraphSAGE	GCN

935 **E SCALING THE SYNTHETIC DATASET**
937

938 In this section, we analyze what happens when either the number of features or the number of nodes
939 in the synthetic dataset is increased. To this end, we constructed three additional synthetic datasets
940 (SYNTHETIC2, SYNTHETIC3, SYNTHETIC4) following the same design principles as SYNTHETIC.
941 Table 5 reports their statistics.

942 As shown in Figure 5, the behavior of the models in this larger-scale setting is consistent with the one
943 observed in our original setup. In this case, we experimented with the *uniform random missingness*
944 mechanism, and we observe a monotonic decrease in performance for all models as the missingness
945 rate μ increases. This confirms that dataset size does not affect the overall trend of performance
946 degradation under feature missingness.

947 To further support this point, we also report the runtime and GPU memory consumption of all models
948 on both the main synthetic dataset (SYNTHETIC) and its larger-scale counterpart (SYNTHETIC3),
949 which features an increased number of features. As shown in Table 6, the runtime and memory
950 requirements remain substantially stable across datasets, with negligible variations between models.
951 This behavior confirms that our approach scales efficiently with the dataset size, as it only involves a
952 standard GNN architecture augmented with a simple MIM mask concatenated to the input features,
953 introducing minimal computational overhead.



954
955 Figure 5: F1 score as a function of feature missingness (μ) for additional synthetic datasets generated
956 with the same procedure as SYNTHETIC, but with either an increased number of nodes or features.
957 For SYNTHETIC4, the model is not reported since training exceeded the 12-hour time limit, while
958 GOODIE is excluded due to out-of-memory errors.
959

960 **F COMPLETE RESULT TABLES – R1 REGIME**
961

972

973

974

Table 5: Datasets information.

Dataset	#Nodes	#Features	Sparsity ↓	Type of features
SYNTHETIC	1000	5	0.0000	Gaussian
SYNTHETIC2	1000	20	0.0000	Gaussian
SYNTHETIC3	1000	50	0.0000	Gaussian
SYNTHETIC4	50000	5	0.0000	Gaussian

980

981

Table 6: Runtime and GPU peak memory consumption for the main synthetic dataset (SYNTHETIC) and the scaled version (SYNTHETIC3). Each value corresponds to the average across all missingness levels under the UMCAR mechanism.

Model	SYNTHETIC		SYNTHETIC4	
	Runtime [s] ↓	GPU Mem [GB] ↓	Runtime [s] ↓	GPU Mem [GB] ↓
GNNmi	1.7	0.03	5.3	0.78
GNNzero	1.6	0.03	5.0	0.77
GNNmedian	1.6	0.03	5.0	0.77
GNNmim	1.8	0.03	6.3	0.77
GCNmf	4.5	0.02	28.0	0.53
FP	1.5	0.02	5.3	0.77
PCFI	1.8	0.02	5.2	0.77
FairAC	3.9	0.04	—	—
GSPN	55.0	0.03	150.0	0.84
GOODIE	2.3	0.06	—	—

997

998

999

Table 7: F1 scores for CORA under mechanism *U-MCAR* and varying μ (GSPN is not reported as it is not designed for categorical features).

μ	GOODIE	FairAC	FP	GNNmi	GCNmf	PCFI	GNNzero	GNNmedian
0.00	0.875 (± 0.00)	0.863 (± 0.01)	0.882 (± 0.00)	0.873 (± 0.00)	0.875 (± 0.00)	0.882 (± 0.00)	0.862 (± 0.02)	0.862 (± 0.02)
0.10	0.867 (± 0.00)	0.866 (± 0.00)	0.877 (± 0.00)	0.876 (± 0.00)	0.856 (± 0.00)	0.878 (± 0.00)	0.868 (± 0.01)	0.868 (± 0.01)
0.20	0.875 (± 0.00)	0.862 (± 0.00)	0.878 (± 0.00)	0.873 (± 0.00)	0.858 (± 0.00)	0.877 (± 0.00)	0.864 (± 0.02)	0.864 (± 0.02)
0.30	0.873 (± 0.00)	0.865 (± 0.00)	0.881 (± 0.00)	0.885 (± 0.00)	0.860 (± 0.00)	0.876 (± 0.00)	0.863 (± 0.01)	0.863 (± 0.01)
0.40	0.869 (± 0.00)	0.857 (± 0.00)	0.878 (± 0.00)	0.873 (± 0.00)	0.860 (± 0.00)	0.884 (± 0.00)	0.860 (± 0.02)	0.860 (± 0.02)
0.50	0.861 (± 0.00)	0.856 (± 0.00)	0.882 (± 0.00)	0.867 (± 0.00)	0.831 (± 0.00)	0.882 (± 0.00)	0.856 (± 0.01)	0.856 (± 0.01)
0.60	0.866 (± 0.00)	0.847 (± 0.00)	0.882 (± 0.00)	0.871 (± 0.00)	0.862 (± 0.00)	0.881 (± 0.00)	0.847 (± 0.01)	0.847 (± 0.01)
0.70	0.866 (± 0.00)	0.858 (± 0.00)	0.869 (± 0.00)	0.865 (± 0.00)	0.847 (± 0.00)	0.877 (± 0.00)	0.849 (± 0.01)	0.849 (± 0.01)
0.80	0.868 (± 0.00)	0.843 (± 0.00)	0.864 (± 0.00)	0.854 (± 0.00)	0.805 (± 0.00)	0.863 (± 0.00)	0.835 (± 0.01)	0.835 (± 0.01)
0.90	0.864 (± 0.00)	0.845 (± 0.00)	0.860 (± 0.00)	0.848 (± 0.00)	0.476 (± 0.00)	0.856 (± 0.00)	0.826 (± 0.00)	0.826 (± 0.00)
0.99	0.776 (± 0.00)	0.298 (± 0.00)	0.066 (± 0.00)	0.066 (± 0.00)	0.183 (± 0.00)	0.065 (± 0.00)	0.655 (± 0.03)	0.625 (± 0.02)

1012

1013

Table 8: F1 scores for CORA under mechanism *S-MCAR* and varying μ (GSPN is not reported as it is not designed for categorical features).

μ	GOODIE	FairAC	FP	GNNmi	GCNmf	PCFI	GNNzero	GNNmedian
0.00	0.875 (± 0.00)	0.863 (± 0.01)	0.882 (± 0.00)	0.872 (± 0.00)	0.875 (± 0.00)	0.868 (± 0.00)	0.862 (± 0.02)	0.862 (± 0.02)
0.10	0.868 (± 0.00)	0.857 (± 0.00)	0.869 (± 0.00)	0.862 (± 0.00)	0.869 (± 0.00)	0.872 (± 0.00)	0.862 (± 0.02)	0.862 (± 0.02)
0.20	0.872 (± 0.00)	0.860 (± 0.00)	0.863 (± 0.00)	0.863 (± 0.00)	0.858 (± 0.00)	0.869 (± 0.00)	0.856 (± 0.02)	0.856 (± 0.02)
0.30	0.865 (± 0.00)	0.850 (± 0.00)	0.854 (± 0.00)	0.855 (± 0.00)	0.852 (± 0.00)	0.858 (± 0.00)	0.857 (± 0.02)	0.857 (± 0.02)
0.40	0.870 (± 0.00)	0.857 (± 0.00)	0.859 (± 0.00)	0.848 (± 0.00)	0.848 (± 0.00)	0.862 (± 0.00)	0.849 (± 0.02)	0.849 (± 0.02)
0.50	0.862 (± 0.00)	0.854 (± 0.00)	0.854 (± 0.00)	0.844 (± 0.00)	0.839 (± 0.00)	0.858 (± 0.00)	0.841 (± 0.01)	0.841 (± 0.01)
0.60	0.855 (± 0.00)	0.854 (± 0.00)	0.853 (± 0.00)	0.837 (± 0.00)	0.837 (± 0.00)	0.856 (± 0.00)	0.826 (± 0.01)	0.826 (± 0.01)
0.70	0.847 (± 0.00)	0.836 (± 0.00)	0.845 (± 0.00)	0.817 (± 0.00)	0.807 (± 0.00)	0.854 (± 0.00)	0.798 (± 0.02)	0.798 (± 0.02)
0.80	0.845 (± 0.00)	0.815 (± 0.00)	0.836 (± 0.00)	0.772 (± 0.00)	0.764 (± 0.00)	0.845 (± 0.00)	0.760 (± 0.02)	0.760 (± 0.02)
0.90	0.822 (± 0.00)	0.760 (± 0.00)	0.806 (± 0.00)	0.696 (± 0.00)	0.610 (± 0.00)	0.836 (± 0.00)	0.661 (± 0.02)	0.661 (± 0.02)
0.99	0.609 (± 0.00)	0.300 (± 0.00)	0.606 (± 0.00)	0.179 (± 0.00)	0.132 (± 0.00)	0.792 (± 0.00)	0.294 (± 0.05)	0.294 (± 0.05)

1025

1026

1027 Table 9: F1 scores for CORA under mechanism *CD-MCAR* and varying μ (GSPNis not reported as
1028 it is not designed for categorical features).

1029

μ	GOODIE	FairAC	FP	GNNmi	GCNmf	PCFI	GNNzero	GNNmedian
0.00	0.875 (± 0.00)	0.863 (± 0.01)	0.882 (± 0.00)	0.873 (± 0.00)	0.875 (± 0.00)	0.868 (± 0.00)	0.862 (± 0.02)	0.862 (± 0.02)
0.10	0.852 (± 0.00)	0.851 (± 0.00)	0.862 (± 0.00)	0.857 (± 0.00)	0.846 (± 0.00)	0.860 (± 0.00)	0.858 (± 0.02)	0.858 (± 0.02)
0.20	0.843 (± 0.00)	0.854 (± 0.00)	0.859 (± 0.00)	0.854 (± 0.00)	0.850 (± 0.00)	0.855 (± 0.00)	0.854 (± 0.02)	0.854 (± 0.02)
0.30	0.843 (± 0.00)	0.856 (± 0.00)	0.859 (± 0.00)	0.855 (± 0.00)	0.846 (± 0.00)	0.852 (± 0.00)	0.853 (± 0.02)	0.853 (± 0.02)
0.40	0.828 (± 0.00)	0.854 (± 0.00)	0.858 (± 0.00)	0.853 (± 0.00)	0.838 (± 0.00)	0.849 (± 0.00)	0.849 (± 0.02)	0.849 (± 0.02)
0.50	0.828 (± 0.00)	0.854 (± 0.00)	0.855 (± 0.00)	0.855 (± 0.00)	0.848 (± 0.00)	0.852 (± 0.00)	0.844 (± 0.02)	0.844 (± 0.02)
0.60	0.812 (± 0.00)	0.847 (± 0.00)	0.853 (± 0.00)	0.844 (± 0.00)	0.837 (± 0.00)	0.841 (± 0.00)	0.825 (± 0.02)	0.825 (± 0.02)
0.70	0.782 (± 0.00)	0.841 (± 0.00)	0.842 (± 0.00)	0.831 (± 0.00)	0.822 (± 0.00)	0.827 (± 0.00)	0.810 (± 0.02)	0.810 (± 0.02)
0.80	0.584 (± 0.00)	0.844 (± 0.00)	0.822 (± 0.00)	0.815 (± 0.00)	0.792 (± 0.00)	0.818 (± 0.00)	0.761 (± 0.01)	0.761 (± 0.01)
0.90	0.297 (± 0.00)	0.824 (± 0.00)	0.777 (± 0.00)	0.793 (± 0.00)	0.760 (± 0.00)	0.778 (± 0.00)	0.653 (± 0.02)	0.654 (± 0.02)
0.99	0.088 (± 0.00)	0.066 (± 0.00)	0.322 (± 0.00)	0.395 (± 0.00)	0.113 (± 0.00)	0.231 (± 0.00)	0.204 (± 0.03)	0.204 (± 0.03)

1038

1039

1040

1041 Table 10: F1 scores for CORA under mechanism *FD-MNAR* and varying μ (GSPNis not reported as
1042 it is not designed for categorical features).

1043

μ	GOODIE	FairAC	FP	GNNmi	GCNmf	PCFI	GNNzero	GNNmedian
0.00	0.875 (± 0.00)	0.863 (± 0.01)	0.882 (± 0.00)	0.873 (± 0.00)	0.875 (± 0.00)	0.868 (± 0.00)	0.864 (± 0.02)	0.864 (± 0.02)
0.10	0.872 (± 0.01)	0.862 (± 0.01)	0.873 (± 0.01)	0.868 (± 0.01)	0.851 (± 0.01)	0.873 (± 0.00)	0.862 (± 0.02)	0.862 (± 0.02)
0.20	0.879 (± 0.00)	0.870 (± 0.01)	0.874 (± 0.00)	0.865 (± 0.01)	0.853 (± 0.01)	0.863 (± 0.01)	0.858 (± 0.01)	0.858 (± 0.01)
0.30	0.880 (± 0.00)	0.864 (± 0.01)	0.869 (± 0.00)	0.867 (± 0.01)	0.847 (± 0.01)	0.864 (± 0.01)	0.864 (± 0.01)	0.864 (± 0.01)
0.40	0.869 (± 0.01)	0.855 (± 0.01)	0.864 (± 0.01)	0.856 (± 0.01)	0.849 (± 0.00)	0.866 (± 0.01)	0.858 (± 0.02)	0.858 (± 0.02)
0.50	0.865 (± 0.01)	0.860 (± 0.01)	0.866 (± 0.01)	0.859 (± 0.01)	0.854 (± 0.01)	0.863 (± 0.01)	0.854 (± 0.02)	0.854 (± 0.02)
0.60	0.866 (± 0.01)	0.853 (± 0.01)	0.865 (± 0.01)	0.863 (± 0.01)	0.829 (± 0.02)	0.864 (± 0.01)	0.851 (± 0.01)	0.851 (± 0.01)
0.70	0.859 (± 0.01)	0.847 (± 0.00)	0.862 (± 0.01)	0.853 (± 0.00)	0.695 (± 0.14)	0.860 (± 0.00)	0.846 (± 0.01)	0.846 (± 0.01)
0.80	0.865 (± 0.01)	0.845 (± 0.01)	0.861 (± 0.01)	0.837 (± 0.00)	0.785 (± 0.05)	0.857 (± 0.01)	0.817 (± 0.02)	0.817 (± 0.02)
0.90	0.854 (± 0.01)	0.833 (± 0.01)	0.855 (± 0.00)	0.833 (± 0.00)	0.465 (± 0.21)	0.854 (± 0.01)	0.819 (± 0.01)	0.819 (± 0.01)
0.99	0.822 (± 0.01)	0.066 (± 0.00)	0.810 (± 0.02)	0.098 (± 0.01)	0.230 (± 0.05)	0.837 (± 0.02)	0.670 (± 0.02)	0.670 (± 0.02)

1052

1053

1054

1055 Table 11: F1 scores for CORA under mechanism *CD-MNAR* and varying μ (GSPNis not reported as
1056 it is not designed for categorical features).

1057

μ	GOODIE	FairAC	FP	GNNmi	GCNmf	PCFI	GNNzero	GNNmedian
0.00	0.875 (± 0.00)	0.863 (± 0.01)	0.882 (± 0.00)	0.873 (± 0.00)	0.875 (± 0.00)	0.868 (± 0.00)	0.863 (± 0.02)	0.863 (± 0.02)
0.10	0.875 (± 0.00)	0.864 (± 0.01)	0.870 (± 0.01)	0.862 (± 0.01)	0.850 (± 0.00)	0.869 (± 0.01)	0.863 (± 0.02)	0.863 (± 0.02)
0.20	0.881 (± 0.01)	0.865 (± 0.00)	0.874 (± 0.01)	0.868 (± 0.01)	0.856 (± 0.01)	0.869 (± 0.01)	0.860 (± 0.02)	0.860 (± 0.02)
0.30	0.882 (± 0.00)	0.858 (± 0.00)	0.873 (± 0.00)	0.871 (± 0.01)	0.854 (± 0.00)	0.866 (± 0.01)	0.860 (± 0.02)	0.860 (± 0.02)
0.40	0.884 (± 0.01)	0.862 (± 0.01)	0.870 (± 0.00)	0.864 (± 0.00)	0.853 (± 0.01)	0.865 (± 0.01)	0.853 (± 0.02)	0.853 (± 0.02)
0.50	0.867 (± 0.01)	0.852 (± 0.01)	0.867 (± 0.00)	0.861 (± 0.00)	0.844 (± 0.02)	0.861 (± 0.01)	0.855 (± 0.02)	0.855 (± 0.02)
0.60	0.864 (± 0.00)	0.847 (± 0.00)	0.860 (± 0.01)	0.856 (± 0.01)	0.849 (± 0.00)	0.857 (± 0.00)	0.842 (± 0.02)	0.842 (± 0.02)
0.70	0.860 (± 0.01)	0.845 (± 0.01)	0.864 (± 0.01)	0.852 (± 0.01)	0.753 (± 0.12)	0.856 (± 0.01)	0.840 (± 0.02)	0.840 (± 0.02)
0.80	0.853 (± 0.01)	0.844 (± 0.02)	0.862 (± 0.01)	0.852 (± 0.01)	0.551 (± 0.10)	0.861 (± 0.01)	0.822 (± 0.03)	0.822 (± 0.03)
0.90	0.848 (± 0.01)	0.835 (± 0.01)	0.852 (± 0.00)	0.831 (± 0.01)	0.271 (± 0.23)	0.855 (± 0.01)	0.771 (± 0.03)	0.771 (± 0.03)
0.99	0.836 (± 0.01)	0.810 (± 0.01)	0.828 (± 0.01)	0.788 (± 0.02)	0.135 (± 0.05)	0.849 (± 0.01)	0.727 (± 0.04)	0.725 (± 0.03)

1066

1067

1068

1069 Table 12: F1 scores for CITESEER under mechanism *U-MCAR* and varying μ (GSPNis not reported as
1070 it is not designed for categorical features).

1071

μ	GOODIE	FairAC	FP	GNNmi	GCNmf	PCFI	GNNzero	GNNmedian
0.00	0.687 (± 0.00)	0.700 (± 0.00)	0.710 (± 0.02)	0.704 (± 0.02)	0.707 (± 0.00)	0.706 (± 0.02)	0.726 (± 0.02)	0.726 (± 0.02)
0.10	0.682 (± 0.00)	0.693 (± 0.00)	0.707 (± 0.00)	0.705 (± 0.00)	0.692 (± 0.00)	0.708 (± 0.00)	0.732 (± 0.02)	0.732 (± 0.02)
0.20	0.684 (± 0.00)	0.693 (± 0.00)	0.706 (± 0.00)	0.695 (± 0.00)	0.698 (± 0.00)	0.705 (± 0.00)	0.728 (± 0.02)	0.728 (± 0.02)
0.30	0.691 (± 0.00)	0.691 (± 0.00)	0.705 (± 0.00)	0.696 (± 0.00)	0.697 (± 0.00)	0.706 (± 0.00)	0.723 (± 0.03)	0.723 (± 0.03)
0.40	0.685 (± 0.00)	0.700 (± 0.00)	0.706 (± 0.00)	0.698 (± 0.00)	0.684 (± 0.00)	0.708 (± 0.00)	0.724 (± 0.02)	0.724 (± 0.02)
0.50	0.669 (± 0.00)	0.697 (± 0.00)	0.702 (± 0.00)	0.695 (± 0.00)	0.675 (± 0.00)	0.711 (± 0.00)	0.722 (± 0.02)	0.722 (± 0.02)
0.60	0.680 (± 0.00)	0.695 (± 0.00)	0.697 (± 0.00)	0.699 (± 0.00)	0.700 (± 0.00)	0.707 (± 0.00)	0.712 (± 0.02)	0.712 (± 0.02)
0.70	0.699 (± 0.00)	0.688 (± 0.00)	0.694 (± 0.00)	0.700 (± 0.00)	0.507 (± 0.00)	0.701 (± 0.00)	0.710 (± 0.02)	0.710 (± 0.02)
0.80	0.675 (± 0.00)	0.687 (± 0.00)	0.694 (± 0.00)	0.696 (± 0.00)	0.368 (± 0.00)	0.707 (± 0.00)	0.701 (± 0.01)	0.701 (± 0.01)
0.90	0.684 (± 0.00)	0.680 (± 0.00)	0.686 (± 0.00)	0.680 (± 0.00)	0.215 (± 0.00)	0.694 (± 0.00)	0.678 (± 0.02)	0.678 (± 0.02)
0.99	0.588 (± 0.00)	0.584 (± 0.00)	0.613 (± 0.00)	0.539 (± 0.00)	0.102 (± 0.00)	0.636 (± 0.00)	0.519 (± 0.03)	0.519 (± 0.03)

1080

1081 Table 13: F1 scores for CITESEER under mechanism *S-MCAR* and varying μ (GSPNis not reported
1082 as it is not designed for categorical features).

1083

μ	GOODIE	FairAC	FP	GNNmi	GCNmf	PCFI	GNNzero	GNNmedian
0.00	0.687 (± 0.00)	0.700 (± 0.00)	0.710 (± 0.02)	-	0.707 (± 0.00)	0.706 (± 0.02)	0.726 (± 0.02)	0.726 (± 0.02)
0.10	0.670 (± 0.00)	0.688 (± 0.00)	0.711 (± 0.00)	0.703 (± 0.00)	0.708 (± 0.00)	0.708 (± 0.00)	0.726 (± 0.03)	0.726 (± 0.03)
0.20	0.675 (± 0.00)	0.685 (± 0.00)	0.707 (± 0.00)	0.697 (± 0.00)	0.707 (± 0.00)	0.706 (± 0.00)	0.725 (± 0.03)	0.725 (± 0.03)
0.30	0.673 (± 0.00)	0.681 (± 0.00)	0.705 (± 0.00)	0.692 (± 0.00)	0.693 (± 0.00)	0.701 (± 0.00)	0.714 (± 0.02)	0.714 (± 0.02)
0.40	0.677 (± 0.00)	0.667 (± 0.00)	0.698 (± 0.00)	0.682 (± 0.00)	0.682 (± 0.00)	0.698 (± 0.00)	0.704 (± 0.03)	0.704 (± 0.03)
0.50	0.658 (± 0.00)	0.659 (± 0.00)	0.685 (± 0.00)	0.680 (± 0.00)	0.676 (± 0.00)	0.683 (± 0.00)	0.689 (± 0.03)	0.689 (± 0.03)
0.60	0.667 (± 0.00)	0.659 (± 0.00)	0.676 (± 0.00)	0.656 (± 0.00)	0.659 (± 0.00)	0.680 (± 0.00)	0.659 (± 0.02)	0.659 (± 0.02)
0.70	0.655 (± 0.00)	0.646 (± 0.00)	0.656 (± 0.00)	0.629 (± 0.00)	0.624 (± 0.00)	0.662 (± 0.00)	0.617 (± 0.02)	0.617 (± 0.02)
0.80	0.621 (± 0.00)	0.593 (± 0.00)	0.629 (± 0.00)	0.575 (± 0.00)	0.531 (± 0.00)	0.628 (± 0.00)	0.553 (± 0.03)	0.553 (± 0.03)
0.90	0.568 (± 0.00)	0.508 (± 0.00)	0.552 (± 0.00)	0.449 (± 0.00)	0.352 (± 0.00)	0.584 (± 0.00)	0.455 (± 0.03)	0.455 (± 0.03)
0.99	0.425 (± 0.00)	0.258 (± 0.00)	0.381 (± 0.00)	0.188 (± 0.00)	0.159 (± 0.00)	0.495 (± 0.00)	0.186 (± 0.01)	0.186 (± 0.01)

1092

1093

1094

1095 Table 14: F1 scores for CITESEER under mechanism *CD-MCAR* and varying μ (GSPNis not reported
1096 as it is not designed for categorical features).

1097

μ	GOODIE	FairAC	FP	GNNmi	GCNmf	PCFI	GNNzero	GNNmedian
0.00	0.687 (± 0.00)	0.700 (± 0.00)	0.710 (± 0.02)	0.704 (± 0.02)	0.707 (± 0.00)	0.706 (± 0.02)	0.726 (± 0.02)	0.726 (± 0.02)
0.10	0.671 (± 0.00)	0.687 (± 0.00)	0.698 (± 0.00)	0.694 (± 0.00)	0.693 (± 0.00)	0.702 (± 0.00)	0.723 (± 0.02)	0.723 (± 0.02)
0.20	0.670 (± 0.00)	0.686 (± 0.00)	0.699 (± 0.00)	0.691 (± 0.00)	0.696 (± 0.00)	0.698 (± 0.00)	0.713 (± 0.02)	0.713 (± 0.02)
0.30	0.666 (± 0.00)	0.682 (± 0.00)	0.697 (± 0.00)	0.691 (± 0.00)	0.694 (± 0.00)	0.699 (± 0.00)	0.711 (± 0.03)	0.711 (± 0.03)
0.40	0.652 (± 0.00)	0.683 (± 0.00)	0.698 (± 0.00)	0.691 (± 0.00)	0.688 (± 0.00)	0.701 (± 0.00)	0.715 (± 0.02)	0.715 (± 0.02)
0.50	0.650 (± 0.00)	0.690 (± 0.00)	0.699 (± 0.00)	0.693 (± 0.00)	0.688 (± 0.00)	0.702 (± 0.00)	0.694 (± 0.02)	0.694 (± 0.02)
0.60	0.622 (± 0.00)	0.686 (± 0.00)	0.685 (± 0.00)	0.685 (± 0.00)	0.681 (± 0.00)	0.704 (± 0.00)	0.684 (± 0.02)	0.684 (± 0.02)
0.70	0.613 (± 0.00)	0.687 (± 0.00)	0.686 (± 0.00)	0.674 (± 0.00)	0.677 (± 0.00)	0.700 (± 0.00)	0.685 (± 0.03)	0.685 (± 0.03)
0.80	0.582 (± 0.00)	0.671 (± 0.00)	0.677 (± 0.00)	0.664 (± 0.00)	0.534 (± 0.00)	0.686 (± 0.00)	0.674 (± 0.02)	0.674 (± 0.02)
0.90	0.456 (± 0.00)	0.671 (± 0.00)	0.650 (± 0.00)	0.650 (± 0.00)	0.607 (± 0.00)	0.648 (± 0.00)	0.593 (± 0.02)	0.593 (± 0.02)
0.99	0.171 (± 0.00)	0.257 (± 0.00)	0.298 (± 0.00)	0.346 (± 0.00)	0.195 (± 0.00)	0.348 (± 0.00)	0.184 (± 0.02)	0.194 (± 0.03)

1096

1097

1098

1099 Table 15: F1 scores for CITESEER under mechanism *FD-MNAR* and varying μ (GSPNis not reported
1100 as it is not designed for categorical features).

1101

μ	GOODIE	FairAC	FP	GNNmi	GCNmf	PCFI	GNNzero	GNNmedian
0.00	0.687 (± 0.00)	0.700 (± 0.00)	0.710 (± 0.02)	0.704 (± 0.02)	0.707 (± 0.00)	0.706 (± 0.02)	0.728 (± 0.02)	0.728 (± 0.02)
0.10	0.689 (± 0.03)	0.691 (± 0.03)	0.706 (± 0.02)	0.699 (± 0.02)	0.699 (± 0.02)	0.708 (± 0.03)	0.729 (± 0.02)	0.729 (± 0.02)
0.20	0.686 (± 0.02)	0.698 (± 0.03)	0.703 (± 0.02)	0.697 (± 0.02)	0.696 (± 0.02)	0.704 (± 0.02)	0.720 (± 0.02)	0.720 (± 0.02)
0.30	0.701 (± 0.04)	0.690 (± 0.03)	0.701 (± 0.03)	0.693 (± 0.02)	0.704 (± 0.02)	0.700 (± 0.03)	0.721 (± 0.03)	0.721 (± 0.03)
0.40	0.696 (± 0.04)	0.699 (± 0.04)	0.695 (± 0.02)	0.695 (± 0.02)	0.692 (± 0.03)	0.701 (± 0.03)	0.717 (± 0.02)	0.717 (± 0.02)
0.50	0.707 (± 0.03)	0.688 (± 0.04)	0.698 (± 0.03)	0.693 (± 0.03)	0.690 (± 0.02)	0.702 (± 0.03)	0.727 (± 0.02)	0.727 (± 0.02)
0.60	0.708 (± 0.02)	0.694 (± 0.03)	0.691 (± 0.03)	0.693 (± 0.03)	0.696 (± 0.02)	0.702 (± 0.03)	0.712 (± 0.03)	0.712 (± 0.03)
0.70	0.678 (± 0.04)	0.688 (± 0.03)	0.688 (± 0.03)	0.686 (± 0.02)	0.649 (± 0.03)	0.690 (± 0.04)	0.705 (± 0.02)	0.705 (± 0.02)
0.80	0.695 (± 0.03)	0.689 (± 0.04)	0.689 (± 0.02)	0.685 (± 0.02)	0.437 (± 0.27)	0.694 (± 0.03)	0.696 (± 0.03)	0.696 (± 0.03)
0.90	0.653 (± 0.03)	0.681 (± 0.04)	0.682 (± 0.02)	0.687 (± 0.03)	0.257 (± 0.17)	0.689 (± 0.02)	0.676 (± 0.02)	0.676 (± 0.02)
0.99	0.601 (± 0.01)	0.566 (± 0.01)	0.611 (± 0.01)	0.535 (± 0.02)	0.118 (± 0.04)	0.633 (± 0.01)	0.538 (± 0.03)	0.538 (± 0.03)

1102

1103

1104

1105 Table 16: F1 scores for CITESEER under mechanism *CD-MNAR* and varying μ (GSPNis not reported
1106 as it is not designed for categorical features).

1107

1108

1109

μ	GOODIE	FairAC	FP	GNNmi	GCNmf	PCFI	GNNzero	GNNmedian
0.00	0.687 (± 0.00)	0.700 (± 0.05)	0.710 (± 0.02)	0.704 (± 0.02)	0.707 (± 0.00)	0.706 (± 0.02)	0.726 (± 0.02)	0.726 (± 0.02)
0.10	0.692 (± 0.04)	0.696 (± 0.04)	0.708 (± 0.02)	0.705 (± 0.02)	0.702 (± 0.03)	0.705 (± 0.02)	0.729 (± 0.02)	0.729 (± 0.02)
0.20	0.690 (± 0.04)	0.689 (± 0.04)	0.703 (± 0.03)	0.702 (± 0.02)	0.705 (± 0.02)	0.704 (± 0.02)	0.727 (± 0.02)	0.727 (± 0.02)
0.30	0.700 (± 0.02)	0.689 (± 0.04)	0.708 (± 0.03)	0.706 (± 0.02)	0.708 (± 0.02)	0.705 (± 0.02)	0.728 (± 0.02)	0.728 (± 0.02)
0.40	0.687 (± 0.04)	0.695 (± 0.04)	0.707 (± 0.03)	0.704 (± 0.02)	0.703 (± 0.03)	0.704 (± 0.03)	0.725 (± 0.02)	0.725 (± 0.02)
0.50	0.675 (± 0.03)	0.692 (± 0.03)	0.699 (± 0.03)	0.700 (± 0.03)	0.697 (± 0.02)	0.706 (± 0.03)	0.718 (± 0.02)	0.718 (± 0.02)
0.60	0.689 (± 0.03)	0.689 (± 0.03)	0.702 (± 0.03)	0.699 (± 0.03)	0.693 (± 0.03)	0.706 (± 0.03)	0.714 (± 0.02)	0.714 (± 0.02)
0.70	0.681 (± 0.03)	0.685 (± 0.03)	0.692 (± 0.03)	0.691 (± 0.03)	0.522 (± 0.20)	0.696 (± 0.03)	0.702 (± 0.03)	0.702 (± 0.03)
0.80	0.676 (± 0.05)	0.685 (± 0.03)	0.690 (± 0.03)	0.689 (± 0.02)	0.359 (± 0.15)	0.696 (± 0.04)	0.689 (± 0.03)	0.689 (± 0.03)
0.90	0.665 (± 0.02)	0.681 (± 0.03)	0.677 (± 0.03)	0.666 (± 0.03)	0.113 (± 0.06)	0.681 (± 0.03)	0.638 (± 0.02)	0.638 (± 0.02)
0.99	0.645 (± 0.03)	0.631 (± 0.02)	0.652 (± 0.02)	0.621 (± 0.02)	0.104 (± 0.06)	0.660 (± 0.02)	0.593 (± 0.03)	0.592 (± 0.03)

1105

1106

1107

1134

1135 Table 17: F1 scores for PUBMED under mechanism *U-MCAR* and varying μ (GSPNis not reported
1136 as it is not designed for categorical features).

1137

μ	GOODIE	FairAC	FP	GNNmi	GCNmf	PCFI	GNNzero	GNNmedian
0.00	0.784 (± 0.01)	0.831 (± 0.00)	0.883 (± 0.00)	0.881 (± 0.00)	0.877 (± 0.00)	0.882 (± 0.00)	0.875 (± 0.00)	0.875 (± 0.00)
0.10	0.787 (± 0.00)	0.830 (± 0.00)	0.877 (± 0.00)	0.879 (± 0.00)	0.830 (± 0.00)	0.874 (± 0.00)	0.871 (± 0.00)	0.871 (± 0.00)
0.20	0.786 (± 0.00)	0.831 (± 0.00)	0.868 (± 0.00)	0.873 (± 0.00)	0.832 (± 0.00)	0.868 (± 0.00)	0.866 (± 0.00)	0.866 (± 0.00)
0.30	0.785 (± 0.00)	0.830 (± 0.00)	0.870 (± 0.00)	0.872 (± 0.00)	0.827 (± 0.00)	0.864 (± 0.00)	0.862 (± 0.00)	0.860 (± 0.00)
0.40	0.782 (± 0.00)	0.828 (± 0.00)	0.861 (± 0.00)	0.869 (± 0.00)	0.828 (± 0.00)	0.858 (± 0.00)	0.857 (± 0.01)	0.857 (± 0.00)
0.50	0.784 (± 0.00)	0.827 (± 0.00)	0.856 (± 0.00)	0.862 (± 0.00)	0.778 (± 0.00)	0.852 (± 0.00)	0.851 (± 0.01)	0.852 (± 0.00)
0.60	0.777 (± 0.00)	0.828 (± 0.00)	0.851 (± 0.00)	0.855 (± 0.00)	0.805 (± 0.00)	0.849 (± 0.00)	0.846 (± 0.00)	0.845 (± 0.00)
0.70	0.772 (± 0.00)	0.824 (± 0.00)	0.847 (± 0.00)	0.845 (± 0.00)	0.726 (± 0.00)	0.844 (± 0.00)	0.834 (± 0.01)	0.835 (± 0.01)
0.80	0.756 (± 0.00)	0.819 (± 0.00)	0.836 (± 0.00)	0.832 (± 0.00)	0.443 (± 0.00)	0.837 (± 0.00)	0.820 (± 0.00)	0.816 (± 0.00)
0.90	0.700 (± 0.00)	0.806 (± 0.00)	0.822 (± 0.00)	0.803 (± 0.00)	0.315 (± 0.00)	0.832 (± 0.00)	0.791 (± 0.01)	0.786 (± 0.01)
0.99	0.452 (± 0.00)	0.262 (± 0.00)	0.793 (± 0.00)	0.327 (± 0.00)	0.315 (± 0.00)	0.814 (± 0.00)	0.674 (± 0.02)	0.693 (± 0.01)

1146

1147

1148

1149 Table 18: F1 scores for PUBMED under mechanism *S-MCAR* and varying μ (GSPNis not reported
1150 as it is not designed for categorical features).

1151

μ	GOODIE	FairAC	FP	GNNmi	GCNmf	PCFI	GNNzero	GNNmedian
0.00	0.784 (± 0.01)	0.831 (± 0.00)	0.883 (± 0.00)	-	0.877 (± 0.00)	0.882 (± 0.00)	0.875 (± 0.00)	0.875 (± 0.00)
0.10	0.786 (± 0.00)	0.831 (± 0.00)	0.875 (± 0.00)	0.875 (± 0.00)	0.870 (± 0.00)	0.871 (± 0.00)	0.868 (± 0.01)	0.866 (± 0.01)
0.20	0.783 (± 0.00)	0.827 (± 0.00)	0.869 (± 0.00)	0.870 (± 0.00)	0.861 (± 0.00)	0.867 (± 0.00)	0.860 (± 0.01)	0.859 (± 0.01)
0.30	0.785 (± 0.00)	0.832 (± 0.00)	0.863 (± 0.00)	0.865 (± 0.00)	0.861 (± 0.00)	0.863 (± 0.00)	0.853 (± 0.01)	0.852 (± 0.00)
0.40	0.785 (± 0.00)	0.828 (± 0.00)	0.856 (± 0.00)	0.857 (± 0.00)	0.848 (± 0.00)	0.856 (± 0.00)	0.846 (± 0.01)	0.847 (± 0.01)
0.50	0.775 (± 0.00)	0.827 (± 0.00)	0.853 (± 0.00)	0.854 (± 0.00)	0.808 (± 0.00)	0.848 (± 0.00)	0.838 (± 0.00)	0.837 (± 0.00)
0.60	0.774 (± 0.00)	0.822 (± 0.00)	0.843 (± 0.00)	0.845 (± 0.00)	0.798 (± 0.00)	0.843 (± 0.00)	0.829 (± 0.00)	0.827 (± 0.00)
0.70	0.760 (± 0.00)	0.813 (± 0.00)	0.832 (± 0.00)	0.827 (± 0.00)	0.762 (± 0.00)	0.836 (± 0.00)	0.815 (± 0.00)	0.814 (± 0.00)
0.80	0.744 (± 0.00)	0.806 (± 0.00)	0.828 (± 0.00)	0.808 (± 0.00)	0.683 (± 0.00)	0.832 (± 0.00)	0.785 (± 0.01)	0.788 (± 0.01)
0.90	0.706 (± 0.00)	0.786 (± 0.00)	0.815 (± 0.00)	0.743 (± 0.00)	0.421 (± 0.00)	0.825 (± 0.00)	0.727 (± 0.01)	0.729 (± 0.00)
0.99	0.441 (± 0.00)	0.259 (± 0.00)	0.765 (± 0.00)	0.333 (± 0.00)	0.310 (± 0.00)	0.794 (± 0.00)	0.446 (± 0.03)	0.458 (± 0.02)

1160

1161

1162

1163 Table 19: F1 scores for PUBMED under mechanism *CD-MCAR* and varying μ (GSPNis not reported
1164 as it is not designed for categorical features).

1165

μ	GOODIE	FairAC	FP	GNNmi	GCNmf	PCFI	GNNzero	GNNmedian
0.00	0.784 (± 0.01)	0.831 (± 0.00)	0.883 (± 0.00)	0.881 (± 0.00)	0.877 (± 0.00)	0.882 (± 0.00)	0.875 (± 0.00)	0.876 (± 0.00)
0.10	0.738 (± 0.00)	0.824 (± 0.00)	0.855 (± 0.00)	0.857 (± 0.00)	0.830 (± 0.00)	0.852 (± 0.00)	0.848 (± 0.00)	0.846 (± 0.00)
0.20	0.700 (± 0.00)	0.820 (± 0.00)	0.845 (± 0.00)	0.851 (± 0.00)	0.828 (± 0.00)	0.844 (± 0.00)	0.837 (± 0.00)	0.836 (± 0.00)
0.30	0.607 (± 0.00)	0.823 (± 0.00)	0.843 (± 0.00)	0.844 (± 0.00)	0.823 (± 0.00)	0.836 (± 0.00)	0.822 (± 0.00)	0.822 (± 0.00)
0.40	0.534 (± 0.00)	0.821 (± 0.00)	0.834 (± 0.00)	0.842 (± 0.00)	0.818 (± 0.00)	0.830 (± 0.00)	0.821 (± 0.01)	0.821 (± 0.01)
0.50	0.509 (± 0.00)	0.814 (± 0.00)	0.818 (± 0.00)	0.823 (± 0.00)	0.797 (± 0.00)	0.820 (± 0.00)	0.808 (± 0.01)	0.806 (± 0.01)
0.60	0.422 (± 0.00)	0.812 (± 0.00)	0.808 (± 0.00)	0.816 (± 0.00)	0.787 (± 0.00)	0.812 (± 0.00)	0.790 (± 0.00)	0.793 (± 0.01)
0.70	0.415 (± 0.00)	0.802 (± 0.00)	0.797 (± 0.00)	0.811 (± 0.00)	0.779 (± 0.00)	0.801 (± 0.00)	0.778 (± 0.01)	0.774 (± 0.01)
0.80	0.396 (± 0.00)	0.779 (± 0.00)	0.749 (± 0.00)	0.783 (± 0.00)	0.713 (± 0.00)	0.754 (± 0.00)	0.738 (± 0.01)	0.749 (± 0.02)
0.90	0.306 (± 0.00)	0.574 (± 0.00)	0.693 (± 0.00)	0.700 (± 0.00)	0.391 (± 0.00)	0.683 (± 0.00)	0.664 (± 0.01)	0.667 (± 0.02)
0.99	0.198 (± 0.00)	0.266 (± 0.00)	0.303 (± 0.00)	0.330 (± 0.00)	0.306 (± 0.00)	0.305 (± 0.00)	0.346 (± 0.02)	0.345 (± 0.02)

1174

1175

1176

1177 Table 20: F1 scores for PUBMED under mechanism *FD-MNAR* and varying μ (GSPNis not reported
1178 as it is not designed for categorical features).

1179

μ	GOODIE	FairAC	FP	GNNmi	GCNmf	PCFI	GNNzero	GNNmedian
0.00	0.784 (± 0.01)	0.831 (± 0.00)	0.883 (± 0.00)	0.881 (± 0.00)	0.877 (± 0.00)	0.882 (± 0.00)	0.875 (± 0.00)	0.874 (± 0.00)
0.10	0.785 (± 0.02)	0.832 (± 0.00)	0.876 (± 0.01)	0.880 (± 0.01)	0.834 (± 0.00)	0.874 (± 0.01)	0.867 (± 0.01)	0.868 (± 0.00)
0.20	0.785 (± 0.02)	0.834 (± 0.00)	0.869 (± 0.00)	0.875 (± 0.00)	0.832 (± 0.00)	0.869 (± 0.01)	0.864 (± 0.01)	0.864 (± 0.00)
0.30	0.785 (± 0.02)	0.830 (± 0.00)	0.865 (± 0.00)	0.870 (± 0.00)	0.829 (± 0.00)	0.860 (± 0.00)	0.858 (± 0.00)	0.858 (± 0.01)
0.40	0.780 (± 0.01)	0.827 (± 0.00)	0.860 (± 0.00)	0.866 (± 0.00)	0.733 (± 0.11)	0.856 (± 0.00)	0.853 (± 0.01)	0.854 (± 0.00)
0.50	0.775 (± 0.02)	0.822 (± 0.00)	0.853 (± 0.00)	0.859 (± 0.00)	0.720 (± 0.12)	0.850 (± 0.00)	0.844 (± 0.01)	0.846 (± 0.00)
0.60	0.763 (± 0.02)	0.824 (± 0.01)	0.847 (± 0.01)	0.850 (± 0.00)	0.746 (± 0.04)	0.842 (± 0.00)	0.836 (± 0.01)	0.836 (± 0.00)
0.70	0.745 (± 0.03)	0.813 (± 0.00)	0.836 (± 0.00)	0.834 (± 0.00)	0.579 (± 0.25)	0.837 (± 0.00)	0.827 (± 0.00)	0.826 (± 0.00)
0.80	0.745 (± 0.03)	0.819 (± 0.00)	0.759 (± 0.04)	0.829 (± 0.00)	0.555 (± 0.14)	0.764 (± 0.00)	0.805 (± 0.01)	0.805 (± 0.01)
0.90	0.336 (± 0.01)	0.806 (± 0.00)	0.693 (± 0.01)	0.812 (± 0.00)	0.529 (± 0.13)	0.653 (± 0.00)	0.780 (± 0.01)	0.777 (± 0.01)
0.99	0.278 (± 0.01)	0.282 (± 0.01)	0.303 (± 0.05)	0.347 (± 0.00)	0.399 (± 0.33)	0.335 (± 0.01)	0.659 (± 0.02)	0.669 (± 0.02)

1188
1189
1190Table 21: F1 scores for PUBMED under mechanism *CD-MNAR* and varying μ (GSPNis not reported as it is not designed for categorical features).

μ	GOODIE	FairAC	FP	GNNmi	GCNmf	PCFI	GNNzero	GNNmedian
0.00	0.784 (± 0.01)	0.831 (± 0.00)	0.883 (± 0.00)	0.881 (± 0.00)	0.877 (± 0.00)	0.882 (± 0.00)	0.874 (± 0.00)	0.875 (± 0.00)
0.10	0.789 (± 0.02)	0.829 (± 0.00)	0.878 (± 0.00)	0.880 (± 0.00)	0.835 (± 0.00)	0.877 (± 0.00)	0.866 (± 0.01)	0.869 (± 0.00)
0.20	0.783 (± 0.01)	0.830 (± 0.00)	0.870 (± 0.00)	0.876 (± 0.00)	0.834 (± 0.00)	0.867 (± 0.01)	0.862 (± 0.00)	0.861 (± 0.00)
0.30	0.783 (± 0.02)	0.828 (± 0.00)	0.863 (± 0.00)	0.871 (± 0.00)	0.823 (± 0.00)	0.866 (± 0.00)	0.860 (± 0.00)	0.859 (± 0.00)
0.40	0.777 (± 0.02)	0.826 (± 0.00)	0.858 (± 0.00)	0.863 (± 0.00)	0.830 (± 0.00)	0.857 (± 0.01)	0.854 (± 0.00)	0.852 (± 0.00)
0.50	0.779 (± 0.01)	0.825 (± 0.00)	0.853 (± 0.00)	0.858 (± 0.00)	0.826 (± 0.00)	0.853 (± 0.00)	0.847 (± 0.00)	0.849 (± 0.00)
0.60	0.769 (± 0.02)	0.824 (± 0.00)	0.847 (± 0.01)	0.848 (± 0.01)	0.784 (± 0.04)	0.848 (± 0.00)	0.840 (± 0.01)	0.840 (± 0.00)
0.70	0.752 (± 0.03)	0.816 (± 0.00)	0.837 (± 0.00)	0.835 (± 0.00)	0.765 (± 0.02)	0.837 (± 0.00)	0.827 (± 0.00)	0.825 (± 0.00)
0.80	0.742 (± 0.03)	0.813 (± 0.00)	0.828 (± 0.00)	0.817 (± 0.00)	0.323 (± 0.10)	0.836 (± 0.00)	0.810 (± 0.01)	0.809 (± 0.00)
0.90	0.605 (± 0.13)	0.628 (± 0.24)	0.812 (± 0.00)	0.770 (± 0.00)	0.280 (± 0.05)	0.823 (± 0.00)	0.760 (± 0.01)	0.763 (± 0.01)
0.99	0.557 (± 0.14)	0.260 (± 0.00)	0.800 (± 0.00)	0.689 (± 0.01)	0.418 (± 0.04)	0.818 (± 0.00)	0.717 (± 0.01)	0.728 (± 0.02)

1200

1201

Table 22: F1 scores for SYNTHETIC under mechanism *U-MCAR* and varying μ

μ	GOODIE	GSPN	FairAC	FP	GNNmi	GCNmf	PCFI	GNNzero	GNNmedian	GNNmim
0.00	0.812 (± 0.00)	0.865 (± 0.00)	0.815 (± 0.00)	0.980 (± 0.00)	0.982 (± 0.00)	0.978 (± 0.00)	0.977 (± 0.00)	0.978 (± 0.01)	0.978 (± 0.01)	0.983 (± 0.01)
0.10	0.810 (± 0.00)	0.822 (± 0.00)	0.828 (± 0.00)	0.910 (± 0.00)	0.902 (± 0.00)	0.875 (± 0.00)	0.898 (± 0.00)	0.902 (± 0.02)	0.903 (± 0.02)	0.901 (± 0.00)
0.20	0.792 (± 0.00)	0.759 (± 0.00)	0.808 (± 0.00)	0.863 (± 0.00)	0.870 (± 0.00)	0.790 (± 0.00)	0.855 (± 0.00)	0.853 (± 0.02)	0.853 (± 0.02)	0.861 (± 0.00)
0.30	0.758 (± 0.00)	0.768 (± 0.00)	0.762 (± 0.00)	0.795 (± 0.00)	0.808 (± 0.00)	0.770 (± 0.00)	0.805 (± 0.00)	0.800 (± 0.03)	0.801 (± 0.03)	0.815 (± 0.00)
0.40	0.758 (± 0.00)	0.749 (± 0.00)	0.759 (± 0.00)	0.764 (± 0.00)	0.771 (± 0.00)	0.745 (± 0.00)	0.763 (± 0.00)	0.766 (± 0.02)	0.766 (± 0.02)	0.791 (± 0.00)
0.50	0.747 (± 0.00)	0.721 (± 0.00)	0.642 (± 0.00)	0.745 (± 0.00)	0.745 (± 0.00)	0.710 (± 0.00)	0.748 (± 0.00)	0.732 (± 0.04)	0.730 (± 0.04)	0.739 (± 0.00)
0.60	0.773 (± 0.00)	0.708 (± 0.00)	0.680 (± 0.00)	0.720 (± 0.00)	0.737 (± 0.00)	0.692 (± 0.00)	0.717 (± 0.00)	0.714 (± 0.04)	0.710 (± 0.04)	0.714 (± 0.00)
0.70	0.742 (± 0.00)	0.629 (± 0.00)	0.611 (± 0.00)	0.683 (± 0.00)	0.689 (± 0.00)	0.673 (± 0.00)	0.678 (± 0.00)	0.687 (± 0.03)	0.693 (± 0.03)	0.693 (± 0.00)
0.80	0.771 (± 0.00)	0.579 (± 0.00)	0.621 (± 0.00)	0.632 (± 0.00)	0.638 (± 0.00)	0.601 (± 0.00)	0.638 (± 0.00)	0.610 (± 0.05)	0.621 (± 0.05)	0.649 (± 0.00)
0.90	0.776 (± 0.00)	0.544 (± 0.00)	0.567 (± 0.00)	0.605 (± 0.00)	0.602 (± 0.00)	0.592 (± 0.00)	0.588 (± 0.00)	0.589 (± 0.04)	0.599 (± 0.04)	0.590 (± 0.00)
0.99	0.762 (± 0.00)	0.499 (± 0.00)	0.391 (± 0.00)	0.542 (± 0.00)	0.367 (± 0.00)	0.471 (± 0.00)	0.547 (± 0.00)	0.548 (± 0.04)	0.411 (± 0.07)	0.535 (± 0.00)

1211

1212

Table 23: F1 scores for SYNTHETIC under mechanism *S-MCAR* and varying μ

μ	GOODIE	GSPN	FairAC	FP	GNNmi	GCNmf	PCFI	GNNzero	GNNmedian	GNNmim
0.00	0.812 (± 0.00)	0.865 (± 0.00)	0.815 (± 0.00)	0.980 (± 0.00)	0.982 (± 0.00)	0.978 (± 0.00)	0.977 (± 0.00)	0.978 (± 0.01)	0.978 (± 0.01)	0.983 (± 0.01)
0.10	0.756 (± 0.00)	0.748 (± 0.00)	0.723 (± 0.00)	0.903 (± 0.00)	0.912 (± 0.00)	0.903 (± 0.00)	0.900 (± 0.00)	0.909 (± 0.01)	0.911 (± 0.01)	0.898 (± 0.00)
0.20	0.769 (± 0.00)	0.733 (± 0.00)	0.727 (± 0.00)	0.883 (± 0.00)	0.883 (± 0.00)	0.872 (± 0.00)	0.870 (± 0.00)	0.844 (± 0.02)	0.843 (± 0.02)	0.875 (± 0.00)
0.30	0.742 (± 0.00)	0.737 (± 0.00)	0.700 (± 0.00)	0.830 (± 0.00)	0.842 (± 0.00)	0.841 (± 0.00)	0.831 (± 0.00)	0.817 (± 0.02)	0.813 (± 0.01)	0.833 (± 0.00)
0.40	0.716 (± 0.00)	0.712 (± 0.00)	0.683 (± 0.00)	0.810 (± 0.00)	0.798 (± 0.00)	0.752 (± 0.00)	0.793 (± 0.00)	0.775 (± 0.02)	0.777 (± 0.02)	0.799 (± 0.00)
0.50	0.700 (± 0.00)	0.711 (± 0.00)	0.704 (± 0.00)	0.785 (± 0.00)	0.788 (± 0.00)	0.705 (± 0.00)	0.780 (± 0.00)	0.746 (± 0.02)	0.748 (± 0.02)	0.779 (± 0.00)
0.60	0.658 (± 0.00)	0.674 (± 0.00)	0.695 (± 0.00)	0.747 (± 0.00)	0.761 (± 0.00)	0.726 (± 0.00)	0.738 (± 0.00)	0.718 (± 0.03)	0.705 (± 0.04)	0.756 (± 0.00)
0.70	0.618 (± 0.00)	0.675 (± 0.00)	0.652 (± 0.00)	0.687 (± 0.00)	0.703 (± 0.00)	0.665 (± 0.00)	0.700 (± 0.00)	0.663 (± 0.03)	0.667 (± 0.02)	0.727 (± 0.00)
0.80	0.584 (± 0.00)	0.649 (± 0.00)	0.616 (± 0.00)	0.653 (± 0.00)	0.667 (± 0.00)	0.645 (± 0.00)	0.638 (± 0.00)	0.647 (± 0.05)	0.656 (± 0.04)	0.676 (± 0.00)
0.90	0.527 (± 0.00)	0.588 (± 0.00)	0.589 (± 0.00)	0.597 (± 0.00)	0.597 (± 0.00)	0.578 (± 0.00)	0.591 (± 0.00)	0.601 (± 0.02)	0.593 (± 0.02)	0.582 (± 0.00)
0.99	0.337 (± 0.00)	0.455 (± 0.00)	0.338 (± 0.00)	0.515 (± 0.00)	0.425 (± 0.00)	0.403 (± 0.00)	0.513 (± 0.00)	0.488 (± 0.02)	0.444 (± 0.05)	0.477 (± 0.00)

1221

1222

Table 24: F1 scores for SYNTHETIC under mechanism *CD-MCAR* and varying μ

μ	GOODIE	GSPN	FairAC	FP	GNNmi	GCNmf	PCFI	GNNzero	GNNmedian	GNNmim
0.00	0.812 (± 0.00)	0.865 (± 0.00)	0.815 (± 0.00)	0.980 (± 0.00)	0.982 (± 0.00)	0.978 (± 0.00)	0.977 (± 0.00)	0.978 (± 0.01)	0.978 (± 0.01)	0.886 (± 0.00)
0.10	0.778 (± 0.00)	0.785 (± 0.00)	0.792 (± 0.00)	0.860 (± 0.00)	0.857 (± 0.00)	0.845 (± 0.00)	0.860 (± 0.00)	0.978 (± 0.01)	0.978 (± 0.01)	0.829 (± 0.00)
0.20	0.760 (± 0.00)	0.731 (± 0.00)	0.705 (± 0.00)	0.788 (± 0.00)	0.770 (± 0.00)	0.741 (± 0.00)	0.772 (± 0.00)	0.699 (± 0.02)	0.699 (± 0.02)	0.780 (± 0.00)
0.30	0.730 (± 0.00)	0.666 (± 0.00)	0.718 (± 0.00)	0.736 (± 0.00)	0.733 (± 0.00)	0.730 (± 0.00)	0.734 (± 0.00)	0.605 (± 0.03)	0.605 (± 0.03)	0.738 (± 0.00)
0.40	0.736 (± 0.00)	0.625 (± 0.00)	0.607 (± 0.00)	0.661 (± 0.00)	0.659 (± 0.00)	0.673 (± 0.00)	0.649 (± 0.00)	0.605 (± 0.03)	0.605 (± 0.03)	0.703 (± 0.00)
0.50	0.761 (± 0.00)	0.547 (± 0.00)	0.542 (± 0.00)	0.619 (± 0.00)	0.618 (± 0.00)	0.628 (± 0.00)	0.613 (± 0.00)	0.605 (± 0.03)	0.605 (± 0.03)	0.682 (± 0.00)
0.60	0.768 (± 0.00)	0.594 (± 0.00)	0.543 (± 0.00)	0.621 (± 0.00)	0.613 (± 0.00)	0.619 (± 0.00)	0.605 (± 0.00)	0.528 (± 0.03)	0.528 (± 0.03)	0.667 (± 0.00)
0.70	0.759 (± 0.00)	0.603 (± 0.00)	0.586 (± 0.00)	0.617 (± 0.00)	0.607 (± 0.00)	0.591 (± 0.00)	0.594 (± 0.00)	0.536 (± 0.03)	0.536 (± 0.03)	0.675 (± 0.00)
0.80	0.758 (± 0.00)	0.613 (± 0.00)	0.486 (± 0.00)	0.617 (± 0.00)	0.622 (± 0.00)	0.631 (± 0.00)	0.620 (± 0.00)	0.536 (± 0.03)	0.536 (± 0.03)	0.666 (± 0.00)
0.90	0.775 (± 0.00)	0.544 (± 0.00)	0.529 (± 0.00)	0.623 (± 0.00)	0.633 (± 0.00)	0.623 (± 0.00)	0.606 (± 0.00)	0.555 (± 0.02)	0.536 (± 0.03)	0.678 (± 0.00)
0.99	0.764 (± 0.00)	0.569 (± 0.00)	0.557 (± 0.00)	0.609 (± 0.00)	0.611 (± 0.00)	0.643 (± 0.00)	0.612 (± 0.00)	0.646 (± 0.03)	0.638 (± 0.03)	0.667 (± 0.00)

1231

1232

Table 25: F1 scores for SYNTHETIC under mechanism *FD-MNAR* and varying μ

μ	GOODIE	GSPN	FairAC	FP	GNNmi	GCNmf	PCFI	GNNzero	GNNmedian	GNNmim
0.00	0.812 (± 0.00)	0.865 (± 0.00)	0.815 (± 0.00)	0.980 (± 0.00)	0.982 (± 0.00)	0.978 (± 0.00)	0.977 (± 0.00)	0.976 (± 0.01)	0.976 (± 0.01)	0.983 (± 0.01)
0.10	0.751 (± 0.05)	0.750 (± 0.03)	0.761 (± 0.02)	0.893 (± 0.01)	0.900 (± 0.02)	0.878 (± 0.02)	0.895 (± 0.01)	0.891 (± 0.02)	0.894 (± 0.02)	0.895 (± 0.01)
0.20	0.750 (± 0.03)	0.721 (± 0.01)	0.699 (± 0.04)	0.836 (± 0.02)	0.845 (± 0.02)	0.785 (± 0.04)	0.847 (± 0.02)	0.849 (± 0.03)	0.854 (± 0.02)	0.843 (± 0.04)
0.30	0.691 (± 0.04)	0.678 (± 0.02)	0.667 (± 0.03)	0.810 (± 0.01)	0.812 (± 0.01)	0.771 (± 0.03)	0.789 (± 0.01)	0.819 (± 0.02)	0.821 (± 0.01)	0.812 (± 0.01)
0.40	0.693 (± 0.03)	0.678 (± 0.03)	0.682 (± 0.03)	0.791 (± 0.02)	0.798 (± 0.02)	0.763 (± 0.02)	0.7			

1242

1243

Table 26: F1 scores for SYNTHETIC under mechanism $CD\text{-MNAR}$ and varying μ

1244

1245

μ	GOODIE	GSPN	FairAC	FP	GNNmi	GCNmf	PCFI	GNNzero	GNNmedian	GNNmim
0.00	0.812 (± 0.00)	0.865 (± 0.00)	0.815 (± 0.00)	0.980 (± 0.00)	0.982 (± 0.00)	0.978 (± 0.00)	0.977 (± 0.00)	0.978 (± 0.01)	0.978 (± 0.01)	0.983 (± 0.01)
0.10	0.756 (± 0.04)	0.757 (± 0.02)	0.752 (± 0.02)	0.913 (± 0.02)	0.918 (± 0.02)	0.882 (± 0.02)	0.912 (± 0.01)	0.912 (± 0.02)	0.912 (± 0.02)	0.913 (± 0.02)
0.20	0.730 (± 0.05)	0.718 (± 0.02)	0.674 (± 0.05)	0.856 (± 0.03)	0.868 (± 0.03)	0.800 (± 0.04)	0.861 (± 0.04)	0.864 (± 0.02)	0.865 (± 0.02)	0.865 (± 0.03)
0.30	0.663 (± 0.05)	0.716 (± 0.02)	0.689 (± 0.03)	0.803 (± 0.02)	0.820 (± 0.02)	0.768 (± 0.03)	0.810 (± 0.03)	0.807 (± 0.02)	0.804 (± 0.02)	0.830 (± 0.03)
0.40	0.530 (± 0.16)	0.678 (± 0.01)	0.718 (± 0.03)	0.744 (± 0.01)	0.749 (± 0.00)	0.753 (± 0.01)	0.739 (± 0.03)	0.756 (± 0.01)	0.742 (± 0.01)	0.776 (± 0.01)
0.50	0.487 (± 0.12)	0.662 (± 0.03)	0.655 (± 0.04)	0.697 (± 0.03)	0.695 (± 0.03)	0.683 (± 0.04)	0.699 (± 0.04)	0.689 (± 0.03)	0.657 (± 0.02)	0.725 (± 0.01)
0.60	0.575 (± 0.06)	0.696 (± 0.03)	0.577 (± 0.02)	0.683 (± 0.03)	0.658 (± 0.03)	0.666 (± 0.02)	0.645 (± 0.03)	0.694 (± 0.04)	0.638 (± 0.03)	0.731 (± 0.03)
0.70	0.553 (± 0.03)	0.616 (± 0.03)	0.583 (± 0.02)	0.613 (± 0.02)	0.600 (± 0.04)	0.617 (± 0.04)	0.592 (± 0.05)	0.642 (± 0.03)	0.603 (± 0.04)	0.668 (± 0.01)
0.80	0.486 (± 0.06)	0.638 (± 0.03)	0.592 (± 0.03)	0.588 (± 0.02)	0.596 (± 0.03)	0.570 (± 0.02)	0.563 (± 0.03)	0.618 (± 0.02)	0.580 (± 0.04)	0.655 (± 0.02)
0.90	0.432 (± 0.08)	0.618 (± 0.05)	0.479 (± 0.10)	0.586 (± 0.04)	0.607 (± 0.03)	0.556 (± 0.03)	0.553 (± 0.01)	0.598 (± 0.03)	0.557 (± 0.04)	0.635 (± 0.04)
0.99	0.468 (± 0.03)	0.545 (± 0.06)	0.396 (± 0.08)	0.594 (± 0.01)	0.537 (± 0.01)	0.475 (± 0.06)	0.549 (± 0.03)	0.550 (± 0.03)	0.485 (± 0.06)	0.568 (± 0.01)

1252

1253

1254

Table 27: F1 scores for AIR under mechanism $U\text{-MCAR}$ and varying μ

1255

1256

μ	GOODIE	GSPN	FairAC	FP	GNNmi	GCNmf	PCFI	GNNzero	GNNmedian	GNNmim
0.00	0.724 (± 0.00)	0.798 (± 0.02)	0.733 (± 0.00)	0.918 (± 0.00)	0.922 (± 0.01)	0.922 (± 0.00)	0.891 (± 0.00)	0.916 (± 0.02)	0.916 (± 0.02)	0.930 (± 0.00)
0.10	0.665 (± 0.00)	0.710 (± 0.00)	0.733 (± 0.00)	0.895 (± 0.00)	0.891 (± 0.00)	0.768 (± 0.00)	0.883 (± 0.00)	0.904 (± 0.03)	0.902 (± 0.03)	0.899 (± 0.00)
0.20	0.669 (± 0.00)	0.582 (± 0.00)	0.709 (± 0.00)	0.848 (± 0.00)	0.833 (± 0.00)	0.747 (± 0.00)	0.852 (± 0.00)	0.874 (± 0.03)	0.865 (± 0.03)	0.859 (± 0.00)
0.30	0.669 (± 0.00)	0.502 (± 0.00)	0.715 (± 0.00)	0.836 (± 0.00)	0.837 (± 0.00)	0.712 (± 0.00)	0.836 (± 0.00)	0.837 (± 0.04)	0.857 (± 0.03)	0.852 (± 0.00)
0.40	0.714 (± 0.00)	0.532 (± 0.00)	0.700 (± 0.00)	0.805 (± 0.00)	0.829 (± 0.00)	0.712 (± 0.00)	0.797 (± 0.00)	0.813 (± 0.02)	0.839 (± 0.02)	0.833 (± 0.00)
0.50	0.666 (± 0.00)	0.553 (± 0.00)	0.669 (± 0.00)	0.801 (± 0.00)	0.805 (± 0.00)	0.711 (± 0.00)	0.802 (± 0.00)	0.832 (± 0.04)	0.815 (± 0.03)	0.767 (± 0.00)
0.60	0.663 (± 0.00)	0.452 (± 0.00)	0.691 (± 0.00)	0.775 (± 0.00)	0.762 (± 0.00)	0.701 (± 0.00)	0.767 (± 0.00)	0.795 (± 0.04)	0.807 (± 0.06)	0.744 (± 0.00)
0.70	0.714 (± 0.00)	0.495 (± 0.00)	0.686 (± 0.00)	0.724 (± 0.00)	0.736 (± 0.00)	0.656 (± 0.00)	0.754 (± 0.00)	0.753 (± 0.07)	0.746 (± 0.05)	0.736 (± 0.00)
0.80	0.666 (± 0.00)	0.559 (± 0.00)	0.667 (± 0.00)	0.712 (± 0.00)	0.677 (± 0.00)	0.647 (± 0.00)	0.637 (± 0.00)	0.709 (± 0.03)	0.715 (± 0.03)	0.713 (± 0.00)
0.90	0.700 (± 0.00)	0.541 (± 0.00)	0.670 (± 0.00)	0.585 (± 0.00)	0.593 (± 0.00)	0.669 (± 0.00)	0.619 (± 0.00)	0.598 (± 0.06)	0.628 (± 0.04)	0.705 (± 0.00)
0.99	0.693 (± 0.00)	0.409 (± 0.00)	0.658 (± 0.00)	0.436 (± 0.00)	0.384 (± 0.00)	0.651 (± 0.00)	0.431 (± 0.00)	0.440 (± 0.05)	0.397 (± 0.04)	0.664 (± 0.00)

1263

1264

1265

Table 28: F1 scores for AIR under mechanism $S\text{-MCAR}$ and varying μ

1266

1267

μ	GOODIE	GSPN	FairAC	FP	GNNmi	GCNmf	PCFI	GNNzero	GNNmedian	GNNmim
0.00	0.724 (± 0.00)	0.798 (± 0.02)	0.733 (± 0.00)	0.918 (± 0.00)	0.922 (± 0.01)	0.922 (± 0.00)	0.891 (± 0.00)	0.916 (± 0.02)	0.916 (± 0.02)	0.930 (± 0.00)
0.10	0.568 (± 0.00)	0.644 (± 0.00)	0.733 (± 0.00)	0.891 (± 0.00)	0.899 (± 0.00)	0.895 (± 0.00)	0.872 (± 0.00)	0.879 (± 0.02)	0.900 (± 0.02)	0.891 (± 0.00)
0.20	0.573 (± 0.00)	0.597 (± 0.00)	0.733 (± 0.00)	0.860 (± 0.00)	0.883 (± 0.00)	0.851 (± 0.00)	0.899 (± 0.00)	0.860 (± 0.03)	0.865 (± 0.03)	0.890 (± 0.00)
0.30	0.630 (± 0.00)	0.527 (± 0.00)	0.665 (± 0.00)	0.850 (± 0.00)	0.847 (± 0.00)	0.820 (± 0.00)	0.852 (± 0.00)	0.838 (± 0.04)	0.853 (± 0.03)	0.835 (± 0.00)
0.40	0.571 (± 0.00)	0.508 (± 0.00)	0.728 (± 0.00)	0.819 (± 0.00)	0.819 (± 0.00)	0.795 (± 0.00)	0.826 (± 0.00)	0.812 (± 0.03)	0.796 (± 0.04)	0.842 (± 0.00)
0.50	0.562 (± 0.00)	0.530 (± 0.00)	0.742 (± 0.00)	0.787 (± 0.00)	0.770 (± 0.00)	0.829 (± 0.00)	0.799 (± 0.00)	0.769 (± 0.03)	0.778 (± 0.03)	0.817 (± 0.00)
0.60	0.549 (± 0.00)	0.532 (± 0.00)	0.739 (± 0.00)	0.750 (± 0.00)	0.737 (± 0.00)	0.809 (± 0.00)	0.761 (± 0.00)	0.736 (± 0.06)	0.718 (± 0.04)	0.797 (± 0.00)
0.70	0.603 (± 0.00)	0.532 (± 0.00)	0.706 (± 0.00)	0.686 (± 0.00)	0.661 (± 0.00)	0.767 (± 0.00)	0.666 (± 0.00)	0.709 (± 0.05)	0.693 (± 0.03)	0.756 (± 0.00)
0.80	0.610 (± 0.00)	0.476 (± 0.00)	0.657 (± 0.00)	0.607 (± 0.00)	0.605 (± 0.00)	0.721 (± 0.00)	0.601 (± 0.00)	0.614 (± 0.04)	0.603 (± 0.04)	0.734 (± 0.00)
0.90	0.504 (± 0.00)	0.389 (± 0.00)	0.692 (± 0.00)	0.549 (± 0.00)	0.505 (± 0.00)	0.677 (± 0.00)	0.522 (± 0.00)	0.537 (± 0.03)	0.511 (± 0.02)	0.699 (± 0.00)
0.99	0.435 (± 0.00)	0.332 (± 0.00)	0.652 (± 0.00)	0.350 (± 0.00)	0.333 (± 0.00)	0.643 (± 0.00)	0.353 (± 0.00)	0.351 (± 0.01)	0.354 (± 0.01)	0.652 (± 0.00)

1274

1275

1276

Table 29: F1 scores for AIR under mechanism $CD\text{-MCAR}$ and varying μ

1277

1278

μ	GOODIE	GSPN	FairAC	FP	GNNmi	GCNmf	PCFI	GNNzero	GNNmedian	GNNmim
0.00	0.724 (± 0.00)	0.798 (± 0.02)	0.733 (± 0.00)	0.918 (± 0.00)	0.922 (± 0.01)	0.922 (± 0.00)	0.891 (± 0.00)	0.916 (± 0.02)	0.916 (± 0.02)	0.930 (± 0.00)
0.10	0.714 (± 0.00)	0.730 (± 0.00)	0.706 (± 0.00)	0.804 (± 0.00)	0.819 (± 0.00)	0.700 (± 0.00)	0.820 (± 0.00)	0.825 (± 0.05)	0.825 (± 0.05)	0.876 (± 0.00)
0.20	0.714 (± 0.00)	0.730 (± 0.00)	0.703 (± 0.00)	0.804 (± 0.00)	0.819 (± 0.00)	0.677 (± 0.00)	0.820 (± 0.00)	0.825 (± 0.05)	0.825 (± 0.05)	0.887 (± 0.00)
0.30	0.710 (± 0.00)	0.613 (± 0.00)	0.721 (± 0.00)	0.697 (± 0.00)	0.696 (± 0.00)	0.696 (± 0.00)	0.726 (± 0.00)	0.725 (± 0.07)	0.725 (± 0.07)	0.744 (± 0.00)
0.40	0.701 (± 0.00)	0.587 (± 0.00)	0.617 (± 0.00)	0.717 (± 0.00)	0.687 (± 0.00)	0.691 (± 0.00)	0.701 (± 0.00)	0.719 (± 0.05)	0.719 (± 0.05)	0.794 (± 0.00)
0.50	0.717 (± 0.00)	0.504 (± 0.00)	0.458 (± 0.00)	0.528 (± 0.00)	0.571 (± 0.00)	0.625 (± 0.00)	0.564 (± 0.00)	0.556 (± 0.08)	0.556 (± 0.08)	0.722 (± 0.00)
0.60	0.717 (± 0.00)	0.504 (± 0.00)	0.450 (± 0.00)	0.528 (± 0.00)	0.571 (± 0.00)	0.625 (± 0.00)	0.564 (± 0.00)	0.556 (± 0.08)	0.556 (± 0.08)	0.737 (± 0.00)
0.70	0.717 (± 0.00)	0.498 (± 0.00)	0.446 (± 0.00)	0.540 (± 0.00)	0.553 (± 0.00)	0.668 (± 0.00)	0.518 (± 0.00)	0.498 (± 0.04)	0.498 (± 0.04)	0.662 (± 0.00)
0.80	0.703 (± 0.00)	0.557 (± 0.00)	0.430 (± 0.00)	0.515 (± 0.00)	0.481 (± 0.00)	0.676 (± 0.00)	0.457 (± 0.00)	0.495 (± 0.05)	0.495 (± 0.05)	0.680 (± 0.00)
0.90	0.703 (± 0.00)	0.498 (± 0.00)	0.338 (± 0.00)	0.515 (± 0.00)	0.481 (± 0.00)	0.676 (± 0.00)	0.457 (± 0.00)	0.495 (± 0.05)	0.495 (± 0.05)	0.674 (± 0.00)
0.99	0.660 (± 0.00)	0.468 (± 0.00)	0.338 (± 0.00)	0.515 (± 0.00)	0.481 (± 0.00)	0.682 (± 0.00)	0.457 (± 0.00)	0.675 (± 0.05)	0.688 (± 0.05)	0.673 (± 0.00)

1285

1286

1287

Table 30: F1 scores for AIR under mechanism $FD\text{-MNAR}$ and varying μ

1288

1289

μ	GOODIE	GSPN	FairAC	FP	GNNmi	GCNmf	PCFI	GNNzero	GNN
-------	--------	------	--------	----	-------	-------	------	---------	-----

1296

1297

1298

1299

1300

1301

1302

1303

1304

1305

1306

1307

1308

1309

1310

1311

1312

1313

1314

1315

1316

1317

1318

1319

1320

1321

1322

1323

1324

1325

1326

1327

1328

1329

1330

1331

1332

1333

1334

1335

1336

1337

1338

1339

1340

1341

1342

1343

1344

1345

1346

1347

1348

1349

Table 31: F1 scores for AIR under mechanism *CD-MNAR* and varying μ

μ	GOODIE	GSPN	FairAC	FP	GNNmi	GCNmf	PCFI	GNNzero	GNNmedian	GNNmim
0.00	0.724 (± 0.00)	0.798 (± 0.02)	0.733 (± 0.00)	0.918 (± 0.00)	0.922 (± 0.01)	0.922 (± 0.00)	0.891 (± 0.00)	0.916 (± 0.02)	0.916 (± 0.02)	0.930 (± 0.00)
0.10	0.598 (± 0.11)	0.667 (± 0.02)	0.722 (± 0.02)	0.888 (± 0.05)	0.887 (± 0.04)	0.851 (± 0.01)	0.891 (± 0.03)	0.860 (± 0.04)	0.883 (± 0.04)	0.895 (± 0.04)
0.20	0.556 (± 0.16)	0.632 (± 0.19)	0.697 (± 0.02)	0.864 (± 0.02)	0.848 (± 0.06)	0.778 (± 0.04)	0.841 (± 0.01)	0.853 (± 0.04)	0.836 (± 0.04)	0.864 (± 0.01)
0.30	0.556 (± 0.16)	0.526 (± 0.13)	0.722 (± 0.03)	0.845 (± 0.01)	0.825 (± 0.04)	0.689 (± 0.02)	0.841 (± 0.03)	0.855 (± 0.02)	0.806 (± 0.04)	0.891 (± 0.04)
0.40	0.480 (± 0.16)	0.691 (± 0.14)	0.601 (± 0.12)	0.833 (± 0.02)	0.805 (± 0.03)	0.722 (± 0.02)	0.860 (± 0.03)	0.856 (± 0.02)	0.811 (± 0.02)	0.860 (± 0.03)
0.50	0.536 (± 0.16)	0.607 (± 0.09)	0.705 (± 0.02)	0.813 (± 0.02)	0.769 (± 0.04)	0.674 (± 0.01)	0.783 (± 0.04)	0.790 (± 0.05)	0.777 (± 0.05)	0.833 (± 0.03)
0.60	0.622 (± 0.06)	0.636 (± 0.04)	0.694 (± 0.01)	0.758 (± 0.05)	0.708 (± 0.07)	0.681 (± 0.01)	0.766 (± 0.06)	0.814 (± 0.03)	0.774 (± 0.07)	0.766 (± 0.06)
0.70	0.580 (± 0.10)	0.672 (± 0.07)	0.681 (± 0.01)	0.757 (± 0.03)	0.724 (± 0.04)	0.644 (± 0.02)	0.753 (± 0.05)	0.755 (± 0.06)	0.720 (± 0.02)	0.726 (± 0.05)
0.80	0.563 (± 0.12)	0.681 (± 0.05)	0.676 (± 0.01)	0.733 (± 0.02)	0.655 (± 0.02)	0.658 (± 0.02)	0.712 (± 0.01)	0.735 (± 0.05)	0.686 (± 0.06)	0.769 (± 0.03)
0.90	0.655 (± 0.03)	0.615 (± 0.04)	0.653 (± 0.01)	0.693 (± 0.04)	0.579 (± 0.04)	0.643 (± 0.04)	0.692 (± 0.06)	0.678 (± 0.03)	0.613 (± 0.04)	0.668 (± 0.02)
0.99	0.654 (± 0.03)	0.522 (± 0.04)	0.660 (± 0.05)	0.524 (± 0.07)	0.473 (± 0.05)	0.650 (± 0.06)	0.424 (± 0.06)	0.523 (± 0.06)	0.411 (± 0.03)	0.631 (± 0.07)

Table 32: F1 scores for ELECTRIC under mechanism *U-MCAR* and varying μ

μ	GOODIE	GSPN	FairAC	FP	GNNmi	GCNmf	PCFI	GNNzero	GNNmedian	GNNmim
0.00	0.588 (± 0.00)	0.915 (± 0.00)	0.963 (± 0.01)	0.885 (± 0.00)	0.929 (± 0.00)	0.861 (± 0.00)	0.903 (± 0.00)	0.912 (± 0.01)	0.909 (± 0.01)	0.938 (± 0.01)
0.10	0.589 (± 0.00)	0.827 (± 0.00)	0.931 (± 0.00)	0.865 (± 0.00)	0.864 (± 0.00)	0.887 (± 0.00)	0.889 (± 0.00)	0.855 (± 0.03)	0.854 (± 0.02)	0.923 (± 0.00)
0.20	0.589 (± 0.00)	0.806 (± 0.00)	0.935 (± 0.00)	0.821 (± 0.00)	0.807 (± 0.00)	0.876 (± 0.00)	0.877 (± 0.00)	0.805 (± 0.03)	0.807 (± 0.03)	0.877 (± 0.00)
0.30	0.588 (± 0.00)	0.770 (± 0.00)	0.924 (± 0.00)	0.758 (± 0.00)	0.780 (± 0.00)	0.889 (± 0.00)	0.872 (± 0.00)	0.742 (± 0.03)	0.781 (± 0.04)	0.868 (± 0.00)
0.40	0.590 (± 0.00)	0.703 (± 0.00)	0.906 (± 0.00)	0.711 (± 0.00)	0.728 (± 0.00)	0.874 (± 0.00)	0.865 (± 0.00)	0.710 (± 0.02)	0.746 (± 0.04)	0.859 (± 0.00)
0.50	0.587 (± 0.00)	0.626 (± 0.00)	0.922 (± 0.00)	0.676 (± 0.00)	0.693 (± 0.00)	0.864 (± 0.00)	0.841 (± 0.00)	0.676 (± 0.03)	0.721 (± 0.04)	0.804 (± 0.00)
0.60	0.584 (± 0.00)	0.567 (± 0.00)	0.881 (± 0.00)	0.598 (± 0.00)	0.614 (± 0.00)	0.877 (± 0.00)	0.793 (± 0.00)	0.597 (± 0.04)	0.663 (± 0.06)	0.779 (± 0.00)
0.70	0.582 (± 0.00)	0.506 (± 0.00)	0.868 (± 0.00)	0.548 (± 0.00)	0.553 (± 0.00)	0.831 (± 0.00)	0.771 (± 0.00)	0.528 (± 0.02)	0.601 (± 0.06)	0.766 (± 0.00)
0.80	0.592 (± 0.00)	0.397 (± 0.00)	0.852 (± 0.00)	0.496 (± 0.00)	0.522 (± 0.00)	0.807 (± 0.00)	0.730 (± 0.00)	0.465 (± 0.03)	0.509 (± 0.06)	0.728 (± 0.00)
0.90	0.593 (± 0.00)	0.389 (± 0.00)	0.744 (± 0.00)	0.361 (± 0.00)	0.423 (± 0.00)	0.701 (± 0.00)	0.628 (± 0.00)	0.407 (± 0.04)	0.395 (± 0.02)	0.646 (± 0.00)
0.99	0.592 (± 0.00)	0.289 (± 0.00)	0.260 (± 0.00)	0.285 (± 0.00)	0.282 (± 0.00)	0.630 (± 0.00)	0.333 (± 0.00)	0.278 (± 0.01)	0.276 (± 0.01)	0.412 (± 0.00)

Table 33: F1 scores for ELECTRIC under mechanism *S-MCAR* and varying μ

μ	GOODIE	GSPN	FairAC	FP	GNNmi	GCNmf	PCFI	GNNzero	GNNmedian	GNNmim
0.00	0.588 (± 0.00)	0.915 (± 0.00)	0.963 (± 0.01)	0.885 (± 0.00)	0.929 (± 0.00)	0.861 (± 0.00)	0.903 (± 0.00)	0.908 (± 0.01)	0.912 (± 0.01)	0.938 (± 0.01)
0.10	0.493 (± 0.00)	0.891 (± 0.00)	0.959 (± 0.00)	0.831 (± 0.00)	0.853 (± 0.00)	0.862 (± 0.00)	0.854 (± 0.00)	0.872 (± 0.01)	0.873 (± 0.02)	0.904 (± 0.00)
0.20	0.484 (± 0.00)	0.855 (± 0.00)	0.945 (± 0.00)	0.821 (± 0.00)	0.851 (± 0.00)	0.867 (± 0.00)	0.870 (± 0.00)	0.833 (± 0.01)	0.842 (± 0.03)	0.878 (± 0.00)
0.30	0.478 (± 0.00)	0.816 (± 0.00)	0.935 (± 0.00)	0.768 (± 0.00)	0.796 (± 0.00)	0.872 (± 0.00)	0.856 (± 0.00)	0.776 (± 0.02)	0.805 (± 0.02)	0.855 (± 0.00)
0.40	0.483 (± 0.00)	0.756 (± 0.00)	0.924 (± 0.00)	0.703 (± 0.00)	0.734 (± 0.00)	0.842 (± 0.00)	0.871 (± 0.00)	0.736 (± 0.03)	0.754 (± 0.01)	0.801 (± 0.00)
0.50	0.431 (± 0.00)	0.708 (± 0.00)	0.926 (± 0.00)	0.656 (± 0.00)	0.665 (± 0.00)	0.839 (± 0.00)	0.844 (± 0.00)	0.682 (± 0.02)	0.712 (± 0.01)	0.810 (± 0.00)
0.60	0.397 (± 0.00)	0.632 (± 0.00)	0.898 (± 0.00)	0.619 (± 0.00)	0.617 (± 0.00)	0.813 (± 0.00)	0.808 (± 0.00)	0.627 (± 0.03)	0.651 (± 0.01)	0.787 (± 0.00)
0.70	0.435 (± 0.00)	0.563 (± 0.00)	0.870 (± 0.00)	0.528 (± 0.00)	0.545 (± 0.00)	0.799 (± 0.00)	0.776 (± 0.00)	0.543 (± 0.04)	0.586 (± 0.05)	0.711 (± 0.00)
0.80	0.490 (± 0.00)	0.522 (± 0.00)	0.806 (± 0.00)	0.475 (± 0.00)	0.455 (± 0.00)	0.764 (± 0.00)	0.770 (± 0.00)	0.477 (± 0.03)	0.493 (± 0.02)	0.676 (± 0.00)
0.90	0.374 (± 0.00)	0.392 (± 0.00)	0.771 (± 0.00)	0.420 (± 0.00)	0.394 (± 0.00)	0.738 (± 0.00)	0.496 (± 0.00)	0.374 (± 0.03)	0.381 (± 0.03)	0.567 (± 0.00)
0.99	0.260 (± 0.00)	0.265 (± 0.00)	0.260 (± 0.00)	0.260 (± 0.00)	0.260 (± 0.00)	0.630 (± 0.00)	0.260 (± 0.00)	0.382 (± 0.01)	0.423 (± 0.02)	0.552 (± 0.00)

Table 34: F1 scores for ELECTRIC under mechanism *CD-MCAR* and varying μ

μ	GOODIE	GSPN	FairAC	FP	GNNmi	GCNmf	PCFI	GNNzero	GNNmedian	GNNmim
0.00	0.588 (± 0.00)	0.915 (± 0.00)	0.963 (± 0.01)	0.885 (± 0.00)	0.929 (± 0.00)	0.861 (± 0.00)	0.903 (± 0.00)	0.911 (± 0.01)	0.913 (± 0.01)	0.938 (± 0.01)
0.10	0.468 (± 0.15)	0.879 (± 0.01)	0.944 (± 0.02)	0.862 (± 0.03)	0.844 (± 0.02)	0.878 (± 0.03)	0.870 (± 0.04)	0.840 (± 0.03)	0.851 (± 0.02)	0.916 (± 0.01)
0.20	0.491 (± 0.13)	0.850 (± 0.01)	0.938 (± 0.01)	0.808 (± 0.02)	0.813 (± 0.02)	0.867 (± 0.01)	0.859 (± 0.02)	0.789 (± 0.02)	0.802 (± 0.03)	0.906 (± 0.00)
0.30	0.496 (± 0.13)	0.800 (± 0.02)	0.922 (± 0.03)	0.744 (± 0.02)	0.793 (± 0.01)	0.864 (± 0.03)	0.861 (± 0.01)	0.727 (± 0.02)	0.798 (± 0.03)	0.877 (± 0.01)
0.40	0.506 (± 0.12)	0.772 (± 0.04)	0.906 (± 0.03)	0.701 (± 0.03)	0.751 (± 0.03)	0.850 (± 0.02)	0.839 (± 0.01)	0.674 (± 0.02)	0.726 (± 0.03)	0.864 (± 0.01)
0.50	0.438 (± 0.12)	0.743 (± 0.01)	0.877 (± 0.01)	0.648 (± 0.03)	0.707 (± 0.02)	0.842 (± 0.02)	0.817 (± 0.03)	0.642 (± 0.05)	0.699 (± 0.08)	0.837 (± 0.02)
0.60	0.331 (± 0.05)	0.688 (± 0.02)	0.836 (± 0.03)	0.594 (± 0.02)	0.663 (± 0.01)	0.807 (± 0.05)	0.775 (± 0.02)	0.590 (± 0.03)	0.607 (± 0.03)	0.806 (± 0.01)
0.70	0.461 (± 0.14)	0.626 (± 0.01)	0.834 (± 0.04)	0.514 (± 0.04)	0.590 (± 0.02)	0.776 (± 0.02)	0.761 (± 0.02)	0.482 (± 0.03)	0.433 (± 0.09)	0.760 (± 0.02)
0.80	0.435 (± 0.12)	0.57								

1350

1351 Table 36: F1 scores for ELECTRIC under mechanism *CD-MNAR* and varying μ

μ	GOODIE	GSPN	FairAC	FP	GNNmi	GCNmf	PCFI	GNNzero	GNNmedian	GNNmim
0.00	0.588 (± 0.00)	0.915 (± 0.00)	0.963 (± 0.01)	0.885 (± 0.00)	0.929 (± 0.00)	0.861 (± 0.00)	0.903 (± 0.00)	0.908 (± 0.01)	0.908 (± 0.01)	0.938 (± 0.01)
0.10	0.486 (± 0.12)	0.888 (± 0.01)	0.962 (± 0.01)	0.869 (± 0.01)	0.874 (± 0.01)	0.908 (± 0.02)	0.885 (± 0.03)	0.839 (± 0.03)	0.860 (± 0.02)	0.922 (± 0.00)
0.20	0.476 (± 0.15)	0.851 (± 0.02)	0.931 (± 0.02)	0.815 (± 0.03)	0.802 (± 0.01)	0.879 (± 0.01)	0.879 (± 0.01)	0.805 (± 0.03)	0.801 (± 0.00)	0.902 (± 0.03)
0.30	0.478 (± 0.16)	0.819 (± 0.04)	0.922 (± 0.00)	0.789 (± 0.03)	0.789 (± 0.01)	0.872 (± 0.01)	0.880 (± 0.01)	0.770 (± 0.05)	0.736 (± 0.01)	0.890 (± 0.00)
0.40	0.431 (± 0.11)	0.807 (± 0.02)	0.902 (± 0.01)	0.775 (± 0.01)	0.762 (± 0.01)	0.835 (± 0.02)	0.865 (± 0.02)	0.749 (± 0.03)	0.685 (± 0.05)	0.869 (± 0.02)
0.50	0.450 (± 0.09)	0.758 (± 0.02)	0.867 (± 0.03)	0.722 (± 0.02)	0.748 (± 0.01)	0.835 (± 0.03)	0.827 (± 0.03)	0.656 (± 0.03)	0.633 (± 0.04)	0.850 (± 0.02)
0.60	0.436 (± 0.10)	0.706 (± 0.01)	0.853 (± 0.05)	0.663 (± 0.02)	0.608 (± 0.01)	0.847 (± 0.03)	0.780 (± 0.02)	0.664 (± 0.03)	0.593 (± 0.04)	0.836 (± 0.02)
0.70	0.337 (± 0.03)	0.604 (± 0.03)	0.812 (± 0.03)	0.585 (± 0.03)	0.538 (± 0.03)	0.770 (± 0.09)	0.729 (± 0.01)	0.560 (± 0.02)	0.514 (± 0.02)	0.765 (± 0.01)
0.80	0.411 (± 0.09)	0.594 (± 0.02)	0.824 (± 0.08)	0.540 (± 0.01)	0.486 (± 0.01)	0.703 (± 0.04)	0.671 (± 0.01)	0.513 (± 0.01)	0.469 (± 0.02)	0.742 (± 0.02)
0.90	0.392 (± 0.11)	0.531 (± 0.02)	0.735 (± 0.07)	0.473 (± 0.03)	0.449 (± 0.02)	0.686 (± 0.06)	0.600 (± 0.04)	0.434 (± 0.02)	0.445 (± 0.04)	0.683 (± 0.02)
0.99	0.304 (± 0.02)	0.329 (± 0.04)	0.264 (± 0.01)	0.303 (± 0.02)	0.294 (± 0.01)	0.629 (± 0.00)	0.312 (± 0.04)	0.305 (± 0.02)	0.292 (± 0.02)	0.561 (± 0.02)

1360

1361

1362

1363 Table 37: F1 scores for TADPOLE under mechanism *U-MCAR* and varying μ

μ	GOODIE	GSPN	FairAC	FP	GNNmi	GCNmf	PCFI	GNNzero	GNNmedian	GNNmim
0.00	0.804 (± 0.00)	0.648 (± 0.01)	0.790 (± 0.00)	0.806 (± 0.00)	0.832 (± 0.02)	0.786 (± 0.00)	0.792 (± 0.00)	0.847 (± 0.03)	0.847 (± 0.03)	0.809 (± 0.00)
0.10	0.789 (± 0.00)	0.590 (± 0.00)	0.795 (± 0.00)	0.801 (± 0.00)	0.832 (± 0.00)	0.809 (± 0.00)	0.821 (± 0.00)	0.841 (± 0.03)	0.837 (± 0.03)	0.820 (± 0.00)
0.20	0.808 (± 0.00)	0.590 (± 0.00)	0.803 (± 0.00)	0.823 (± 0.00)	0.836 (± 0.00)	0.779 (± 0.00)	0.802 (± 0.00)	0.833 (± 0.03)	0.827 (± 0.04)	0.799 (± 0.00)
0.30	0.814 (± 0.00)	0.567 (± 0.00)	0.791 (± 0.00)	0.806 (± 0.00)	0.825 (± 0.00)	0.757 (± 0.00)	0.803 (± 0.00)	0.811 (± 0.03)	0.813 (± 0.03)	0.802 (± 0.00)
0.40	0.804 (± 0.00)	0.610 (± 0.00)	0.831 (± 0.00)	0.800 (± 0.00)	0.820 (± 0.00)	0.794 (± 0.00)	0.799 (± 0.00)	0.830 (± 0.01)	0.819 (± 0.02)	0.805 (± 0.00)
0.50	0.752 (± 0.00)	0.581 (± 0.00)	0.813 (± 0.00)	0.809 (± 0.00)	0.830 (± 0.00)	0.799 (± 0.00)	0.810 (± 0.00)	0.797 (± 0.03)	0.790 (± 0.03)	0.814 (± 0.00)
0.60	0.756 (± 0.00)	0.575 (± 0.00)	0.808 (± 0.00)	0.785 (± 0.00)	0.797 (± 0.00)	0.722 (± 0.00)	0.791 (± 0.00)	0.810 (± 0.05)	0.771 (± 0.04)	0.799 (± 0.00)
0.70	0.610 (± 0.00)	0.552 (± 0.00)	0.795 (± 0.00)	0.740 (± 0.00)	0.772 (± 0.00)	0.729 (± 0.00)	0.762 (± 0.00)	0.779 (± 0.04)	0.767 (± 0.03)	0.802 (± 0.00)
0.80	0.669 (± 0.00)	0.552 (± 0.00)	0.804 (± 0.00)	0.757 (± 0.00)	0.728 (± 0.00)	0.669 (± 0.00)	0.775 (± 0.00)	0.760 (± 0.05)	0.736 (± 0.04)	0.764 (± 0.00)
0.90	0.759 (± 0.00)	0.590 (± 0.00)	0.241 (± 0.00)	0.758 (± 0.00)	0.408 (± 0.00)	0.608 (± 0.00)	0.767 (± 0.00)	0.786 (± 0.02)	0.704 (± 0.02)	0.763 (± 0.00)
0.99	0.707 (± 0.00)	0.523 (± 0.00)	0.241 (± 0.00)	0.241 (± 0.00)	0.353 (± 0.00)	0.241 (± 0.00)	0.507 (± 0.22)	0.241 (± 0.00)	0.700 (± 0.00)	

1371

1372

1373

1374 Table 38: F1 scores for TADPOLE under mechanism *S-MCAR* and varying μ

μ	GOODIE	GSPN	FairAC	FP	GNNmi	GCNmf	PCFI	GNNzero	GNNmedian	GNNmim
0.00	0.804 (± 0.00)	0.648 (± 0.01)	0.790 (± 0.00)	0.806 (± 0.00)	0.832 (± 0.02)	0.786 (± 0.00)	0.792 (± 0.00)	0.847 (± 0.03)	0.847 (± 0.03)	0.831 (± 0.04)
0.10	0.554 (± 0.00)	0.542 (± 0.00)	0.803 (± 0.00)	0.815 (± 0.00)	0.751 (± 0.00)	0.804 (± 0.00)	0.848 (± 0.02)	0.846 (± 0.02)	0.846 (± 0.02)	0.810 (± 0.00)
0.20	0.497 (± 0.00)	0.486 (± 0.00)	0.818 (± 0.00)	0.818 (± 0.00)	0.811 (± 0.00)	0.737 (± 0.00)	0.814 (± 0.00)	0.846 (± 0.02)	0.845 (± 0.03)	0.794 (± 0.00)
0.30	0.523 (± 0.00)	0.502 (± 0.00)	0.775 (± 0.00)	0.799 (± 0.00)	0.825 (± 0.00)	0.777 (± 0.00)	0.818 (± 0.00)	0.837 (± 0.02)	0.838 (± 0.02)	0.775 (± 0.00)
0.40	0.482 (± 0.00)	0.581 (± 0.00)	0.769 (± 0.00)	0.797 (± 0.00)	0.794 (± 0.00)	0.719 (± 0.00)	0.784 (± 0.00)	0.820 (± 0.03)	0.823 (± 0.04)	0.790 (± 0.00)
0.50	0.501 (± 0.00)	0.523 (± 0.00)	0.757 (± 0.00)	0.777 (± 0.00)	0.769 (± 0.00)	0.739 (± 0.00)	0.798 (± 0.00)	0.803 (± 0.02)	0.797 (± 0.03)	0.795 (± 0.00)
0.60	0.539 (± 0.00)	0.498 (± 0.00)	0.802 (± 0.00)	0.769 (± 0.00)	0.734 (± 0.00)	0.693 (± 0.00)	0.804 (± 0.00)	0.804 (± 0.05)	0.799 (± 0.04)	0.816 (± 0.00)
0.70	0.480 (± 0.00)	0.453 (± 0.00)	0.748 (± 0.00)	0.719 (± 0.00)	0.738 (± 0.00)	0.642 (± 0.00)	0.752 (± 0.00)	0.784 (± 0.03)	0.777 (± 0.05)	0.795 (± 0.00)
0.80	0.502 (± 0.00)	0.422 (± 0.00)	0.689 (± 0.00)	0.736 (± 0.00)	0.703 (± 0.00)	0.555 (± 0.00)	0.730 (± 0.00)	0.739 (± 0.02)	0.740 (± 0.06)	0.812 (± 0.00)
0.90	0.377 (± 0.00)	0.280 (± 0.00)	0.503 (± 0.00)	0.680 (± 0.00)	0.650 (± 0.00)	0.420 (± 0.00)	0.739 (± 0.00)	0.662 (± 0.07)	0.557 (± 0.06)	0.742 (± 0.00)
0.99	0.272 (± 0.00)	0.249 (± 0.00)	0.241 (± 0.00)	0.384 (± 0.00)	0.241 (± 0.00)	0.361 (± 0.00)	0.337 (± 0.00)	0.292 (± 0.00)	0.323 (± 0.05)	0.241 (± 0.00)

1393

1394

1395

1396 Table 40: F1 scores for TADPOLE under mechanism *FD-MNAR* and varying μ

μ	GOODIE	GSPN	FairAC	FP	GNNmi	GCNmf	PCFI	GNNzero	GNNmedian	GNNmim
0.00	0.804 (± 0.00)	0.648 (± 0.01)	0.790 (± 0.00)	0.806 (± 0.00)	0.832 (± 0.02)	0.786 (± 0.00)	0.792 (± 0.00)	0.846 (± 0.03)	0.849 (± 0.03)	0.831 (± 0.04)
0.10	0.546 (± 0.07)	0.643 (± 0.01)	0.801 (± 0.01)	0.797 (± 0.01)	0.822 (± 0.02)	0.830 (± 0.04)	0.838 (± 0.03)	0.841 (± 0.03)	0.842 (± 0.03)	0.846 (± 0.04)
0.20	0.531 (± 0.11)	0.624 (± 0.05)	0.793 (± 0.04)	0.836 (± 0.01)	0.810 (± 0.01)	0.832 (± 0.02)	0.827 (± 0.01)	0.832 (± 0.03)	0.817 (± 0.03)	0.796 (± 0.00)
0.30	0.573 (± 0.12)	0.580 (± 0.04)	0.804 (± 0.05)	0.811 (± 0.03)	0.806 (± 0.04)	0.829 (± 0.04)	0.831 (± 0.02)	0.827 (± 0.03)	0.802 (± 0.03)	0.828 (± 0.03)
0.40	0.562 (± 0.09)	0.615 (± 0.03)	0.751 (± 0.03)	0.803 (± 0.04)	0.793 (± 0.04)	0.811 (± 0.02)	0.802 (± 0.03)	0.806 (± 0.03)	0.803 (± 0.03)	0.781 (± 0.02)
0.50	0.673 (± 0.04)	0.646 (± 0.07)</								

1404
 1405
 1406
 1407
 1408
 1409
 1410
 1411
 1412
 1413
 1414
 1415
 1416
 1417
 1418
 1419
 1420
 1421
 1422
 1423
 1424
 1425
 1426

Table 41: F1 scores for TADPOLE under mechanism *CD-MNAR* and varying μ

μ	GOODIE	GSPN	FairAC	FP	GNNmi	GCNmf	PCFI	GNNzero	GNNmedian	GNNmim
0.00	0.804 (± 0.00)	0.648 (± 0.01)	0.790 (± 0.00)	0.806 (± 0.00)	0.832 (± 0.02)	0.786 (± 0.00)	0.792 (± 0.00)	0.847 (± 0.03)	0.847 (± 0.03)	0.809 (± 0.00)
0.10	0.553 (± 0.06)	0.534 (± 0.09)	0.793 (± 0.05)	0.813 (± 0.03)	0.829 (± 0.04)	0.792 (± 0.03)	0.806 (± 0.03)	0.842 (± 0.02)	0.826 (± 0.04)	0.803 (± 0.01)
0.20	0.485 (± 0.06)	0.515 (± 0.04)	0.804 (± 0.03)	0.812 (± 0.03)	0.832 (± 0.03)	0.810 (± 0.02)	0.806 (± 0.02)	0.849 (± 0.01)	0.826 (± 0.04)	0.815 (± 0.02)
0.30	0.441 (± 0.02)	0.584 (± 0.06)	0.805 (± 0.03)	0.785 (± 0.02)	0.811 (± 0.03)	0.786 (± 0.02)	0.812 (± 0.02)	0.828 (± 0.03)	0.813 (± 0.04)	0.827 (± 0.03)
0.40	0.502 (± 0.07)	0.671 (± 0.03)	0.828 (± 0.01)	0.818 (± 0.03)	0.808 (± 0.02)	0.793 (± 0.02)	0.814 (± 0.03)	0.824 (± 0.02)	0.826 (± 0.03)	0.830 (± 0.01)
0.50	0.448 (± 0.02)	0.621 (± 0.04)	0.784 (± 0.02)	0.804 (± 0.04)	0.799 (± 0.04)	0.756 (± 0.03)	0.803 (± 0.05)	0.819 (± 0.02)	0.800 (± 0.04)	0.828 (± 0.04)
0.60	0.457 (± 0.01)	0.529 (± 0.03)	0.791 (± 0.01)	0.781 (± 0.03)	0.803 (± 0.03)	0.710 (± 0.07)	0.797 (± 0.03)	0.823 (± 0.04)	0.783 (± 0.03)	0.792 (± 0.03)
0.70	0.485 (± 0.07)	0.590 (± 0.09)	0.639 (± 0.29)	0.797 (± 0.05)	0.787 (± 0.04)	0.710 (± 0.05)	0.822 (± 0.02)	0.813 (± 0.03)	0.784 (± 0.07)	0.818 (± 0.01)
0.80	0.376 (± 0.10)	0.605 (± 0.04)	0.434 (± 0.27)	0.785 (± 0.05)	0.767 (± 0.09)	0.744 (± 0.01)	0.798 (± 0.05)	0.819 (± 0.04)	0.776 (± 0.04)	0.800 (± 0.02)
0.90	0.362 (± 0.09)	0.563 (± 0.03)	0.241 (± 0.00)	0.788 (± 0.01)	0.730 (± 0.08)	0.689 (± 0.05)	0.776 (± 0.06)	0.771 (± 0.06)	0.704 (± 0.05)	0.803 (± 0.05)
0.99	0.324 (± 0.12)	0.547 (± 0.08)	0.241 (± 0.00)	0.255 (± 0.02)	0.241 (± 0.00)	0.348 (± 0.05)	0.241 (± 0.00)	0.558 (± 0.15)	0.241 (± 0.00)	0.652 (± 0.04)

1436
 1437
 1438
 1439
 1440
 1441
 1442
 1443
 1444
 1445
 1446
 1447
 1448
 1449
 1450
 1451
 1452
 1453
 1454
 1455
 1456
 1457

1458 **G COMPLETE RESULT TABLES – R2 REGIME**
1459

1460 This appendix complements the analysis of Research Question 3 (Section 4). It reports the complete
1461 set of results for the R2 regime, where training and test data are subject to different missingness
1462 mechanisms. We include both numerical tables (F1-score mean \pm std over 5 runs) and extended
1463 visualizations across all models and datasets.

1464 **G.1 NUMERICAL RESULTS**
1465

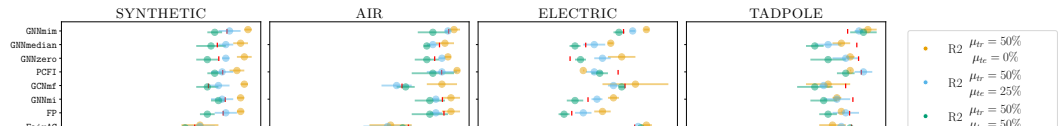
1466 Table 42 reports the full F1-scores for all models, datasets, and shift configurations considered in
1467 the R2 regime.

1469 Table 42: F1 (mean \pm std over 5 runs). Setup: **R2** missingness distribution shift, where training
1470 data are subject to either *FD-MNAR* or *CD-MNAR*, while test data have either no missingness, 25%
1471 or 50% of *U-MCAR*

Task	Train mech.	μ_{Test}	GOODIE	GSPN	FairAC	GCNmf	PCFI	FP	GNNmi	GNNzero	GNNmedian	GNNmim
SYNTHETIC	<i>FD-MNAR</i>	0	0.50 (± 0.15)	0.68 (± 0.01)	0.69 (± 0.05)	0.81 (± 0.01)	0.79 (± 0.02)	0.80 (± 0.01)	0.81 (± 0.02)	0.80 (± 0.02)	0.82 (± 0.01)	
	<i>FD-MNAR</i>	0.25	0.47 (± 0.13)	0.64 (± 0.03)	0.69 (± 0.04)	0.74 (± 0.03)	0.75 (± 0.03)	0.76 (± 0.03)	0.75 (± 0.03)	0.76 (± 0.01)	0.76 (± 0.02)	0.77 (± 0.03)
	<i>CD-MNAR</i>	0.50	0.47 (± 0.13)	0.64 (± 0.02)	0.65 (± 0.04)	0.71 (± 0.03)	0.73 (± 0.02)	0.71 (± 0.02)	0.74 (± 0.02)	0.71 (± 0.03)	0.72 (± 0.04)	0.73 (± 0.02)
	<i>CD-MNAR</i>	0	0.71 (± 0.07)	0.70 (± 0.03)	0.70 (± 0.05)	0.80 (± 0.04)	0.81 (± 0.02)	0.80 (± 0.02)	0.78 (± 0.02)	0.82 (± 0.02)	0.76 (± 0.02)	0.85 (± 0.04)
	<i>CD-MNAR</i>	0.25	0.66 (± 0.05)	0.68 (± 0.05)	0.68 (± 0.03)	0.75 (± 0.06)	0.78 (± 0.04)	0.77 (± 0.04)	0.77 (± 0.02)	0.78 (± 0.03)	0.72 (± 0.03)	0.80 (± 0.03)
	<i>CD-MNAR</i>	0.50	0.56 (± 0.10)	0.64 (± 0.04)	0.65 (± 0.01)	0.73 (± 0.02)	0.72 (± 0.03)	0.72 (± 0.05)	0.72 (± 0.01)	0.72 (± 0.04)	0.70 (± 0.01)	0.75 (± 0.03)
AIR	<i>FD-MNAR</i>	0	0.50 (± 0.14)	0.33 (± 0.04)	0.66 (± 0.07)	0.83 (± 0.05)	0.88 (± 0.01)	0.86 (± 0.03)	0.86 (± 0.03)	0.85 (± 0.01)	0.84 (± 0.03)	0.87 (± 0.02)
	<i>FD-MNAR</i>	0.25	0.51 (± 0.12)	0.42 (± 0.04)	0.65 (± 0.08)	0.68 (± 0.05)	0.83 (± 0.05)	0.81 (± 0.02)	0.81 (± 0.01)	0.83 (± 0.01)	0.80 (± 0.02)	0.85 (± 0.01)
	<i>FD-MNAR</i>	0.50	0.52 (± 0.11)	0.55 (± 0.03)	0.70 (± 0.03)	0.71 (± 0.03)	0.80 (± 0.07)	0.79 (± 0.06)	0.79 (± 0.05)	0.78 (± 0.04)	0.78 (± 0.01)	0.80 (± 0.05)
	<i>CD-MNAR</i>	0	0.56 (± 0.16)	0.35 (± 0.02)	0.65 (± 0.08)	0.60 (± 0.20)	0.88 (± 0.01)	0.71 (± 0.07)	0.86 (± 0.06)	0.83 (± 0.07)	0.82 (± 0.03)	0.85 (± 0.00)
	<i>CD-MNAR</i>	0.25	0.56 (± 0.16)	0.45 (± 0.50)	0.70 (± 0.05)	0.70 (± 0.05)	0.84 (± 0.05)	0.75 (± 0.05)	0.84 (± 0.04)	0.80 (± 0.05)	0.79 (± 0.03)	0.84 (± 0.06)
	<i>CD-MNAR</i>	0.50	0.62 (± 0.07)	0.47 (± 0.04)	0.68 (± 0.07)	0.70 (± 0.02)	0.80 (± 0.05)	0.72 (± 0.03)	0.76 (± 0.05)	0.74 (± 0.03)	0.76 (± 0.02)	
ELECTRIC	<i>FD-MNAR</i>	0	0.45 (± 0.11)	0.67 (± 0.11)	0.92 (± 0.02)	0.88 (± 0.12)	0.69 (± 0.00)	0.76 (± 0.03)	0.80 (± 0.02)	0.83 (± 0.05)	0.79 (± 0.01)	0.92 (± 0.01)
	<i>FD-MNAR</i>	0.25	0.53 (± 0.10)	0.68 (± 0.06)	0.89 (± 0.00)	0.80 (± 0.02)	0.73 (± 0.03)	0.69 (± 0.03)	0.74 (± 0.02)	0.76 (± 0.03)	0.73 (± 0.04)	0.87 (± 0.01)
	<i>FD-MNAR</i>	0.50	0.50 (± 0.10)	0.68 (± 0.01)	0.90 (± 0.02)	0.83 (± 0.01)	0.75 (± 0.03)	0.62 (± 0.02)	0.66 (± 0.03)	0.68 (± 0.02)	0.66 (± 0.02)	0.82 (± 0.02)
	<i>CD-MNAR</i>	0	0.52 (± 0.10)	0.78 (± 0.04)	0.92 (± 0.02)	0.86 (± 0.01)	0.88 (± 0.01)	0.83 (± 0.05)	0.81 (± 0.01)	0.81 (± 0.01)	0.79 (± 0.02)	0.94 (± 0.00)
	<i>CD-MNAR</i>	0.25	0.50 (± 0.10)	0.78 (± 0.01)	0.88 (± 0.01)	0.86 (± 0.02)	0.85 (± 0.02)	0.74 (± 0.04)	0.73 (± 0.03)	0.72 (± 0.01)	0.73 (± 0.02)	0.85 (± 0.03)
	<i>CD-MNAR</i>	0.50	0.49 (± 0.12)	0.70 (± 0.02)	0.87 (± 0.02)	0.82 (± 0.03)	0.81 (± 0.00)	0.66 (± 0.01)	0.70 (± 0.03)	0.65 (± 0.02)	0.68 (± 0.02)	0.83 (± 0.02)
TADPOLE	<i>FD-MNAR</i>	0	0.52 (± 0.07)	0.53 (± 0.00)	0.75 (± 0.03)	0.74 (± 0.05)	0.79 (± 0.00)	0.77 (± 0.00)	0.76 (± 0.01)	0.79 (± 0.01)	0.77 (± 0.02)	0.83 (± 0.02)
	<i>FD-MNAR</i>	0.25	0.48 (± 0.03)	0.48 (± 0.02)	0.77 (± 0.01)	0.73 (± 0.01)	0.82 (± 0.02)	0.78 (± 0.03)	0.76 (± 0.03)	0.78 (± 0.03)	0.74 (± 0.03)	0.81 (± 0.01)
	<i>FD-MNAR</i>	0.50	0.48 (± 0.04)	0.53 (± 0.02)	0.79 (± 0.02)	0.71 (± 0.04)	0.78 (± 0.02)	0.74 (± 0.02)	0.73 (± 0.03)	0.74 (± 0.04)	0.71 (± 0.02)	0.82 (± 0.03)
	<i>CD-MNAR</i>	0	0.60 (± 0.02)	0.26 (± 0.02)	0.79 (± 0.05)	0.75 (± 0.04)	0.80 (± 0.04)	0.80 (± 0.03)	0.79 (± 0.05)	0.79 (± 0.04)	0.75 (± 0.04)	0.79 (± 0.06)
	<i>CD-MNAR</i>	0.25	0.47 (± 0.09)	0.52 (± 0.02)	0.82 (± 0.05)	0.78 (± 0.01)	0.80 (± 0.04)	0.80 (± 0.04)	0.77 (± 0.04)	0.78 (± 0.04)	0.73 (± 0.06)	0.75 (± 0.03)
	<i>CD-MNAR</i>	0.50	0.49 (± 0.07)	0.62 (± 0.05)	0.81 (± 0.03)	0.75 (± 0.00)	0.79 (± 0.01)	0.82 (± 0.02)	0.76 (± 0.03)	0.76 (± 0.05)	0.73 (± 0.06)	0.74 (± 0.02)

1490 **G.2 EXTENDED VISUALIZATIONS**
1491

1492 In addition to Figure 3 in the main paper, Figures 6 and 8 report the full results for all models under
1493 both training mechanisms.



1502 Figure 6: Full results for all models trained with *FD-MNAR* at $\mu_{\text{tr}} = 50\%$, tested on *U-MCAR* with
1503 $\mu_{\text{te}} \in \{0\%, 25\%, 50\%\}$. Each panel corresponds to one dataset; each row to one model. Reported
1504 values are mean \pm std over 5 runs.

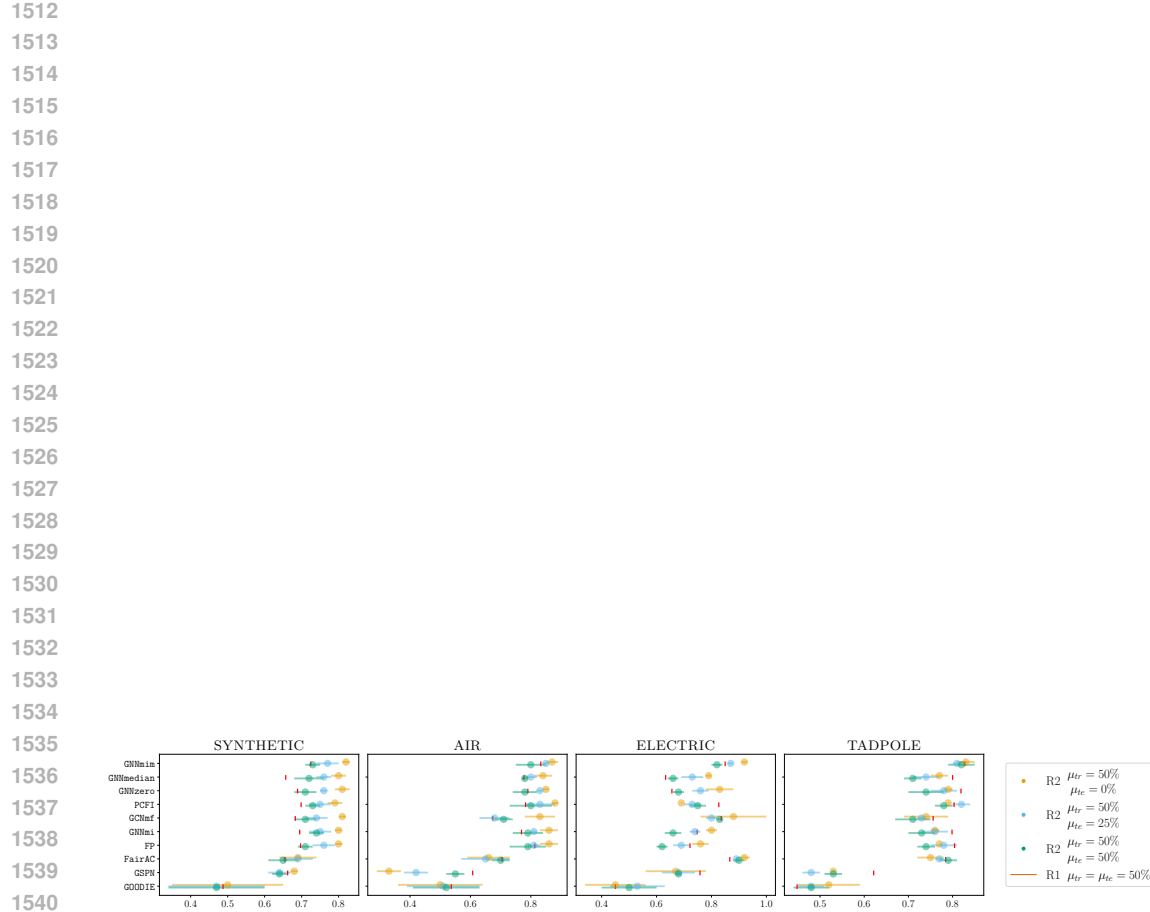
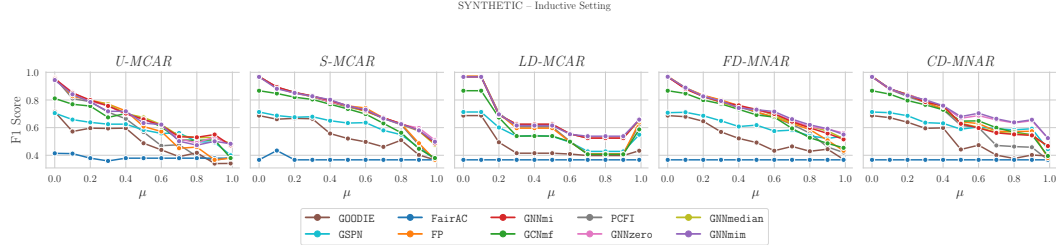


Figure 7: Full results for all models trained with *CD-MNAR* at $\mu_{tr} = 50\%$, tested on *U-MCAR* with $\mu_{te} \in \{0\%, 25\%, 50\%\}$. Same layout as Figure 6.

1566 H INDUCTIVE SYNTHETIC SETTING

1568 In addition to the transductive experiments reported in the main paper, we also ran a set of experiments
 1569 in an inductive setting to demonstrate that our model, GNNmim, is not restricted to transductive
 1570 scenarios. As shown in Figure 8, GNNmim remains competitive with all other baselines even under
 1571 this inductive setup.



1581 Figure 8: Performance of GNNmim and all competitors in an inductive setting. The synthetic dataset
 1582 is constructed so that test nodes form a separate graph component and are never connected to training
 1583 nodes, ensuring that no message can propagate between the two sets during training. Despite this
 1584 strictly inductive setup, GNNmim remains competitive with all baselines.

1586 Table 43: F1 scores for under mechanism *CDMNAR* and varying μ

μ	GOODIE	GSPN	FairAC	FP	GNNmi	GCNmf	PCFI	GNNzero	GNNmedian	GNNmim
0.00	0.687 (± 0.166)	0.713 (± 0.045)	0.367 (± 0.000)	0.972 (± 0.011)	0.968 (± 0.011)	0.867 (± 0.023)	0.970 (± 0.011)	0.968 (± 0.011)	0.968 (± 0.011)	0.967 (± 0.011)
0.10	0.672 (± 0.167)	0.708 (± 0.022)	0.367 (± 0.000)	0.880 (± 0.014)	0.881 (± 0.014)	0.842 (± 0.010)	0.876 (± 0.011)	0.875 (± 0.018)	0.878 (± 0.020)	0.883 (± 0.020)
0.20	0.639 (± 0.151)	0.686 (± 0.048)	0.367 (± 0.000)	0.836 (± 0.015)	0.838 (± 0.022)	0.796 (± 0.026)	0.825 (± 0.018)	0.840 (± 0.022)	0.842 (± 0.020)	0.832 (± 0.019)
0.30	0.595 (± 0.122)	0.636 (± 0.031)	0.367 (± 0.000)	0.785 (± 0.020)	0.785 (± 0.034)	0.765 (± 0.036)	0.782 (± 0.023)	0.796 (± 0.029)	0.793 (± 0.026)	0.801 (± 0.020)
0.40	0.598 (± 0.119)	0.631 (± 0.043)	0.367 (± 0.000)	0.734 (± 0.019)	0.758 (± 0.024)	0.729 (± 0.021)	0.731 (± 0.008)	0.754 (± 0.017)	0.750 (± 0.023)	0.759 (± 0.017)
0.50	0.442 (± 0.092)	0.589 (± 0.029)	0.367 (± 0.000)	0.643 (± 0.036)	0.628 (± 0.040)	0.647 (± 0.041)	0.616 (± 0.029)	0.668 (± 0.023)	0.632 (± 0.030)	0.680 (± 0.018)
0.60	0.473 (± 0.063)	0.605 (± 0.034)	0.367 (± 0.000)	0.629 (± 0.031)	0.597 (± 0.029)	0.649 (± 0.041)	0.600 (± 0.052)	0.687 (± 0.013)	0.602 (± 0.033)	0.704 (± 0.021)
0.70	0.401 (± 0.070)	0.592 (± 0.024)	0.367 (± 0.000)	0.574 (± 0.016)	0.562 (± 0.007)	0.559 (± 0.064)	0.471 (± 0.041)	0.656 (± 0.023)	0.566 (± 0.018)	0.664 (± 0.027)
0.80	0.377 (± 0.012)	0.584 (± 0.026)	0.367 (± 0.000)	0.571 (± 0.026)	0.551 (± 0.020)	0.567 (± 0.044)	0.463 (± 0.069)	0.634 (± 0.025)	0.557 (± 0.016)	0.638 (± 0.028)
0.90	0.402 (± 0.062)	0.592 (± 0.031)	0.367 (± 0.000)	0.574 (± 0.048)	0.544 (± 0.020)	0.548 (± 0.052)	0.458 (± 0.046)	0.650 (± 0.033)	0.547 (± 0.028)	0.657 (± 0.020)
0.99	0.395 (± 0.052)	0.444 (± 0.060)	0.367 (± 0.000)	0.380 (± 0.022)	0.467 (± 0.020)	0.395 (± 0.035)	0.367 (± 0.000)	0.524 (± 0.045)	0.464 (± 0.013)	0.524 (± 0.045)

1597 Table 44: F1 scores for under mechanism *FDMNAR* and varying μ

μ	GOODIE	GSPN	FairAC	FP	GNNmi	GCNmf	PCFI	GNNzero	GNNmedian	GNNmim
0.00	0.687 (± 0.166)	0.708 (± 0.045)	0.367 (± 0.000)	0.972 (± 0.011)	0.967 (± 0.011)	0.867 (± 0.022)	0.968 (± 0.013)	0.967 (± 0.011)	0.967 (± 0.011)	0.968 (± 0.011)
0.10	0.679 (± 0.166)	0.711 (± 0.012)	0.367 (± 0.000)	0.888 (± 0.013)	0.879 (± 0.024)	0.847 (± 0.013)	0.885 (± 0.014)	0.882 (± 0.022)	0.886 (± 0.020)	0.889 (± 0.017)
0.20	0.646 (± 0.154)	0.686 (± 0.033)	0.367 (± 0.000)	0.834 (± 0.024)	0.825 (± 0.024)	0.799 (± 0.016)	0.832 (± 0.026)	0.830 (± 0.022)	0.825 (± 0.025)	0.826 (± 0.028)
0.30	0.569 (± 0.133)	0.649 (± 0.013)	0.367 (± 0.000)	0.800 (± 0.042)	0.786 (± 0.034)	0.772 (± 0.028)	0.796 (± 0.025)	0.789 (± 0.036)	0.782 (± 0.032)	0.793 (± 0.036)
0.40	0.522 (± 0.134)	0.608 (± 0.037)	0.367 (± 0.000)	0.759 (± 0.021)	0.761 (± 0.027)	0.732 (± 0.032)	0.753 (± 0.026)	0.757 (± 0.032)	0.743 (± 0.028)	0.742 (± 0.032)
0.50	0.492 (± 0.135)	0.618 (± 0.008)	0.367 (± 0.000)	0.714 (± 0.016)	0.731 (± 0.015)	0.692 (± 0.027)	0.710 (± 0.028)	0.724 (± 0.017)	0.736 (± 0.018)	0.730 (± 0.019)
0.60	0.433 (± 0.084)	0.575 (± 0.025)	0.367 (± 0.000)	0.675 (± 0.031)	0.699 (± 0.032)	0.676 (± 0.022)	0.674 (± 0.039)	0.702 (± 0.030)	0.687 (± 0.027)	0.716 (± 0.031)
0.70	0.464 (± 0.090)	0.582 (± 0.020)	0.367 (± 0.000)	0.630 (± 0.031)	0.643 (± 0.037)	0.594 (± 0.040)	0.623 (± 0.035)	0.651 (± 0.037)	0.635 (± 0.033)	0.661 (± 0.019)
0.80	0.429 (± 0.065)	0.540 (± 0.009)	0.367 (± 0.000)	0.586 (± 0.021)	0.598 (± 0.027)	0.527 (± 0.053)	0.560 (± 0.030)	0.607 (± 0.029)	0.609 (± 0.019)	0.620 (± 0.024)
0.90	0.444 (± 0.082)	0.522 (± 0.034)	0.367 (± 0.000)	0.508 (± 0.015)	0.558 (± 0.049)	0.486 (± 0.061)	0.460 (± 0.129)	0.589 (± 0.042)	0.575 (± 0.044)	0.592 (± 0.023)
0.99	0.370 (± 0.089)	0.538 (± 0.041)	0.367 (± 0.000)	0.433 (± 0.093)	0.515 (± 0.035)	0.454 (± 0.076)	0.420 (± 0.105)	0.561 (± 0.036)	0.521 (± 0.040)	0.550 (± 0.040)

1620

1621

1622

1623

1624

1625

Table 45: F1 scores for under mechanism *LDMCAR* and varying μ

μ	GOODIE	GSPN	FairAC	FP	GNNmi	GCNmf	PCFI	GNNzero	GNNmedian	GNNmim
0.00	0.687 (± 0.166)	0.713 (± 0.045)	0.367 (± 0.000)	0.972 (± 0.011)	0.968 (± 0.011)	0.867 (± 0.023)	0.970 (± 0.011)	0.968 (± 0.011)	0.968 (± 0.011)	0.967 (± 0.011)
0.10	0.687 (± 0.166)	0.713 (± 0.045)	0.367 (± 0.000)	0.972 (± 0.011)	0.968 (± 0.011)	0.867 (± 0.023)	0.970 (± 0.011)	0.968 (± 0.011)	0.968 (± 0.011)	0.967 (± 0.011)
0.20	0.494 (± 0.117)	0.601 (± 0.039)	0.367 (± 0.000)	0.701 (± 0.023)	0.692 (± 0.031)	0.673 (± 0.036)	0.705 (± 0.019)	0.692 (± 0.031)	0.692 (± 0.031)	0.690 (± 0.029)
0.30	0.415 (± 0.076)	0.537 (± 0.032)	0.367 (± 0.000)	0.596 (± 0.010)	0.624 (± 0.010)	0.539 (± 0.028)	0.606 (± 0.006)	0.624 (± 0.010)	0.624 (± 0.010)	0.615 (± 0.011)
0.40	0.415 (± 0.076)	0.543 (± 0.037)	0.367 (± 0.000)	0.596 (± 0.010)	0.624 (± 0.010)	0.539 (± 0.028)	0.606 (± 0.006)	0.624 (± 0.010)	0.624 (± 0.010)	0.615 (± 0.011)
0.50	0.415 (± 0.076)	0.537 (± 0.032)	0.367 (± 0.000)	0.596 (± 0.010)	0.624 (± 0.010)	0.539 (± 0.028)	0.606 (± 0.006)	0.624 (± 0.010)	0.624 (± 0.010)	0.615 (± 0.011)
0.60	0.409 (± 0.053)	0.495 (± 0.044)	0.367 (± 0.000)	0.497 (± 0.015)	0.555 (± 0.019)	0.498 (± 0.022)	0.501 (± 0.022)	0.555 (± 0.019)	0.555 (± 0.019)	0.552 (± 0.027)
0.70	0.398 (± 0.037)	0.428 (± 0.030)	0.367 (± 0.000)	0.410 (± 0.027)	0.524 (± 0.044)	0.407 (± 0.051)	0.407 (± 0.025)	0.524 (± 0.044)	0.524 (± 0.044)	0.538 (± 0.023)
0.80	0.398 (± 0.037)	0.428 (± 0.030)	0.367 (± 0.000)	0.410 (± 0.027)	0.524 (± 0.044)	0.407 (± 0.051)	0.407 (± 0.025)	0.524 (± 0.044)	0.524 (± 0.044)	0.538 (± 0.023)
0.90	0.398 (± 0.037)	0.428 (± 0.030)	0.367 (± 0.000)	0.410 (± 0.027)	0.524 (± 0.044)	0.407 (± 0.051)	0.407 (± 0.025)	0.524 (± 0.044)	0.524 (± 0.044)	0.538 (± 0.023)
0.99	0.433 (± 0.069)	0.549 (± 0.024)	0.367 (± 0.000)	0.637 (± 0.036)	0.659 (± 0.029)	0.587 (± 0.031)	0.623 (± 0.027)	0.660 (± 0.025)	0.652 (± 0.025)	0.658 (± 0.023)

1633

1634

1635

1636

1637

1638

1639

1640

1641

1642

1643

Table 46: F1 scores for under mechanism *SMCAR* and varying μ

μ	GOODIE	GSPN	FairAC	FP	GNNmi	GCNmf	PCFI	GNNzero	GNNmedian	GNNmim
0.00	0.687 (± 0.166)	0.713 (± 0.045)	0.367 (± 0.000)	0.972 (± 0.011)	0.968 (± 0.011)	0.867 (± 0.023)	0.970 (± 0.011)	0.968 (± 0.011)	0.968 (± 0.011)	0.967 (± 0.011)
0.10	0.661 (± 0.148)	0.687 (± 0.013)	0.434 (± 0.133)	0.887 (± 0.012)	0.894 (± 0.016)	0.847 (± 0.025)	0.891 (± 0.018)	0.894 (± 0.017)	0.890 (± 0.021)	0.881 (± 0.018)
0.20	0.667 (± 0.157)	0.675 (± 0.056)	0.367 (± 0.000)	0.850 (± 0.017)	0.855 (± 0.027)	0.820 (± 0.030)	0.856 (± 0.025)	0.847 (± 0.018)	0.851 (± 0.027)	0.851 (± 0.028)
0.30	0.664 (± 0.155)	0.679 (± 0.034)	0.367 (± 0.000)	0.830 (± 0.016)	0.829 (± 0.032)	0.804 (± 0.028)	0.822 (± 0.025)	0.828 (± 0.032)	0.824 (± 0.034)	0.827 (± 0.038)
0.40	0.557 (± 0.152)	0.650 (± 0.029)	0.367 (± 0.000)	0.785 (± 0.030)	0.796 (± 0.035)	0.769 (± 0.018)	0.785 (± 0.029)	0.785 (± 0.043)	0.790 (± 0.039)	0.802 (± 0.032)
0.50	0.521 (± 0.152)	0.633 (± 0.045)	0.367 (± 0.000)	0.757 (± 0.029)	0.758 (± 0.018)	0.735 (± 0.019)	0.748 (± 0.030)	0.760 (± 0.018)	0.755 (± 0.019)	0.756 (± 0.009)
0.60	0.497 (± 0.135)	0.636 (± 0.058)	0.367 (± 0.000)	0.742 (± 0.030)	0.722 (± 0.034)	0.698 (± 0.021)	0.723 (± 0.038)	0.724 (± 0.039)	0.716 (± 0.031)	0.730 (± 0.027)
0.70	0.461 (± 0.125)	0.580 (± 0.062)	0.367 (± 0.000)	0.670 (± 0.018)	0.671 (± 0.029)	0.631 (± 0.036)	0.666 (± 0.038)	0.673 (± 0.030)	0.672 (± 0.028)	0.666 (± 0.035)
0.80	0.509 (± 0.121)	0.549 (± 0.071)	0.367 (± 0.000)	0.628 (± 0.053)	0.629 (± 0.025)	0.563 (± 0.070)	0.621 (± 0.044)	0.623 (± 0.013)	0.622 (± 0.025)	0.625 (± 0.037)
0.90	0.402 (± 0.071)	0.455 (± 0.068)	0.367 (± 0.000)	0.487 (± 0.070)	0.580 (± 0.043)	0.447 (± 0.060)	0.474 (± 0.092)	0.597 (± 0.026)	0.575 (± 0.039)	0.580 (± 0.027)
0.99	0.367 (± 0.000)	0.372 (± 0.010)	0.367 (± 0.000)	0.367 (± 0.000)	0.486 (± 0.027)	0.380 (± 0.019)	0.367 (± 0.000)	0.509 (± 0.038)	0.476 (± 0.024)	0.498 (± 0.031)

1652

1653

1654

1655

1656

1657

1658

1659

1660

1661

1662

Table 47: F1 scores for under mechanism *UMCAR* and varying μ

μ	GOODIE	GSPN	FairAC	FP	GNNmi	GCNmf	PCFI	GNNzero	GNNmedian	GNNmim
0.00	0.715 (± 0.096)	0.705 (± 0.033)	0.414 (± 0.055)	0.960 (± 0.009)	0.953 (± 0.006)	0.811 (± 0.030)	0.960 (± 0.009)	0.953 (± 0.006)	0.953 (± 0.006)	0.944 (± 0.017)
0.10	0.572 (± 0.137)	0.658 (± 0.031)	0.412 (± 0.057)	0.827 (± 0.050)	0.851 (± 0.043)	0.769 (± 0.112)	0.810 (± 0.034)	0.855 (± 0.044)	0.846 (± 0.047)	0.841 (± 0.051)
0.20	0.596 (± 0.165)	0.638 (± 0.025)	0.379 (± 0.000)	0.798 (± 0.033)	0.799 (± 0.020)	0.756 (± 0.032)	0.788 (± 0.027)	0.790 (± 0.028)	0.788 (± 0.021)	0.785 (± 0.021)
0.30	0.594 (± 0.145)	0.625 (± 0.014)	0.359 (± 0.040)	0.771 (± 0.037)	0.757 (± 0.046)	0.674 (± 0.133)	0.712 (± 0.045)	0.758 (± 0.049)	0.771 (± 0.042)	0.718 (± 0.047)
0.40	0.596 (± 0.132)	0.625 (± 0.005)	0.379 (± 0.000)	0.721 (± 0.055)	0.702 (± 0.044)	0.702 (± 0.055)	0.664 (± 0.080)	0.697 (± 0.049)	0.701 (± 0.048)	0.718 (± 0.029)
0.50	0.487 (± 0.113)	0.583 (± 0.040)	0.379 (± 0.000)	0.608 (± 0.067)	0.660 (± 0.027)	0.664 (± 0.053)	0.568 (± 0.074)	0.659 (± 0.021)	0.674 (± 0.022)	0.633 (± 0.035)
0.60	0.439 (± 0.118)	0.558 (± 0.034)	0.379 (± 0.000)	0.572 (± 0.077)	0.617 (± 0.081)	0.606 (± 0.081)	0.469 (± 0.102)	0.617 (± 0.038)	0.622 (± 0.039)	0.622 (± 0.062)
0.70	0.390 (± 0.074)	0.561 (± 0.019)	0.379 (± 0.000)	0.451 (± 0.092)	0.534 (± 0.073)	0.511 (± 0.095)	0.476 (± 0.118)	0.518 (± 0.076)	0.541 (± 0.089)	0.502 (± 0.092)
0.80	0.418 (± 0.123)	0.499 (± 0.029)	0.379 (± 0.000)	0.459 (± 0.074)	0.530 (± 0.060)	0.508 (± 0.088)	0.392 (± 0.087)	0.490 (± 0.059)	0.528 (± 0.044)	0.473 (± 0.052)
0.90	0.340 (± 0.048)	0.493 (± 0.022)	0.379 (± 0.000)	0.367 (± 0.046)	0.550 (± 0.139)	0.511 (± 0.082)	0.362 (± 0.041)	0.532 (± 0.134)	0.529 (± 0.131)	0.501 (± 0.122)
0.99	0.341 (± 0.045)	0.400 (± 0.025)	0.379 (± 0.000)	0.379 (± 0.000)	0.472 (± 0.022)	0.380 (± 0.003)	0.384 (± 0.011)	0.476 (± 0.038)	0.485 (± 0.018)	0.483 (± 0.033)

1670

1671

1672

1673

1674 I GAIN USING MIM WITH COMPETITORS

1676 Tables 48 through 51 report the performance gain observed when all competitor models described
 1677 in the main paper are equipped with the MIM mask, mirroring the setup used for GNNmim. Consis-
 1678 tently, basic imputation methods that replace missing features with a constant, such as GNNmi and
 1679 GNNmedian, show a positive and comparable performance increase when supplied with the same
 1680 mask. This suggests that the improvement comes from the model's ability to selectively ignore the
 1681 padded or imputed feature values indicated by the mask.

1682 Table 48: F1 gain from using mask on SYNTHETIC under mechanism *U-MCAR*

μ	FairAC	FP	GCNmF	GNNmedian	GNNmi	GOODIE	GSPN	PCFI	GNNzero
0.00	-0.087	-0.016	-0.145	0.002	0.003	-0.256	-0.094	-0.020	0.005
0.10	-0.094	-0.022	-0.065	0.006	0.005	-0.253	-0.080	-0.004	0.001
0.20	-0.102	-0.013	-0.005	0.002	0.004	-0.215	-0.052	-0.001	0.008
0.30	-0.078	0.002	-0.021	0.012	0.014	-0.198	-0.068	-0.008	0.015
0.40	-0.082	0.008	-0.022	0.012	0.07	-0.223	-0.075	0.006	0.025
0.50	0.011	-0.006	-0.010	0.005	0.09	-0.268	-0.079	-0.018	0.007
0.60	-0.025	-0.004	-0.029	0.004	0.013	-0.346	-0.072	-0.001	0.000
0.70	0.013	0.001	-0.044	0.005	0.004	-0.321	-0.008	0.006	0.006
0.80	-0.070	-0.008	0.009	0.002	0.015	-0.429	0.015	-0.014	0.039
0.90	-0.020	-0.017	-0.011	0.011	0.014	-0.346	0.053	0.001	0.001
0.99	0.052	-0.007	0.056	-0.020	-0.013	-0.422	0.024	-0.011	-0.013

1696 Table 49: F1 gain from using mask on SYNTHETIC under mechanism *S-MCAR*

μ	FairAC	FP	GCNmF	GNNmedian	GNNmi	GOODIE	GSPN	PCFI	GNNzero
0.00	-0.080	-0.016	-0.145	0.002	0.003	-0.256	-0.091	0.05	0.005
0.10	0.013	0.001	-0.077	0.03	0.04	-0.211	0.005	-0.11	-0.011
0.20	-0.018	-0.039	-0.086	0.003	0.007	-0.245	-0.019	-0.026	0.031
0.30	0.000	-0.026	-0.083	0.006	0.015	-0.234	-0.013	-0.015	0.016
0.40	0.010	-0.034	-0.012	0.002	0.019	-0.185	-0.014	-0.018	0.024
0.50	-0.062	-0.048	0.005	0.006	0.016	-0.207	-0.036	-0.039	0.033
0.60	-0.045	-0.028	-0.038	0.018	0.032	-0.161	0.001	-0.026	0.038
0.70	0.009	-0.007	-0.025	0.011	0.025	-0.153	-0.015	-0.033	0.064
0.80	0.010	-0.011	-0.046	0.011	0.02	-0.136	-0.002	0.004	0.029
0.90	-0.045	0.003	-0.018	0.002	-0.002	-0.071	0.043	-0.000	-0.019
0.99	0.128	-0.024	0.074	0.002	-0.015	0.048	0.033	-0.025	-0.011

1710 Table 50: F1 gain from using mask on SYNTHETIC under mechanism *LD-MCAR*

μ	FairAC	FP	GCNmF	GNNmedian	GNNmi	GOODIE	GSPN	PCFIGNNzero	
0.00	-0.073	-0.016	-0.145	0.002	0.003	-0.256	-0.094	-0.020	0.005
0.10	-0.047	0.104	-0.012	0.026	0.095	-0.222	-0.014	0.097	-0.08
0.20	-0.105	-0.078	-0.081	0.004	0.075	-0.251	-0.092	-0.067	0.081
0.30	-0.106	-0.119	-0.106	0.015	0.101	-0.331	-0.091	-0.118	0.133
0.40	0.014	-0.044	-0.049	0.015	0.039	-0.337	-0.054	-0.033	0.098
0.50	0.080	-0.002	-0.004	0.015	0.002	-0.362	0.027	0.003	0.077
0.60	-0.079	-0.073	-0.068	0.004	0.081	-0.386	-0.046	-0.069	0.139
0.70	-0.111	-0.084	-0.034	0.001	0.070	-0.423	-0.039	-0.060	0.139
0.80	0.001	-0.084	-0.074	0.001	0.085	-0.422	-0.056	-0.086	0.130
0.90	-0.067	-0.090	-0.066	0.001	0.096	-0.439	0.023	-0.072	0.143
0.99	0.046	0.037	-0.054	0.007	0.014	-0.359	0.025	0.039	0.020

1728

1729

1730

1731

1732

1733

1734

1735

Table 51: F1 gain from using mask on SYNTHETIC under mechanism *FD-MNAR*

μ	FairAC	FP	GCNmf	GNNmedian	GNNmi	GOODIE	GSPN	PCFIGNNzero
0.00	-0.080	-0.018	-0.141	0.002	0.003	-0.256	-0.081	-0.018
0.10	-0.035	-0.006	-0.057	0.007	0.013	-0.216	-0.002	-0.001
0.20	0.018	0.015	0.024	0.06	0.005	-0.193	-0.012	-0.009
0.30	0.021	0.002	-0.005	0.002	0.007	-0.138	0.015	0.016
0.40	0.001	-0.007	-0.031	0.006	0.011	-0.186	-0.032	0.003
0.50	-0.025	-0.011	-0.020	0.008	0.013	-0.208	-0.009	-0.007
0.60	0.011	0.006	-0.019	0.012	0.008	-0.121	0.030	0.013
0.70	0.022	0.029	0.004	0.000	0.003	-0.063	0.044	0.013
0.80	0.010	0.013	-0.010	0.002	0.001	-0.006	-0.017	0.033
0.90	0.053	0.032	-0.032	0.005	0.011	0.048	-0.023	0.020
0.99	0.156	0.002	-0.008	0.001	0.010	-0.015	0.006	-0.003

1747

1748

1749

1750

1751

1752

1753

1754

1755

1756

1757

1758

1759

1760

1761

1762

1763

Table 52: F1 gain from using mask on SYNTHETIC under mechanism *CD-MNAR*

μ	FairAC	FP	GCNmf	GNNmedian	GNNmi	GOODIE	GSPN	PCFIGNNzero
0.00	-0.078	-0.016	-0.145	0.002	0.003	-0.256	-0.091	-0.020
0.10	-0.025	-0.002	-0.060	0.004	0.010	-0.239	-0.019	-0.005
0.20	0.023	0.006	-0.003	0.004	0.002	-0.202	-0.029	0.004
0.30	-0.005	0.017	-0.004	0.009	0.007	-0.121	-0.030	-0.006
0.40	-0.045	0.017	-0.015	0.014	0.017	0.005	-0.024	0.021
0.50	-0.035	0.010	0.001	0.048	0.010	-0.035	-0.042	0.009
0.60	0.054	0.036	-0.011	0.019	0.015	-0.111	-0.047	0.073
0.70	0.038	0.051	0.001	0.025	0.028	-0.064	0.031	0.072
0.80	0.045	0.046	0.047	0.017	0.011	-0.028	-0.021	0.086
0.90	0.136	0.033	0.039	0.011	0.021	-0.009	-0.047	0.075
0.99	0.098	-0.041	0.057	0.017	0.015	-0.050	0.044	0.013

1775

1776

1777

1778

1779

1780

1781